

“Design & Development of Compact Low Pass and Band Pass Filters for Microwave Receivers Applications”

Summer Practical Training Report

*Submitted in Partial Fulfilment of the
Requirements for the Degree of*

BACHELOR OF TECHNOLOGY

IN

ELECTRONICS AND COMMUNICATION ENGINEERING

By

**Sneh Ashish Shah
(22BEC121)**



**Department of Electronics and Communication
Engineering, Institute of Technology,**

**Nirma University,
Ahmedabad 382481**

July 2025

ACKNOWLEDGEMENT

I would like to express my profound gratitude to all those who contributed to the successful completion of this project.

Firstly, I would like to express my gratitude towards **Smt. Harshita Tolani**, Head, MSRD, MSRG, MRSA for letting me work under her division and dive into the domain of RF/Microwave.

I am especially indebted to my guide, **Sri Vinit Kumar**, whose expert guidance, constructive feedback, and unwavering support were instrumental throughout the duration of this work. Their insights and encouragement have been invaluable.

I would also like to extend my sincere thanks to the other supportive personals, **Dr. Anamiya Bhattacharya, Sri Vivan Prakash, Sri Prashant, Smt. Shrija Bhattacharya**, whose assistance, and constant support made everything seem approachable for me.

My appreciation also goes to my peers and colleagues, **Sri Abhay Nathani, Ms. Nisha Bagadia, Krishanu, Pravesh, Saurabh and Uttam** for their helpful discussions, collaboration, and moral support, which played a significant role in overcoming challenges during this endeavour.

Finally, I am deeply grateful to my family for their patience, understanding, and continued encouragement, without which this work would not have been possible.

Sneh Ashish Shah

22BEC121

ABSTRACT

The project titled “**Design & Development of Compact Low Pass and Band Pass Filters for Microwave Receivers Applications**” focuses on the theoretical and practical development of microstrip bandpass filter suitable for the **L&S-Band** application. Filters are crucial in the domain of satellite communication systems, radar systems, and various other systems. Filters can both be realised in the form of lumped components or in the form of distributive components. This project report aims to develop an microstrip filter that meets the stringent performance criteria while ensuring the satisfaction of the provided specifications.

The design and implementation of band pass filters using lumped components play a critical role in the development of modern communication systems. This report explores the design of a compact band pass filter using lumped components operating in the MHz frequency range, **with centred at 312.5 MHz**, covering the passband from **252.5 MHz to 372.5 MHz**. The filter also **rejects, frequencies beyond 187.5 – 437.5 MHz** with an attenuation **greater than 20dBc**. The filter is designed to achieve high performance with low insertion loss better than 3dB, minimal return loss, and a **butterworth** response, making it suitable for a variety of RF communication systems.

The design and implementation of microstrip lowpass filters play a critical role in the development of modern communication systems, particularly for **wideband (WB)** applications. This report explores the design of a compact microstrip lowpass filter operating in the WB frequency range, **with cut-off at 2.475 GHz**, covering the passband from **0 GHz to 2.75 GHz**. The filter also **rejects, frequencies from 2.75 - 17.25 GHz** with an attenuation **greater than 20dBc** and **frequencies from 7.725 - 10.125 GHz** with an attenuation **greater than 30dBc**. The filter is designed to achieve high performance with low insertion loss, minimal return loss, and a **0.1 dB ripple** response, making it suitable for a variety of RF communication systems.

In addition, both the designs are constrained to a **compact area of $\frac{3}{4}$ inch $\times \frac{3}{4}$ inch**, ensuring its applicability in space-limited environments. The use of high-dielectric substrates and precise electromagnetic simulations allows for optimization of the filter’s electrical and physical characteristics. The resulting filter meets the stringent requirements for communication systems, providing a robust solution for modern wireless applications that demand wide frequency coverage, low loss, and high selectivity. This work also discusses the design challenges associated with achieving such performance under physical and manufacturing constraints.

INDEX

CHAPTER-1: INTRODUCTION	
1.1 Company Profile.....	8
1.2 Group Profile	9
1.3 Prologue.....	10
1.4 Introduction	11
1.5 Scope of the Training	11
1.6 Gantt Chart.....	12
1.7 Organization of the Rest of the Report	13
1.8 Scope of the Project	13
CHAPTER-2: BASICS CONCEPTS OF FILTERS	14
2.1 Transfer Functions.....	14
2.1.1 Poles and Zeros of Complex Plane:	15
2.1.2 Butterworth (Maximally Flat) Response:.....	15
2.1.3 Chebyshev Response:	16
2.1.4 Elliptic Function Response:.....	18
2.1.5 Gaussian (Maximally Flat Group-Delay) Response:.....	18
2.2 Low pass Prototype Filters and Elements.....	19
2.2.1 Butterworth Low Pass Prototype Filters.....	19
2.2.2 Chebyshev Low Pass Prototype Filters	20
2.2.3 Elliptic Function Low Pass Prototype Filters	21
2.3 Frequency and Element Transformations.....	21
2.3.1 Low pass Transformation	22
2.3.2 High pass Transformation.....	23
2.3.3 Band pass Transformation.....	24
2.3.4 Band stop Transformation.....	26
2.4 Filter Design by The Insertion Loss Method.....	27
2.5 Filter Implementation.....	27
2.5.1 Richards' Transformation	28
2.5.2 Kuroda's Identities	29
2.5.3 Impedance and Admittance Inverters	30
CHAPTER-3: TRANSMISSION LINES AND COMPONENTS	31
3.1 Micro strip Lines.....	31
3.1.1 Micro strip Structure.....	31
3.1.2 Waves in Micro strips	31
3.1.3 Quasi-TEM Approximation.....	31
3.1.4 Effective Dielectric Constant and Characteristic Impedance.....	32

3.1.5 Guided Wavelength, Propagation Constant, Phase Velocity, and Electrical Length	32
3.1.6 Synthesis of W/h.....	33
3.1.7 Effect of Strip Thickness.....	33
3.2 Microstrip Discontinuities.....	34
3.2.1 Steps in Width.....	34
3.2.2 Open Ends.....	35
3.2.3 Gaps	37
3.2.4 Bends	38
3.3 Quasilumped Elements.....	38
3.3.1 High- and Low-Impedance Short Line Sections	39
3.3.2 Open- and Short-Circuited Stubs	40
3.4 Resonators.....	42
3.5 Scattering Parameters (S-Parameters).....	42
Why Use S-Parameters Instead of Z, Y, or H Parameters?	43
CHAPTER-4 FILTER - 1: FILTER DESIGN METHODOLOGY	44
4.1 Problem Statement (Filter Specifications).....	44
4.2 Literature Survey	44
4.3 Theoretical Approach	45
4.3.1 Substrate Analysis.....	45
4.3.2 Filter Design Analysis	46
4.4 Practical Implementation	46
4.4.1 3 rd Order Lumped Band Pass Filter Design	46
4.4.2 4 th Order Lumped Band Pass Filter Design with Ideal Elements.....	48
4.4.3 3 rd order Lumped Band Pass Filter with Non-Ideal Elements.....	49
CHAPTER-5 FILTER - 2: FILTER DESIGN METHODOLOGY	52
5.1 Problem Statement (Filter Specifications).....	52
5.2 Literature Survey	52
5.3 Theoretical Approach	54
5.3.1 Substrate Analysis.....	54
5.3.2 Filter Design Analysis	55
5.4 Practical Implementation	56
5.4.1 6 th Order Stepped-Impedance Filter Design	58
5.4.2 10 th Order Stepped-Impedance Filter Design	60
5.4.3 10 th Order Open-Stub Filter Design	62
5.4.4 7 th Order Stepped-Impedance with $\lambda/4$ Open-Circuited Stubs Filter Design	64
5.4.5 7 th Order LC Open-Stub Filter Design.....	66
5.4.6 7 th Order LC Open-Stub Filter Design with Radial Stubs.....	68

5.4.7 7 th Order LC Open-Stub Filter Design with Radial Stubs – 2	70
5.4.8 LPF+LPF Finalizing the Design	73
CHAPTER-6 FINAL PROPOSED DESIGNS.....	76
6.1 Band Pass Filter using Lumped Components (Filter – 1)	76
6.1.1 Layout Designed for BPF using Lumped Elements.....	76
6.1.2 Schematic with Co-Simulation	77
6.1.3 S-Parameters for Co-Simulation	78
6.2 Micro-strip Low Pass Filter (Filter – 2).....	79
6.2.1 Layout Designed for Micro-Strip LPF Layout	79
6.2.2 S-Parameters for Final Micro Strip LPF	80
6.2.3 Layout for Final Micro Strip LPF with Tuning Pads	81
CONCLUSION	82
SCOPE OF FUTURE WORK	83
REFERENCES.....	84

List of Figures:

Chapter	Figure No.	Figure Title
Chapter 1	Figure 1.1	Butterworth Filter Response
	Figure 1.2	Butterworth Filter Response (Duplicate or Second Version)
	Figure 1.3	Chebyshev Filter Response
	Figure 1.4	Pole Location for Chebyshev Filter Response
	Figure 1.5	Elliptic Filter Response
	Figure 1.6	Gaussian Filter Response (a) Amplitude (b) Phase Delay
	Figure 1.7	Lowpass prototype filters for elliptic function filters
	Figure 1.8	Low pass prototype to low pass transformation for basic elements
	Figure 1.9	Low pass prototype to high pass transformation for basic element
	Figure 1.10	Low pass prototype to band pass transformation for basic element
	Figure 1.11	Low pass prototype to band pass transformation for basic element
	Figure 1.12	Richards' Transformation (a) Inductor to Short Stub (b) Capacitor to Open Stub
	Figure 1.13	The four Kuroda Identities
	Figure 1.14	Filter Response for Lumped and Distributed Elements
Chapter 2	Figure 2.1	General Microstrip Structure
	Figure 2.2	Microstrip Discontinuity (Steps in Width)
	Figure 2.3	Microstrip Discontinuity (Open End)
	Figure 2.4	Microstrip Discontinuity (Gap)
	Figure 2.5	Microstrip Discontinuity (Bend)
	Figure 2.6	High-Impedance Short-Line Element
	Figure 2.7	Low-Impedance Short-Line Element
	Figure 2.8	Short Stub Elements: (a) Open-Circuited Stub; (b) Short-Circuited Stub
	Figure 2.9	Quarter-Wave Resonators
	Figure 2.10	Half-Wave Resonators
Chapter 3	Figure 3.1	Substrate Structure Used for Design
	Figure 3.2	Schematic Representation of 3rd Order Filter
	Figure 3.3	S-Parameters from Schematic Simulation (3rd Order)
	Figure 3.4	Schematic Representation of 4th Order Filter

Chapter	Figure No.	Figure Title
	Figure 3.5	S-Parameters from Schematic Simulation (4th Order)
	Figure 3.6	Schematic of 3rd Order Filter with Non-Ideal Elements
	Figure 3.7	S-Parameters from Simulation (3rd Order, Non-Ideal Elements)
Chapter 4	Figure 4.1	Substrate Structure Used for Design
	Figure 4.2	LineCalc Tool in ADS
	Figure 4.3	Schematic Representation of 6th Order Filter
	Figure 4.4	S-Parameters from Simulation (6th Order)
	Figure 4.5	Schematic Representation of 6th Order Filter (Layout)
	Figure 4.6	S-Parameters from Simulation (10th Order)
	Figure 4.7	Schematic Representation of 10th Order Filter
	Figure 4.8	S-Parameters from Schematic Simulation (10th Order)
	Figure 4.9	Schematic for 7th Order Filter Design
	Figure 4.10	Layout for 7th Order Filter Design
	Figure 4.11	S-Parameters from Layout Simulation (7th Order)
	Figure 4.12	Layout for 7th Order Filter
	Figure 4.13	S-Parameters from Layout (7th Order Filter)
	Figure 4.14	Layout of 7th Order Filter with Radial Stubs
	Figure 4.15	Simulation Result of 7th Order Filter with Radial Stubs
	Figure 4.16	Layout of 7th Order Filter with More Radial Stubs
	Figure 4.17	Simulation Result of 7th Order Filter with More Radial Stubs
	Figure 4.18	Layout of 7th Order Filter with Radial Stubs – 2
	Figure 4.19	Simulation Result of 7th Order Filter with Radial Stubs – 2
	Figure 4.20	Layout of 7th + 5th Order Filter with Radial Stubs
	Figure 4.21	Simulation Result of 7th + 5th Order Filter with Radial Stubs
	Figure 4.22	Layout Representation of LPF + LPF Filter
	Figure 4.23	Simulation Result of LPF + LPF Filter
	Figure 4.24	Layout of LPF + LPF Filter with Increased Order
	Figure 4.25	Simulation Result of LPF + LPF Filter with Increased Order
Chapter 5	Figure 5.1	Footprints for Lumped Elements

Chapter Figure No. Figure Title

- Figure 5.2 Layout for BPF using Lumped Elements
- Figure 5.3 Co-Simulation Schematic for BPF using Lumped Elements
- Figure 5.4 S-Parameters for Co-Simulations
- Figure 5.5 Layout for Final Microstrip LPF
- Figure 5.6 S-Parameters for Final Microstrip LPF
- Figure 5.7 Layout for Final Microstrip LPF with Tuning Pads

List of Tables:

Table	Details
1	Filter Specifications
2	Obtained values for 3 rd order Lumped Band Pass Filter
3	Obtained values for 4 th order Lumped Band Pass Filter Optimized
4	Obtained values for 3 rd order Filter
5	Filter Specifications
6	Obtained values for 6 th order Stepped-Impedance Filter
7	Obtained values for 10 th order Stepped-Impedance Filter
8	Obtained values for 10 th order Open Stub Filter
9	Obtained values for 7 th order Stepped-Impedance Filter
10	Final values for 3 rd order BPF

1.1 Company Profile

The **Space Applications Centre (SAC)** is a vital wing of the **Indian Space Research Organisation (ISRO)**, operating under the Department of Space, Government of India. Established in **1972** and headquartered in **Ahmedabad, Gujarat**, SAC has played a pioneering role in transforming space technology into practical applications for national development. It has been instrumental in designing payloads and systems that power India's ambitious satellite programs for communications, remote sensing, meteorology, and scientific exploration.

SAC was envisioned by **Dr. Vikram Sarabhai**, the founding father of India's space program, who believed that space science must be harnessed for the benefit of society, especially in areas like education, agriculture, weather forecasting, natural resource management, and rural development. Today, SAC stands as a realization of that vision, continually innovating and translating satellite capabilities into real-world services.

The **vision** of SAC is in alignment with ISRO's broader objective: "*Harness space technology for national development while pursuing space science research and planetary exploration.*" SAC's mission centers on the design, development, and operationalization of payloads and applications in support of communication, Earth observation, navigation, meteorology, and space sciences.

SAC is responsible for the end-to-end development of **payloads for Indian national satellites**, including INSAT, IRS, GSAT, RISAT, Cartosat, and others. These payloads serve diverse functions such as telecommunication, television broadcasting, resource mapping, urban planning, environmental monitoring, disaster management, and defense surveillance. The centre also designs advanced optical and microwave sensors, onboard software, RF and antenna systems, and data reception and processing infrastructure.

The Centre operates from **multiple campuses in Ahmedabad**:

- **SAC Main Campus** at Jodhpur Tekra, housing core R&D facilities.
- **Bopal Campus**, focusing on antenna systems and microwave technology.
- **Vikram Sarabhai Space Exhibition (VSSE)**, a public outreach facility educating visitors about India's space programs.

The **products** developed at SAC include:

- Earth observation payloads (optical, microwave, hyperspectral)
- Telecommunication transponders
- Meteorological sensors (INSAT-3D/3DR)
- Scientific instrumentation (Chandrayaan, Mars Orbiter, Aditya-L1)
- Ground support systems (data processing software, antenna terminals)

The **Services** offered by SAC extend to:

- Data acquisition and dissemination
- Capacity building for satellite-based services
- Support to user agencies in resource management and planning
- Development of satellite-based tele-education and telemedicine platforms

Over the decades, SAC has contributed significantly to key national missions such as **Chandrayaan-1 & 2**, **Mangalyaan (Mars Orbiter Mission)**, **INSAT-3D/3DR**, **RISAT**, **Cartosat** series, and the recently launched **Aditya-L1** solar mission. It has also collaborated with international agencies like NASA, CNES, and ESA on sensor calibration and Earth observation programs.

In essence, SAC remains a beacon of **indigenous innovation**, integrating advanced space technologies with development goals. It not only represents India's technological prowess in space but also embodies the ethical responsibility to use science for social welfare.

1.2 Group Profile

At the **Space Applications Centre (SAC)** of **ISRO**, the organizational structure is divided into thematic groups and divisions, each tasked with specialized functions to support the Centre's mission of developing space-based applications and technologies. Among these, the **Microwave Sensors and Radar Group (MSRG)** — also referred to as **Microwave Sensors and Radar Systems Group (MSRD)** — is a key technical group involved in the design, development, and analysis of active microwave sensors and radar systems for Earth observation and planetary missions.

The **Microwave Sensors and Radar Group (MSRG)** comprises multiple subdivisions and working groups, such as the **Microwave Remote Sensing Area (MRSA)**, which houses experts in hardware and system development of spaceborne synthetic aperture radars (SAR), scatterometers, altimeters, and radiometers. These instruments are central to all-weather, day-and-night remote sensing applications, particularly for monitoring land, ocean, ice, and atmosphere.

This group has made critical contributions to major missions including **RISAT-1**, **RISAT-2B**, **Oceansat**, **Scatsat**, and **NISAR** (NASA-ISRO SAR mission). MRSA works in coordination with both national and international partners to meet the growing demand for high-resolution radar imagery and oceanographic data.

Organizational Structure

The group hierarchy follows a streamlined **project and function-oriented structure** under SAC's Director, with technical oversight from Deputy Directors and Group Heads. The typical hierarchy is:

- **Director, SAC**
 - **Deputy Director (EPSA/RESPOND/MRSA etc.)**
 - **Group Director (MSRG/MSRD)**
 - **Division Heads/Project Leaders (SAR, Altimeter, Scatterometer, Radiometer Systems)**
 - **Section/Team Leaders**
 - **Engineers, Scientists, Research Scholars, Interns**

The MSRG group works collaboratively across SAC's campuses, with system integration often occurring at dedicated cleanroom facilities and testing labs equipped with vector network analyzers, compact antenna test ranges (CATR), and high-frequency simulation tools.

In addition to its core R&D activities, MSRG/MRSA supports:

- **Technology transfer** to Indian industries
- **Feasibility studies** for future missions like **Dual-band SAR, Airborne SAR, and spaceborne radar altimeters**
- **Algorithm development** for SAR image processing and geophysical parameter retrieval
- **Training programs** for young scientists, project trainees, and collaborators

The group fosters an interdisciplinary environment, combining **RF engineering, antenna design, digital signal processing, system integration, and software development** under a unified vision of advancing ISRO's radar remote sensing capabilities.

With decades of expertise and several successful mission deployments, the **MSRG/MSRD/MRSA** group continues to push the frontier of microwave sensing technology, contributing both to India's strategic remote sensing programs and global scientific initiatives.

1.3 Prologue

The advancements in modern technology have greatly accelerated the way we understand and interact with the world around us. Among these advancements, the use of space-based systems for communication, Earth observation, and scientific exploration has been transformative. The Indian Space Research Organisation (ISRO), through its various centers such as the Space Applications Centre (SAC), continues to lead the nation in harnessing space technology for practical applications that benefit society.

This report presents a detailed account of the work carried out as part of a focused training/internship program under the guidance of experts at SAC-ISRO. The primary objective of the project was to understand the end-to-end process of RF and microwave filter design, simulation, and implementation — with an emphasis on microstrip and lumped element filter technologies. These filters play a crucial role in satellite payloads and ground systems by ensuring signal integrity, minimizing noise, and selecting desired frequency bands.

Through this project, significant insights were gained into the theoretical foundations of filter design, including Butterworth, Chebyshev, and other standard responses, as well as practical aspects such as layout design, simulation using advanced tools, and performance validation using S-parameters. The exposure to SAC's structured workflow, technical rigor, and collaborative research environment provided an excellent opportunity to apply academic knowledge in a real-world, mission-driven context.

The following pages document the journey of this project — from the initial literature review to the final proposed designs — and reflect the learning, challenges, and outcomes experienced during the internship. It is hoped that this report not only serves as a technical record but also contributes to a broader understanding of space-grade RF component design and its significance in the field of microwave remote sensing and satellite communications.

1.4 Introduction

In the rapidly evolving landscape of modern wireless communication systems, the demand for high-performance components such as **filters** has seen a sharp increase. Filters play a fundamental role in the design of communication systems by selectively allowing signals within a specified frequency range to pass through while blocking unwanted frequencies. Among various types of filters, **low pass filters** and **band pass filters** are crucial in **RF** (Radio Frequency) and **microwave** applications, where they are used to isolate desired frequency bands from the surrounding noise and interference. With the rise of **Wideband (WB)** communication systems, which require broad frequency coverage and minimal interference, the role of high-performance filters has become even more prominent. These systems, which operate over a wide range of frequencies, demand filters that can provide excellent performance, even at higher frequencies, while maintaining compactness and integration capabilities.

Wideband (WB) communication systems are a class of systems that operate over a very large frequency range, typically spanning from **3.1 GHz to 10.6 GHz** in most commercial applications. However, WB technologies can also extend beyond these ranges, offering high data rates, low power consumption, and high-resolution sensing capabilities. WB systems have found widespread applications in areas like **wireless personal area networks (WPANs)**, **radar** and **positioning systems**, as well as in **medical imaging** and **sensor networks**. The inherent advantage of WB systems lies in their ability to transmit large amounts of data over short distances with minimal interference, making them ideal for both **high-speed communication** and **precision timing applications**.

Despite these advantages, WB systems come with their own set of challenges. The wide frequency spectrum over which these systems operate requires filters that can provide high selectivity and low insertion loss, particularly over a broad passband. The filter must effectively reject signals outside the desired frequency range, ensuring that the communication signal is clear and free of interference. Additionally, with the increasing demand for portable and compact devices, it is necessary for these filters to be **small yet highly efficient**.

1.5 Scope of the Training

The internship at **Space Applications Centre (SAC-ISRO)** provided a unique opportunity to gain hands-on experience in the field of **microwave filter design**, an essential domain within space electronics and RF systems. The training was designed to bridge the gap between academic learning and real-world engineering practices followed at one of India's premier space research institutions.

The scope of this internship revolved around the **design, simulation, analysis, and optimization** of various RF filters used in satellite communication and remote sensing payloads. This included the study and practical implementation of both **lumped element filters** and **microstrip-based filters**. Key technical areas covered during the training included:

- Understanding the **fundamentals of filter theory**, including transfer functions, pole-zero placement, and response characteristics such as Butterworth, Chebyshev, Elliptic, and Gaussian.
- Design and simulation of **lumped bandpass filters** of various orders (3rd, 4th), considering both ideal and non-ideal components.

- Development of **high-order stepped-impedance and stub-based low-pass filters** using **microstrip technology**.
- Advanced filter structures such as **LC open-stub filters with radial stubs** and layout optimization using **tuning pads**.
- **Co-simulation using ADS (Advanced Design System)**, along with analysis of **S-parameters**, performance validation, and layout realization.
- Exposure to key concepts like **Richards' transformation**, **Kuroda identities**, and **frequency scaling techniques**.

Additionally, the training provided insight into SAC's rigorous workflow for satellite payload development, exposing the intern to practical constraints such as layout miniaturization, component selection, and manufacturing considerations. The experience also enhanced technical proficiency in EM simulation tools, design documentation, and interpreting test results in the context of real mission requirements.

Overall, the training contributed significantly to both theoretical understanding and practical skills in RF/microwave engineering, laying a strong foundation for future contributions in space-grade communication and sensing systems.

1.6 Gantt Chart

The below is the image for Gantt Chart which shows the timeline of the internship and the work done.



Task – 1 → Reading books and research papers

Task – 2 → Learning Software

Task – 3 → Filter – 1 and 2

Task – 4 → Filter – 2

1.7 Organization of the Rest of the Report

The remainder of this report is structured into well-defined chapters that document the complete journey of the internship, beginning with foundational concepts and culminating in practical design implementations and final results. **Chapter 2** introduces the basic concepts of filters, covering transfer functions, filter responses, and transformations essential for RF filter design. **Chapter 3** focuses on transmission lines and microwave components, including microstrip structures, discontinuities, and resonators, which form the backbone of physical filter realization.

Chapter 4 outlines the methodology adopted in the first major filter design project (Filter-1), which involves lumped element bandpass filters. It includes the problem definition, theoretical approach, and practical layout and simulation results. **Chapter 5** extends the design methodology to more complex microstrip-based filters (Filter-2), including stepped-impedance and stub-based designs, offering a comprehensive look at higher-order implementations with varied design strategies.

Chapter 6 presents the final proposed designs derived from iterative improvements and layout optimization, complete with S-parameter analysis and tuning techniques. The report ends with a section on the **scope for future work**, references in IEEE format, and supporting appendices. This logical flow ensures clarity, coherence, and a progressive buildup of knowledge from theory to application.

1.8 Scope of the Project

The scope of the project undertaken during the internship at **Space Applications Centre (SAC-ISRO)** primarily involved the **design, analysis, simulation, and implementation of RF and microwave filters**, with a strong emphasis on both theoretical understanding and practical realization using modern simulation tools.

The project covered the end-to-end workflow of filter design — starting from defining specifications based on desired frequency response and system requirements, selecting appropriate filter types (such as lumped or distributed), performing analytical calculations, and proceeding to simulation and layout design using industry-standard tools like **ADS (Advanced Design System)**. This included:

- Designing **low-pass and band-pass filters** using **lumped elements**, considering both ideal and real-world component models.
- Implementing **microstrip-based filter structures**, including **stepped-impedance filters, open- and short-stub filters**, and **LC stub-based configurations**.
- Validating designs through **S-parameter analysis**, observing key performance metrics like return loss, insertion loss, and bandwidth.

The project was not limited to design alone but also involved understanding substrate selection, layout constraints, fabrication feasibility, and co-simulation practices that are integral to flight-qualified hardware. The results obtained serve as building blocks for filters that could potentially be integrated into future satellite systems. Thus, the scope of the project encompassed a **complete design cycle** — from **concept to simulation-ready hardware**, while simultaneously reinforcing fundamental RF principles, enhancing practical design skills, and providing exposure to the highly disciplined and structured development practices followed at ISRO.

CHAPTER-2: BASICS CONCEPTS OF FILTERS

A filter is a two-port network used to control the frequency response of a certain point in an RF or microwave system by providing transmission at frequencies within the passband of the filter and attenuation in the stopband of the filter. Typical filter responses include low-pass, high-pass, band pass, and band-reject characteristics. Applications can be found in virtually any type of RF or microwave communication, radar, or test and measurement system.

This chapter describes basic concepts and theories that form the foundation for design of general RF/microwave filters.

2.1 Transfer Functions

General Definition: The transfer function of a two-port filter network is a mathematical description of network response characteristics, namely, a mathematical expression of S_{21} . On many occasions, an amplitude-squared transfer function for a lossless passive filter network is defined as

$$|S_{21}(j\Omega)|^2 = \frac{1}{1 + \epsilon^2 F_n^2(\Omega)}$$

Where,

ϵ : Ripple constant.

$F_n(\Omega)$: Filtering or characteristic function.

Ω : Frequency variable (radian frequency variable of a low pass prototype filter with cut-off frequency at $\Omega = \Omega_c$ for $\Omega_c = 1$ rad/s)

For linear, time-invariant networks, the transfer function may be defined as a rational function, that is

$$S_{21}(p) = \frac{N(p)}{D(p)}$$

Where, $N(p)$ and $D(p)$ are polynomials in a complex frequency variable $p = \sigma + j\Omega$. For lossless passive network, the neper frequency is 0 and $p = j\Omega$.

For a given transfer function, the insertion loss response of the filter is given by:

$$L_A(\Omega) = 10 \log \frac{1}{|S_{21}(j\Omega)|^2} \text{dB}$$

2.1.1 Poles and Zeros of Complex Plane:

The (σ, Ω) plane, where a rational transfer function is defined, is called the complex plane or the p-plane. The horizontal axis of this plane is called the real or σ -axis, and the vertical axis is called the imaginary or $j\Omega$ -axis. The values of p at which the function becomes zero are the zeroes of the function, and the values of p at which the function becomes infinite are singularities (usually the poles) of the function. Therefore, the zeroes of $S_{21}(p)$ are the roots of the numerator $N(p)$ and the poles are the roots of denominator $D(p)$.

These poles will be the natural frequencies of the filter whose response is described by $S_{21}(p)$. For the filter to be stable, these frequencies must lie in the left half of the p-plane, or on the imaginary axis. If this were not so, the oscillations would be of exponentially increasing magnitude with respect to time, which is impossible in any passive network.

The poles and zeros of a rational transfer function may be depicted on the p-plane. Based on their locations there are different types of transfer functions which we are going to discuss now.

2.1.2 Butterworth (Maximally Flat) Response:

The amplitude-squared transfer function for Butterworth filters that have an insertion loss $L_{Ar} = 3.01$ dB at the cutoff frequency $\Omega_c = 1$ is given by

$$|S_{21}(j\Omega)|^2 = \frac{1}{1 + \Omega^{2n}}$$

Where n is the degree or the order of filter, which corresponds to the number of reactive elements required in the low pass prototype filter. This type response is also referred to as maximally flat because its amplitude-squared transfer function defined above have the maximum number of $(2n-1)$ zero derivatives at $\Omega=0$. Therefore. The maximally flat approximation to the ideal lowpass filter in the passband is best at $\Omega=0$, but deteriorates as Ω approaches the cutoff frequency Ω_c .

A rational transfer function can be constructed from the above amplitude-squared function:

$$S_{21}(p) = \frac{1}{\prod_{i=1}^n (p - p_i)}$$

with

$$p_i = j \exp \left[\frac{(2i-1)\pi}{2n} \right]$$

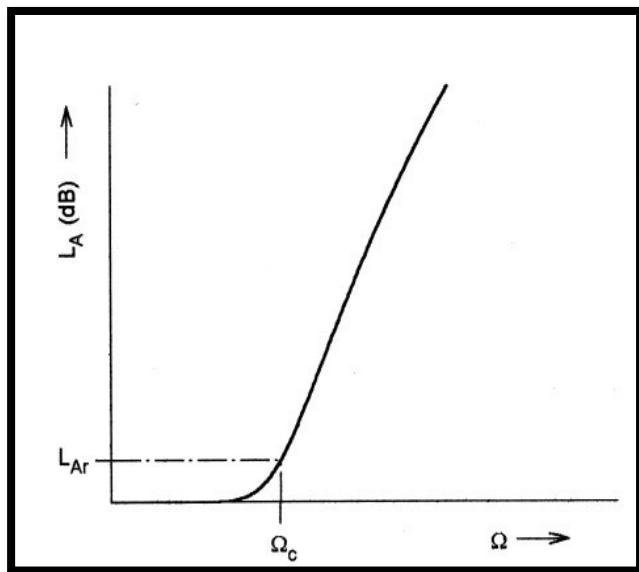


Figure 2.1 Butterworth Filter Response

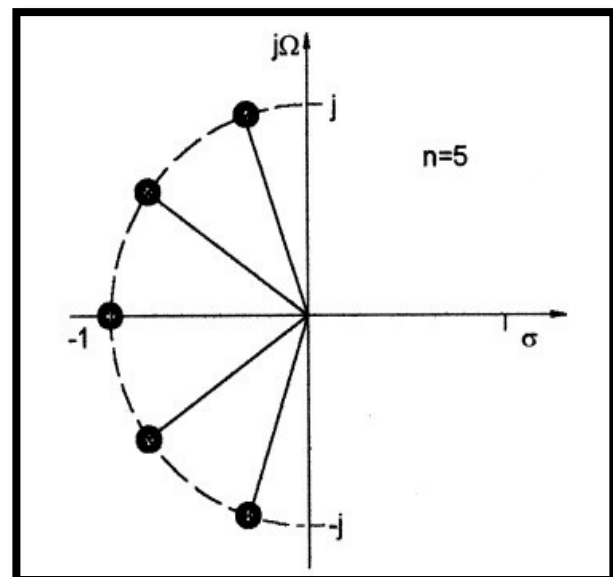


Figure 2.2 Pole Locations for Butterworth Filter Response

2.1.3 Chebyshev Response:

The Chebyshev response that exhibits the equal-ripple passband and maximally flat stopband is shown below. The amplitude-squared transfer function that describes this type of response is

$$|S_{21}(j\Omega)|^2 = \frac{1}{1 + \varepsilon^2 T_n^2(\Omega)}$$

where the ripple constant ε is related to a given passband ripple L_{Ar} in dB by

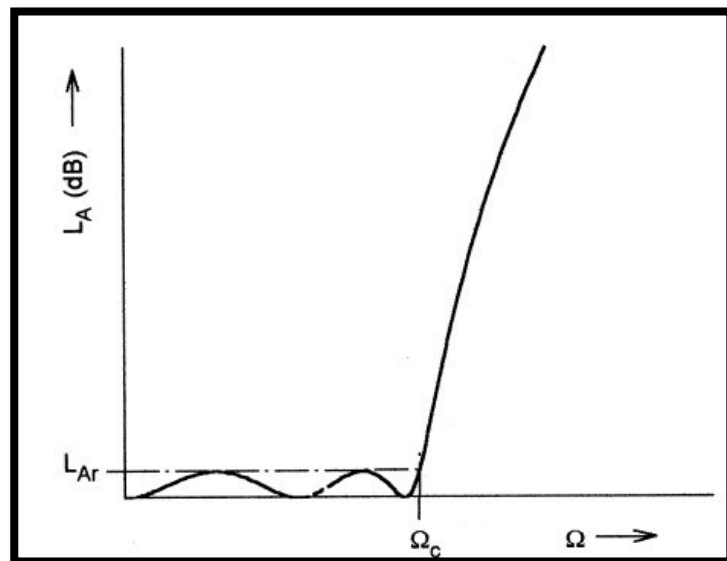


Figure 2.3 Chebyshev Filter Response

$T_n(\Omega)$ is a Chebyshev function of the first kind of order n , which is defined as

$$T_n(\Omega) = \begin{cases} \cos(n \cos^{-1} \Omega) & |\Omega| \leq 1 \\ \cosh(n \cosh^{-1} \Omega) & |\Omega| \geq 1 \end{cases}$$

Hence, the filters realized from these equations are commonly known as Chebyshev filters. General formula of the rational transfer function for the Chebyshev filter is given by

$$S_{21}(p) = \frac{\prod_{i=1}^n [\eta^2 + \sin^2(i\pi/n)]^{1/2}}{\prod_{i=1}^n (p + p_i)}$$

with

$$p_i = j \cos \left[\sin^{-1} j\eta + \frac{(2i-1)\pi}{2n} \right]$$

$$\eta = \sinh \left(\frac{1}{n} \sinh^{-1} \frac{1}{\varepsilon} \right)$$

Like the maximally flat case, all the transmission zeros of $S_{21}(p)$ are located at infinity. Therefore, the Butterworth and Chebyshev filters dealt with so far are sometimes referred to as all-pole filters. However, the pole locations for the Chebyshev case are different, and lie on an ellipse in the left half-plane. The major axis of the ellipse is on the $j\Omega$ -axis and its size is

$\sqrt{1 + \eta^2}$; the minor axis is on the σ -axis and is of the size η . The pole distribution is shown, for $n=5$.

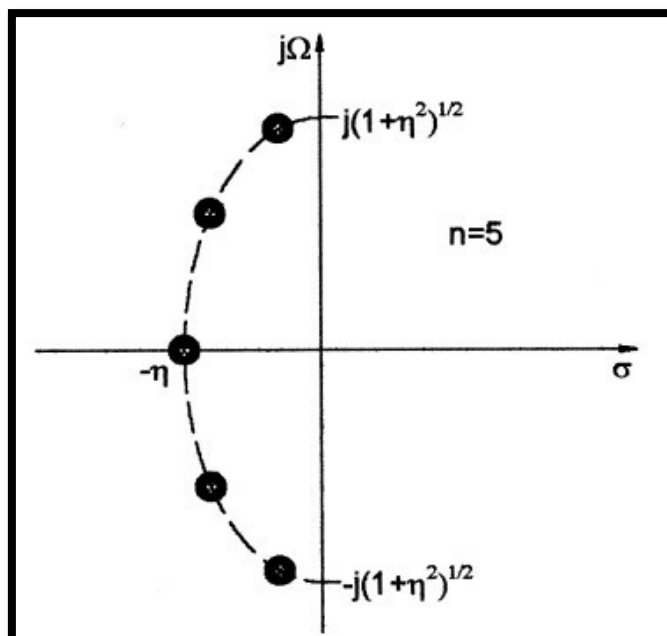


Figure 2.4 Pole Location for Chebyshev Filter Response

2.1.4 Elliptic Function Response:

The response that is equal-ripple in both the passband and stopband is the elliptic function response. The transfer function for this type of response is

$$|S_{21}(j\Omega)|^2 = \frac{1}{1 + \varepsilon^2 F_n^2(\Omega)}$$

with

$$F_n(\Omega) = \begin{cases} M \frac{\prod_{i=1}^{n/2} (\Omega_i^2 - \Omega^2)}{\prod_{i=1}^{n/2} (\Omega_s^2/\Omega_i^2 - \Omega^2)} & \text{for } n \text{ even} \\ N \frac{\Omega \prod_{i=1}^{(n-1)/2} (\Omega_i^2 - \Omega^2)}{\prod_{i=1}^{(n-1)/2} (\Omega_s^2/\Omega_i^2 - \Omega^2)} & \text{for } n (\geq 3) \text{ odd} \end{cases}$$

Where Ω_i ($0 < \Omega_i < 1$) and $\Omega_s > 1$ represents some critical frequencies; M and N are constants.

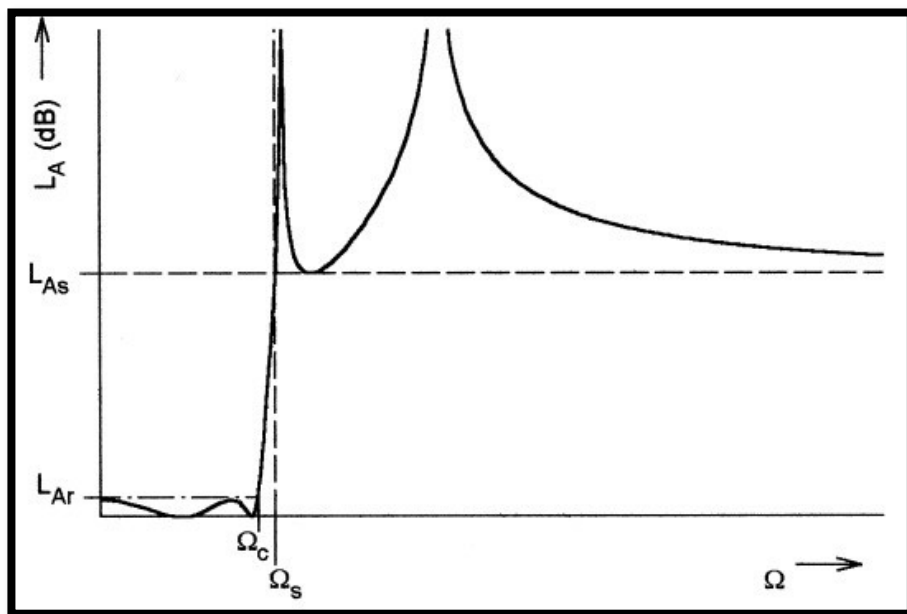


Figure 2.5 Elliptic Filter Response

2.1.5 Gaussian (Maximally Flat Group-Delay) Response:

The Gaussian response is approximated by a rational transfer function

$$S_{21}(p) = \frac{a_0}{\sum_{k=0}^n a_k p^k}$$

Where $p=\sigma+j\Omega$ is the normalized complex frequency variable, and the coefficients

$$a_k = \frac{(2n-k)!}{2^{n-k} k! (n-k)!}$$

This transfer function possesses a group delay that has maximum possible number of zero derivatives with respect to Ω at $\Omega = 0$, which is why it is said to have maximally flat group delay around $\Omega = 0$ and is in a sense complementary to the Butterworth response, which has a maximally flat amplitude. The filters of this type are also known as Bessel filters.

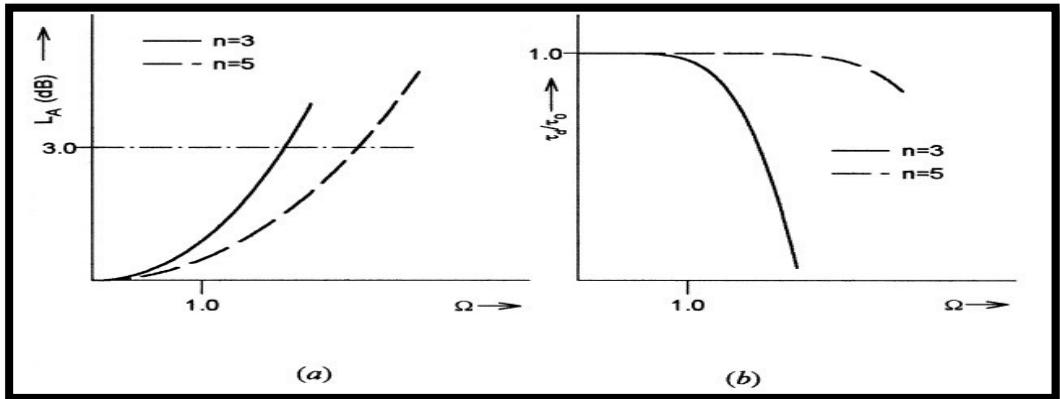


Figure 2.6 Gaussian Filter Response (a) Amplitude (b) Phase Delay

2.2 Low pass Prototype Filters and Elements

Filter syntheses for realizing the transfer functions that are discussed above, usually result in the so-called low pass prototype filters. A low pass prototype filter is in general defined as the low pass filter whose element values are normalized to make the source resistance or conductance equal to one denoted by $g_0 = 1$, and the cut-off angular frequency to be unity, denoted by $\Omega_c = 1$ (rad/s). This type of low pass filter can serve as a prototype for designing many practical filters with frequency and element transformations. This will be addressed in the next section. Below are the prototype filters for different type of filter responses.

2.2.1 Butterworth Low Pass Prototype Filters

For Butterworth or maximally flat low pass prototype filters having a transfer function given above with an insertion loss $L_{Ar} = 3.01$ dB at the cut-off $\Omega_c = 1$, the element values may be computed by

$$g_0 = 1.0$$

$$g_i = 2 \sin\left(\frac{(2i-1)\pi}{2n}\right) \quad \text{for } i = 1 \text{ to } n$$

$$g_{n+1} = 1.0$$

As can be seen, the two-port Butterworth filters considered here are always symmetrical in network structure, namely, $g_0 = g_{n+1}$, $g_1 = g_n$ and so on.

To determine the degree of a Butterworth low pass prototype, a specification that is usually the minimum stopband attenuation L_{As} dB at $\Omega = \Omega_s$ for $\Omega_s > 1$ is given. Hence

$$n \geq \frac{\log(10^{0.1L_{AS}} - 1)}{2\log\Omega_s}$$

2.2.2 Chebyshev Low Pass Prototype Filters

For Chebyshev low pass prototype filters having a transfer function given earlier with a passband ripple L_{Ar} dB and the cutoff frequency $\Omega_c = 1$, the element values for the two-port networks may be computed using the following formulas:

$$g_0 = 1.0$$

$$g_1 = \frac{2}{\gamma} \sin\left(\frac{\pi}{2n}\right)$$

$$g_i = \frac{1}{g_{i-1}} \frac{4 \sin\left[\frac{(2i-1)\pi}{2n}\right] \cdot \sin\left[\frac{(2i-3)\pi}{2n}\right]}{\gamma^2 + \sin^2\left[\frac{(i-1)\pi}{n}\right]} \quad \text{for } i = 2, 3, \dots, n$$

$$g_{n+1} = \begin{cases} 1.0 & \text{for } n \text{ odd} \\ \coth^2\left(\frac{\beta}{4}\right) & \text{for } n \text{ even} \end{cases}$$

where

$$\beta = \ln\left[\coth\left(\frac{L_{Ar}}{17.37}\right)\right]$$

$$\gamma = \sinh\left(\frac{\beta}{2n}\right)$$

For the required passband ripple L_{Ar} dB, the minimum stopband attenuation L_{As} dB at $\Omega = \Omega_s$, the degree of a Chebyshev low pass prototype, which will meet this specification, can be found by

$$n \geq \frac{\cosh^{-1} \sqrt{\frac{10^{0.1L_{As}} - 1}{10^{0.1L_{Ar}} - 1}}}{\cosh^{-1} \Omega_s}$$

Sometimes, the minimum return loss L_R or the maximum voltage standing wave ratio VSWR in the passband is specified instead of the passband ripple L_{Ar} . If the return loss is defined and the minimum passband return loss is L_R dB ($L_R < 0$), the corresponding passband ripple is

$$L_{Ar} = -10 \log(1 - 10^{0.1L_R}) \text{ dB}$$

2.2.3 Elliptic Function Low Pass Prototype Filters

Figure 1.7 illustrates two commonly used network structures for elliptic function low pass prototype filters. In Figure 1.7(a), the series branches of parallel-resonant circuits are introduced for realizing the finite-frequency transmission zeros, since they block transmission by having infinite series impedance (open-circuit) at resonance. For this form of the elliptic function low pass prototype [Figure 1.7(a)], g_i for odd i ($i = 1, 3, \dots$) represent the capacitance of a shunt capacitor, g_i for even i ($i = 2, 4, \dots$) represent the inductance of an inductor, and the primed g'_i for even i ($i = 2, 4, \dots$) are the capacitance of a capacitor in a series branch of parallel-resonant circuit. For the dual realization form in Figure 1.7(b), the shunt branches of series-resonant circuits are used for implementing the finite-frequency transmission zeros, since they short out transmission at resonance. In this case, referring to Figure 1.7(b), g_i for odd i ($i = 1, 3, \dots$) are the inductance of a series inductor, g_i for even i ($i = 2, 4, \dots$) are the capacitance of a capacitor, and primed g'_i for even i ($i = 2, 4, \dots$) indicate the inductance of an inductor in a shunt branch of series-resonant circuit. Again, either form may be used, because both give the same response.

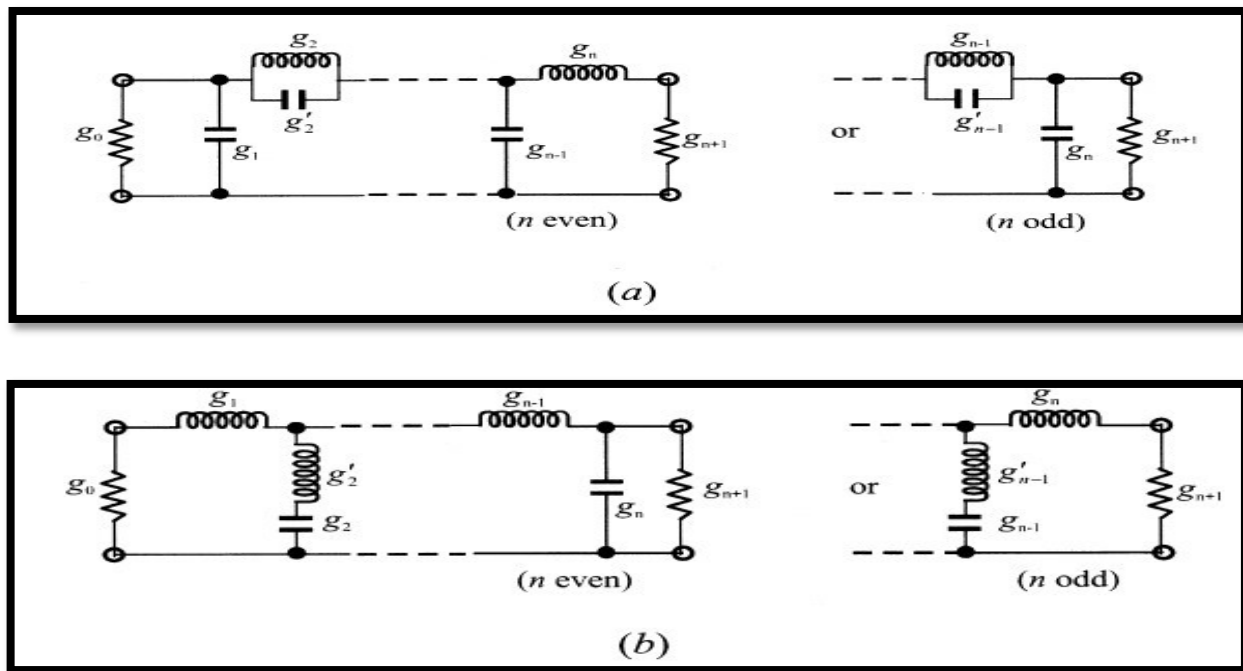


Figure 2.7 Lowpass prototype filters for elliptic function filters with (a) series parallel-resonant

Unlike the Butterworth and Chebyshev low pass prototype filters, there is no simple formula available for determining element values of the elliptic function low pass prototype filters.

2.3 Frequency and Element Transformations

So far, we have only considered the low pass prototype filters, which have a normalized source resistance/conductance $g_0 = 1$ and a cut-off frequency $\Omega_c = 1$. To obtain frequency characteristics and element

values for practical filters based on the low pass prototype, one may apply frequency and element transformations, which will be addressed in this section.

The frequency transformation, which is also referred to as frequency mapping, is required to map a response such as Chebyshev response in the low pass prototype frequency domain ω to that in the frequency domain Ω in which a practical filter response such as low pass, high pass, band pass, and band stop are expressed. The frequency transformation will influence all the reactive elements accordingly, but no effect on the resistive elements. In addition to the frequency mapping, impedance scaling is also required to accomplish the element transformation. The impedance scaling will remove the $g_0 = 1$ normalization and adjust the filter to work for any value of the source impedance denoted by Z_0 . For our formulation, it is convenient to define an impedance scaling factor γ_0 as

$$\gamma_0 = \begin{cases} Z_0/g_0 & \text{for } g_0 \text{ being the resistance} \\ g_0/Y_0 & \text{for } g_0 \text{ being the conductance} \end{cases}$$

where $Y_0 = 1/Z_0$ is the source admittance. In principle, applying the impedance scaling upon a filter network in such a way that has no effect on the response shape.

$$L \rightarrow \gamma_0 L \quad R \rightarrow \gamma_0 R$$

$$C \rightarrow C/\gamma_0 \quad G \rightarrow G/\gamma_0$$

Let g be the generic term for the low pass prototype elements in the element transformation to be discussed. Because it is independent of the frequency transformation, the following resistive element transformation holds for any type of filter:

$$R = \gamma_0 g \quad \text{for } g \text{ representing the resistance}$$

$$G = \frac{g}{\gamma_0} \quad \text{for } g \text{ representing the conductance}$$

2.3.1 Low pass Transformation

The frequency transformation from a low pass prototype to a practical low pass filter having a cut-off frequency ω_c in the angular frequency axis ω is simply given by

$$\Omega = \left(\frac{\Omega_c}{\omega_c} \right) \omega$$

Applying the above formula together with the impedance scaling described earlier yields the element transformation:

$$L = \left(\frac{\Omega_c}{\omega_c} \right) \gamma_0 g \quad \text{for } g \text{ representing the inductance}$$

$$C = \left(\frac{\Omega_c}{\omega_c} \right) \frac{g}{\gamma_0} \quad \text{for } g \text{ representing the capacitance}$$

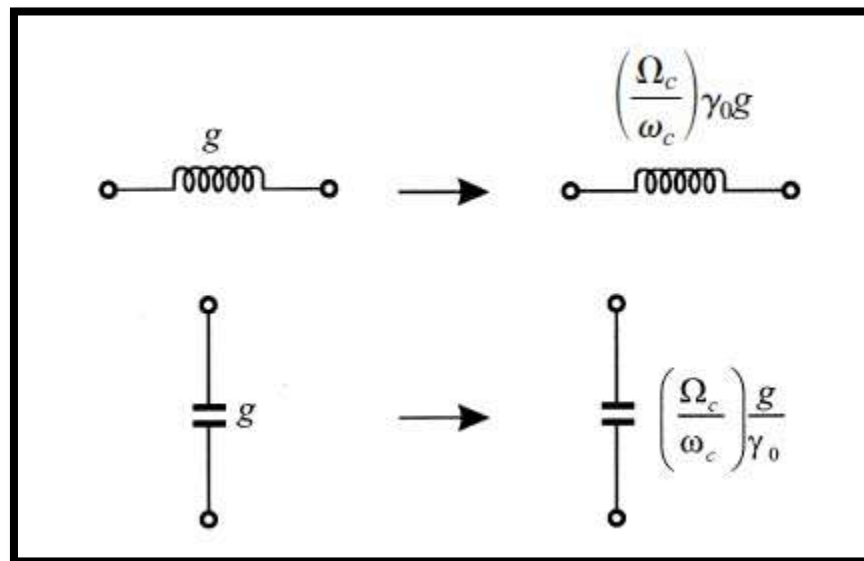


Figure 2.8 Lowpass prototype to lowpass transformation for basic elements

2.3.2 High pass Transformation

For high pass filters with a cut-off frequency ω_c in the ω -axis, the frequency transformation is

$$\Omega = - \frac{\omega_c \Omega_c}{\omega}$$

Applying this frequency transformation to a reactive element g in the low pass prototype leads to

$$j\Omega g \rightarrow \frac{\omega_c \Omega_c g}{j\omega}$$

It is then obvious that an inductive/capacitive element in the low pass prototype will be inversely transformed to a capacitive/inductive element in the high pass filter. With impedance scaling, the element transformation is given by

$$C = \left(\frac{1}{\omega_c \Omega_c} \right) \frac{1}{\gamma_0 g} \quad \text{for } g \text{ representing the inductance}$$

$$L = \left(\frac{1}{\omega_c \Omega_c} \right) \frac{\gamma_0}{g} \quad \text{for } g \text{ representing the capacitance}$$

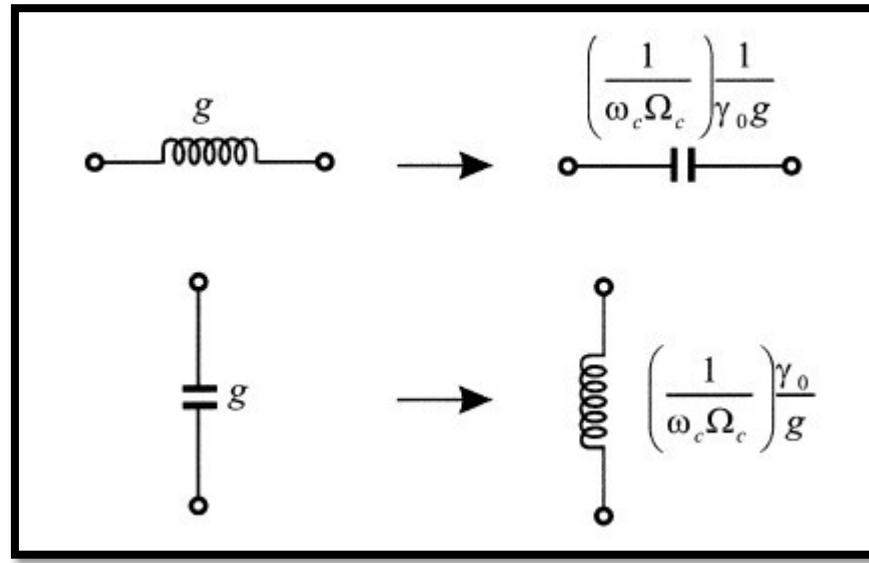


Figure 2.9 Low pass prototype to high pass transformation for basic element transformation

2.3.3 Band pass Transformation

Assume that a low pass prototype response is to be transformed to a band pass response having a passband $\omega_2 - \omega_1$, where ω_1 and ω_2 indicate the passband-edge angular frequency. The required frequency transformation is

$$\Omega = \frac{\Omega_c}{FBW} \left(\frac{\omega}{\omega_0} - \frac{\omega_0}{\omega} \right)$$

with

$$FBW = \frac{\omega_2 - \omega_1}{\omega_0}$$

$$\omega_0 = \sqrt{\omega_1 \omega_2}$$

where ω_0 denotes the center angular frequency and FBW is defined as the fractional bandwidth. If we apply this frequency transformation to a reactive element g of the low pass prototype, we have

$$j\Omega g \rightarrow j\omega \frac{\Omega_c g}{FBW \omega_0} + \frac{1}{j\omega} \frac{\Omega_c \omega_0 g}{FBW}$$

which implies that an g in the low pass prototype will transform to a inductive/capacitive element series/parallel LC resonant circuit in the band pass filter. The elements for the series LC resonator in the band pass filter are

$$L_s = \left(\frac{\Omega_c}{FBW\omega_0} \right) \gamma_0 g$$

for g representing the inductance

$$C_s = \left(\frac{FBW}{\omega_0 \Omega_c} \right) \frac{1}{\gamma_0 g}$$

Where the impedance scaling has been considered as well. Similarly, the elements for the parallel LC resonator in the band pass filter are

$$C_p = \left(\frac{\Omega_c}{FBW\omega_0} \right) \frac{g}{\gamma_0}$$

for g representing the capacitance

$$L_p = \left(\frac{FBW}{\omega_0 \Omega_c} \right) \frac{\gamma_0}{g}$$

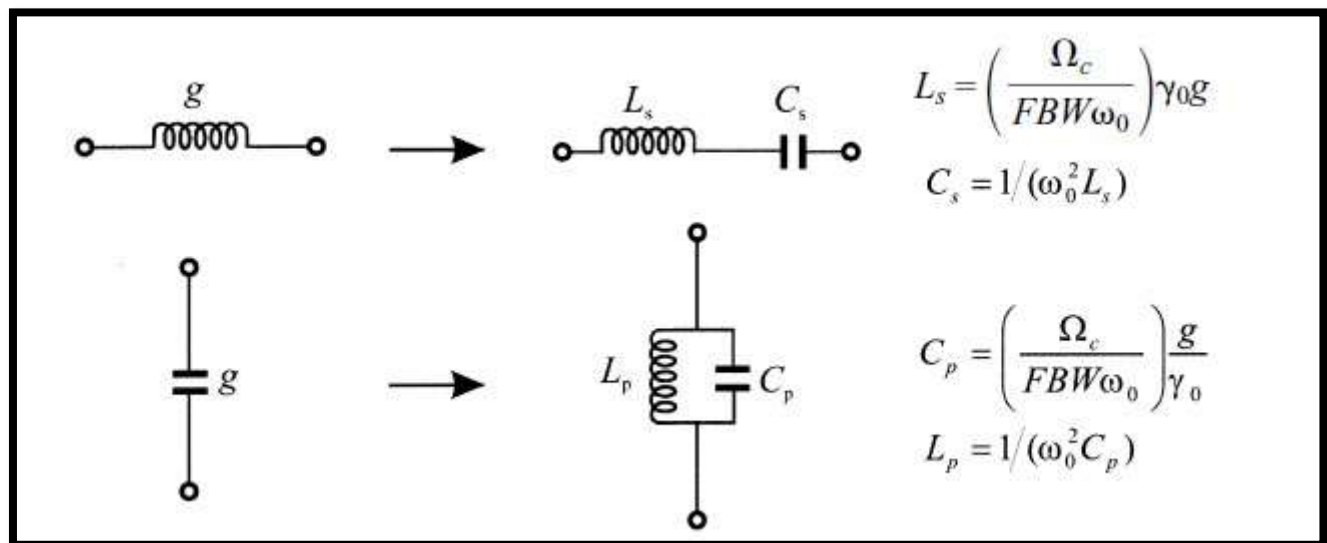


Figure 2.10 Lowpass prototype to bandpass transformation for basic element transformation

2.3.4 Band stop Transformation

The frequency transformation from low pass prototype to band stop is achieved by the frequency mapping

$$\Omega = \frac{\Omega_c FBW}{(\omega_0/\omega - \omega/\omega_0)}$$

$$\omega_0 = \sqrt{\omega_1\omega_2}$$

$$FBW = \frac{\omega_2 - \omega_1}{\omega_0}$$

where $\omega_2 - \omega_1$ is the bandwidth. This form of the transformation is opposite to the band pass transformation in that an inductive/capacitive element g in the low pass prototype will transform to a parallel/series LC resonant circuit in the band stop filter. The elements for the LC resonators transformed to the band stop filter are

$$C_p = \left(\frac{1}{FBW\omega_0\Omega_c} \right) \frac{1}{\gamma_0 g}$$

for g representing the inductance

$$L_p = \left(\frac{\Omega_c FBW}{\omega_0} \right) \gamma_0 g$$

$$L_s = \left(\frac{1}{FBW\omega_0\Omega_c} \right) \frac{\gamma_0}{g}$$

for g representing the capacitance

$$C_s = \left(\frac{\Omega_c FBW}{\omega_0} \right) \frac{g}{\gamma_0}$$

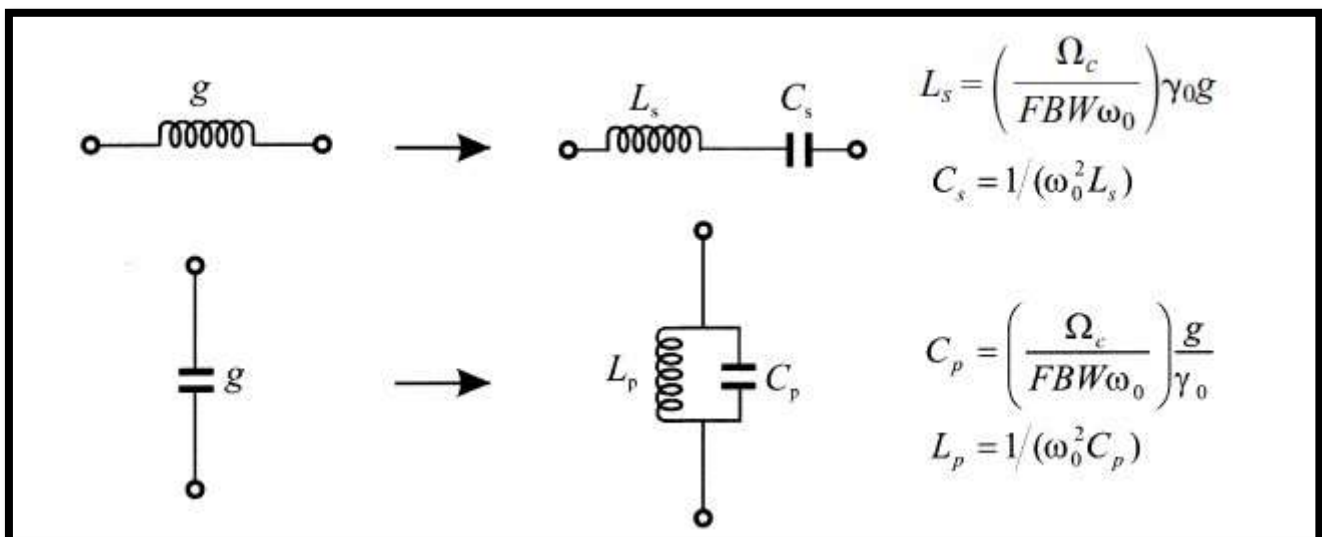


Figure 2.11 Lowpass prototype to bandpass transformation for basic element transformation

2.4 Filter Design by The Insertion Loss Method

A perfect filter would have zero insertion loss in the passband, infinite attenuation in the stopband, and a linear phase response (to avoid signal distortion) in the passband. Of course, such filters do not exist in practice, so compromises must be made; herein lies the art of filter design. The image parameter method of the previous section may yield a usable filter response for some applications, but there is no methodical way of improving the design. The insertion loss method, however, allows a high degree of control over the passband and stopband amplitude and phase characteristics, with a systematic way to synthesize a desired response. The necessary design trade-offs can be evaluated to best meet the application requirements. If, for example, a minimum insertion loss is most important, a binomial response could be used; a Chebyshev response would satisfy a requirement for the sharpest cut-off. If it is possible to sacrifice the attenuation rate, a better phase response can be obtained by using a linear phase filter design. In addition, in all cases, the insertion loss method allows filter performance to be improved in a straightforward manner, at the expense of a higher order filter. For the filter prototypes to be discussed below, the order of the filter is equal to the number of reactive elements.

Characterisation by Power Loss Ratio:

In the insertion loss method, a filter response is defined by its insertion loss, or *power loss ratio*, P_{LR} :

$$P_{LR} = \frac{\text{Power available from source}}{\text{Power delivered to load}} = \frac{P_{inc}}{P_{load}} = \frac{1}{1 - |\Gamma(\omega)|^2}.$$

Observe that this quantity is the reciprocal of $|S_{21}|^2$ if both load and source are matched. The insertion loss (IL) in dB is given by:

$$\text{IL} = 10 \log P_{LR}$$

2.5 Filter Implementation

The lumped-element filter designs discussed in the previous sections generally work well at low frequencies, but two problems arise at higher RF and microwave frequencies. First, lumped-element inductors and capacitors are generally available only for a limited range of values, and can be difficult to implement at microwave frequencies. Distributed elements, such as open-circuited or short-circuited transmission line stubs, are often used to approximate ideal lumped elements. In addition, at microwave frequencies the distances between filter components is not negligible. The first problem is treated with Richards' transformation, which can be used to convert lumped elements to transmission line sections. Kuroda's identities can then be used to physically separate filter elements by using transmission line sections. Because such additional transmission line sections do not affect the filter response, this type of design is called redundant filter synthesis. It is possible to design microwave filters that take advantage of these sections to improve the filter response; such no redundant synthesis does not have a lumped-element counterpart.

2.5.1 Richards' Transformation

The transformation

$$\Omega = \tan \beta \ell = \tan \left(\frac{\omega \ell}{v_p} \right)$$

maps the ω plane to the Ω plane, which repeats with a period of $\omega l / v_p = 2\pi$. This transformation was introduced by P. Richards to synthesize an LC network using open- and short-circuited transmission line stubs. Thus, if we replace the frequency variable ω with, we can write the reactance of an inductor as

$$jX_L = j\Omega L = jL \tan \beta \ell,$$

and the susceptance of a capacitor as

$$jB_C = j\Omega C = jC \tan \beta \ell$$

These results indicate that an inductor can be replaced with a short-circuited stub of length β and characteristic impedance L , while a capacitor can be replaced with an open-circuited stub of length β and characteristic impedance $1/C$. A unity filter impedance is assumed. Cutoff occurs at unity frequency for a low-pass filter prototype; to obtain the same cutoff frequency for the Richards'-transformation filter, shows that

$$\Omega = 1 = \tan \beta \ell,$$

which gives a stub length of $= \lambda/8$, where λ is the wavelength of the line at the cutoff frequency, ω_c . At the frequency $\omega_0 = 2\omega_c$, the lines will be $\lambda/4$ long, and an attenuation pole will occur. At frequencies away from ω_c , the impedances of the stubs will no longer match the original lumped-element impedances, and the filter response will differ from the desired prototype response. In addition, the response will be periodic in frequency, repeating every $4\omega_c$. In principle, then, Richards' transformation allows the inductors and capacitors of a lumpedelement filter to be replaced with short-circuited and open-circuited transmission line stubs, as illustrated in Figure 1.12. Since the electrical lengths of all the stubs are the same ($\lambda/8$ at ω_c), these lines are called commensurate lines.

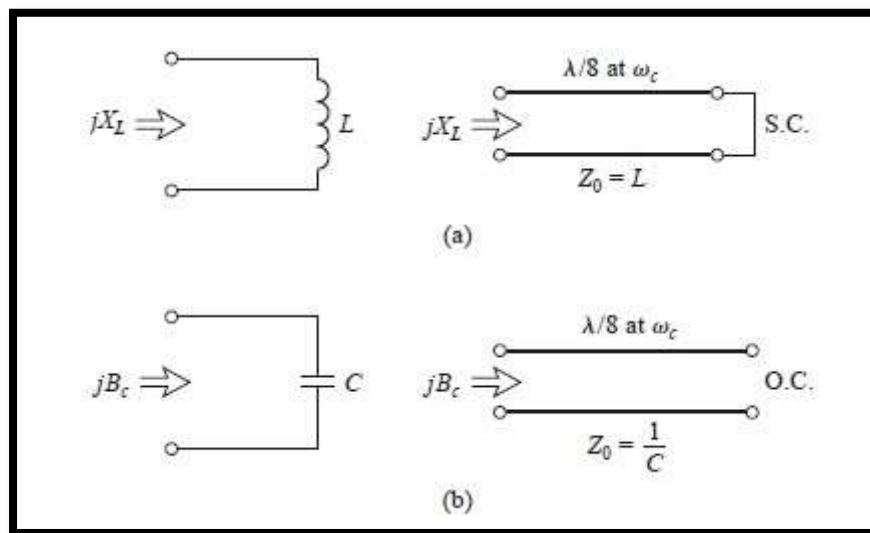


Figure 2.12 Richards' Transformation (a) For inductor to a short-circuited stub (b) For a capacitor to an open-circuited stub

2.5.2 Kuroda's Identities

The four Kuroda identities use redundant transmission line sections to achieve a more practical microwave filter implementation by performing any of the following operations:

- Physically separate transmission line stubs
- Transform series stubs into shunt stubs, or vice versa
- Change impractical characteristic impedance into more realizable values

The additional transmission line sections are called unit elements and are $\lambda/8$ long at ω_c ; the unit elements are thus commensurate with the stubs used to implement the inductors and capacitors of the prototype design. The four Kuroda identities are illustrated in the following table, where each box represents a unit element, or transmission line, of the indicated characteristic impedance and length ($\lambda/8$ at ω_c). The inductors and capacitors represent shortcircuit and open-circuit stubs, respectively.

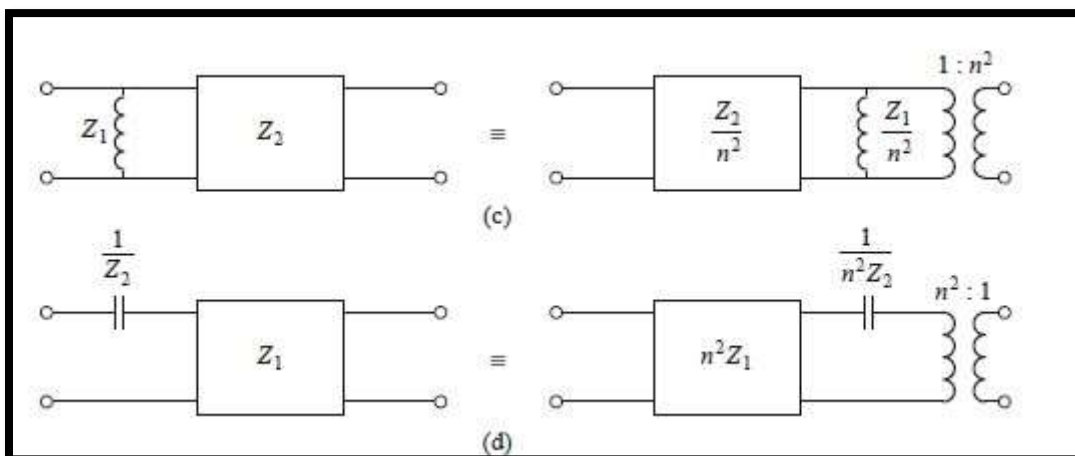
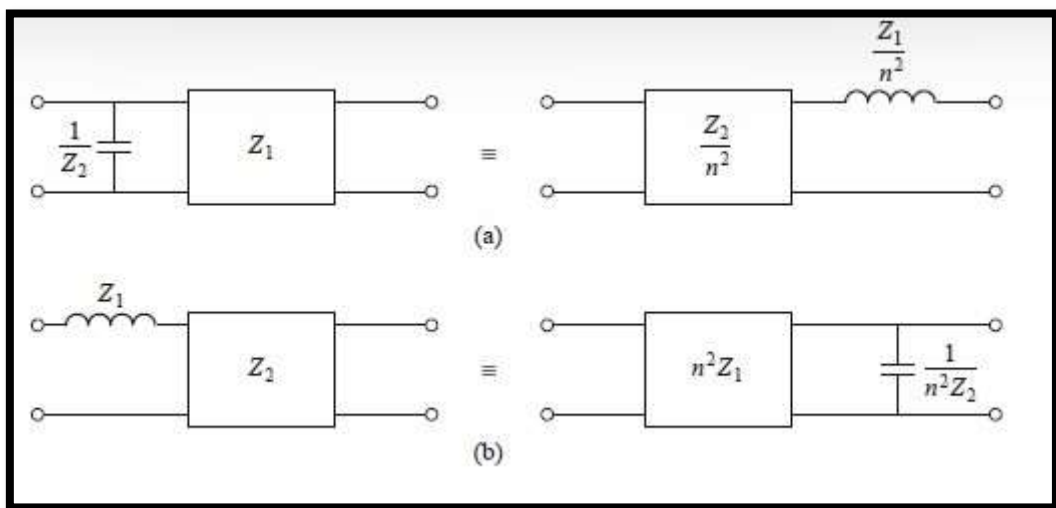


Figure 2.13 The four Kuroda Identities

The following graph shows the response of a low-pass filter response with a cut-off at 4Ghz and impedance of 50Ω , designed using both lumped and distributed elements.

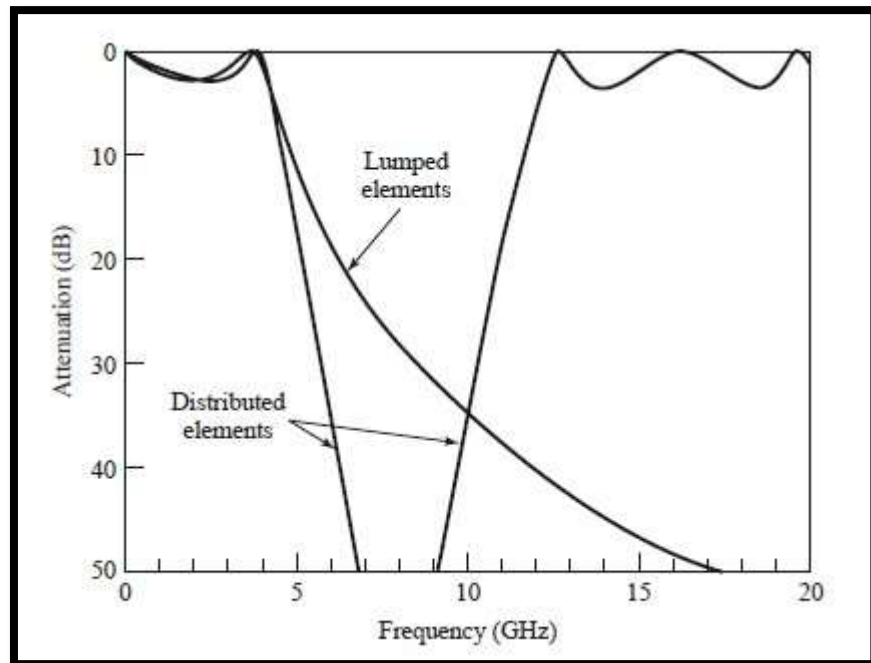


Figure 2.14 Filter Response for both lumped and distributed elements

As we can see, even though the passband characteristics are very similar up to 4Ghz, but the distributed-element filter has a sharper cutoff. Also, the response of distributed-element filter repeats every 16Ghz, because of the periodicity of Richards' transformation.

2.5.3 Impedance and Admittance Inverters

As we have seen, it is often desirable to use only series, or only shunt, elements when implementing a filter with a particular type of transmission line. The Kuroda identities can be used for conversions of this form, but another possibility is to use impedance (K) or admittance (J) inverters. Such inverters are especially useful for bandpass or bandstop filters with narrow ($<10\%$) bandwidths. The conceptual operation of impedance and admittance inverters is illustrated in Figure 8.38; since these inverters essentially form the inverse of the load impedance or admittance, they can be used to transform series-connected elements to shunt connected elements, or vice versa.

CHAPTER-3: TRANSMISSION LINES AND COMPONENTS

In this chapter, basic concepts, and design equations for micro strip lines, coupled micro strip lines, discontinuities, and components useful for design of filters are briefly described.

3.1 Micro strip Lines

3.1.1 Micro strip Structure

The general structure of a micro strip is illustrated in Figure 2.1. A conducting strip (micro strip line) with a width W and a thickness t is on the top of a dielectric substrate that has a relative dielectric constant ϵ_r and a thickness h , and the bottom of the substrate is a ground (conducting) plane.

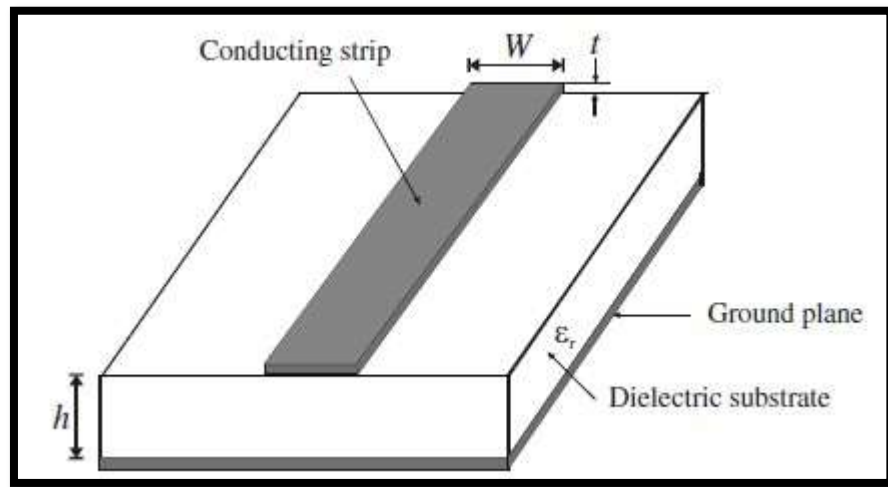


Figure 3.1 General Microstrip Structure

3.1.2 Waves in Micro strips

The fields in the micro strip extend within two media—air above and dielectric below—so that the structure is inhomogeneous. Due to this inhomogeneous nature, the micro strip does not support a pure TEM wave. This is because that a pure TEM wave has only transverse components, and its propagation velocity depends only on the material properties, namely the permittivity ϵ and the permeability μ . However, with the presence of the two guided-wave media (the dielectric substrate and the air), the waves in a micro strip line will have no vanished longitudinal components of electric and magnetic fields, and their propagation velocities will depend not only on the material properties, but also on the physical dimensions of the micro strip.

3.1.3 Quasi-TEM Approximation

When the longitudinal components of the fields for the dominant mode of a micro strip line remain very much smaller than the transverse components, they may be neglected. In this case, the dominant mode then behaves like a TEM mode, and the TEM transmission line theory is applicable for the micro strip line as well. This is called the quasi-TEM approximation and it is valid over most of the operating frequency ranges of micro strip.

3.1.4 Effective Dielectric Constant and Characteristic Impedance

In the quasi-TEM approximation, a homogeneous dielectric material with an effective dielectric permittivity replaces the inhomogeneous dielectric-air media of micro strip. Transmission characteristics of micro strips are described by two parameters, namely, the effective dielectric constant ϵ_{re} and characteristic impedance Z_c , which may then be obtained by quasistatic analysis [1]. In quasi-static analysis, the fundamental mode of wave propagation in a micro strip is assumed to be pure TEM. The above two parameters of micro strips are then determined from the values of two capacitances as follows

$$\epsilon_{re} = \frac{C_d}{C_a}$$

$$Z_c = \frac{1}{c\sqrt{C_a C_d}}$$

in which C_d is the capacitance per unit length with the dielectric substrate present, C_a is the capacitance per unit length with the dielectric substrate replaced by air, and c is the velocity of electromagnetic waves in free space ($c = 3.0 \times 10^8$ m/s). For very thin conductors (i.e., $t > 0$), the closed-form expressions that provide an accuracy better than 1% are given as follows:

$$\epsilon_{re} = \frac{\epsilon_r + 1}{2} + \frac{\epsilon_r - 1}{2} \left[\left(1 + 12 \frac{h}{W} \right)^{-0.5} + 0.04 \left(1 - \frac{W}{h} \right)^2 \right]$$

$$Z_c = \frac{\eta}{2\pi\sqrt{\epsilon_{re}}} \ln \left(\frac{8h}{W} + 0.25 \frac{W}{h} \right)$$

where $\eta = 120\pi$ ohms is the wave impedance in free space. For $W/h \geq 1$:

$$\epsilon_{re} = \frac{\epsilon_r + 1}{2} + \frac{\epsilon_r - 1}{2} \left(1 + 12 \frac{h}{W} \right)^{-0.5}$$

$$Z_c = \frac{\eta}{\sqrt{\epsilon_{re}}} \left\{ \frac{W}{h} + 1.393 + 0.677 \ln \left(\frac{W}{h} + 1.444 \right) \right\}^{-1}$$

3.1.5 Guided Wavelength, Propagation Constant, Phase Velocity, and Electrical Length

Once the effective dielectric constant of a microstrip is determined, the guided wavelength of the quasi-TEM mode of microstrip is given by

$$\lambda_g = \frac{\lambda_0}{\sqrt{\epsilon_{re}}}$$

where λ_0 is the free space wavelength at operation frequency f . More conveniently, where the frequency is given in gigahertz (GHz), the guided wavelength can be evaluated directly in millimetres as follows:

$$\lambda_g = \frac{300}{f(\text{GHz})\sqrt{\epsilon_{re}}} \text{ mm}$$

The associated propagation constant β and phase velocity v_p can be determined by

$$\beta = \frac{2\pi}{\lambda_g}$$

$$v_p = \frac{\omega}{\beta} = \frac{c}{\sqrt{\epsilon_r}}$$

where c is the velocity of light in free space. The electrical length θ for a given physical length l of the microstrip is defined by

$$\theta = \beta l$$

Therefore $= \pi/2$ when $l = \lambda_g/4$, and $\theta = \pi$ when $l = \lambda_g/2$. These so-called quarter wavelength and half-wavelength micro strip lines are important for design of micro strip filters.

3.1.6 Synthesis of W/h

Approximate expressions for W/h in terms of Z_c and ϵ_r are given as follows:

For $W/h \leq 2$

$$\frac{W}{h} = \frac{8 \exp(A)}{\exp(2A) - 2}$$

with

$$A = \frac{Z_c}{60} \left\{ \frac{\epsilon_r + 1}{2} \right\}^{0.5} + \frac{\epsilon_r - 1}{\epsilon_r + 1} \left\{ 0.23 + \frac{0.11}{\epsilon_r} \right\}$$

and for $W/h \geq 2$

$$\frac{W}{h} = \frac{2}{\pi} \left\{ (B - 1) - \ln(2B - 1) + \frac{\epsilon_r - 1}{2\epsilon_r} \left[\ln(B - 1) + 0.39 - \frac{0.61}{\epsilon_r} \right] \right\}$$

with

$$B = \frac{60\pi^2}{Z_c \sqrt{\epsilon_r}}$$

These expressions also provide accuracy better than 1%. If more accurate values are needed, an iterative or optimization process based on the more accurate analysis models can be employed.

3.1.7 Effect of Strip Thickness

So far, we have not considered the effect of conducting strip thickness t (as referring to Figure 2.1). The thickness t is usually very small when the micro strip line is realized by conducting thin films; therefore, its effect may quite often be neglected. Nevertheless, its effect on the characteristic impedance and effective dielectric constant may be included

For $W/h \leq 1$:

$$Z_c(t) = \frac{\eta}{2\pi\sqrt{\epsilon_{re}}} \ln \left\{ \frac{8}{W_e(t)/h} + 0.25 \frac{W_e(t)}{h} \right\}$$

For $W/h \geq 1$:

$$Z_c(t) = \frac{\eta}{\sqrt{\epsilon_{re}}} \left\{ \frac{W_e(t)}{h} + 1.393 + 0.667 \ln \left(\frac{W_e(t)}{h} + 1.444 \right) \right\}$$

where

$$\frac{W_e(t)}{h} = \begin{cases} \frac{W}{h} + \frac{1.25}{\pi} \frac{t}{h} \left(1 + \ln \frac{4\pi W}{t} \right) & (W/h \leq 0.5\pi) \\ \frac{W}{h} + \frac{1.25}{\pi} \frac{t}{h} \left(1 + \ln \frac{2h}{t} \right) & (W/h \geq 0.5\pi) \end{cases}$$

$$\epsilon_{re}(t) = \epsilon_{re} - \frac{\epsilon_r - 1}{4.6} \frac{t/h}{\sqrt{W/h}}$$

In the above expressions, ϵ_{re} is the effective dielectric constant for $t = 0$. It can be observed that the effect of strip thickness on both the characteristic impedance and effective dielectric constant is insignificant for small values of t/h . However, the effect of strip thickness is significant for conductor loss of the micro strip line.

3.2 Microstrip Discontinuities

Microstrip discontinuities commonly encountered in the layout of practical filters include steps, open-ends, bends, gaps, and junctions. Figure 4.4 illustrates some typical structures and their equivalent circuits. The effects of discontinuities can be more accurately modelled and considered in the filter designs with full-wave electromagnetic (EM) simulations, which will be addressed in due course later. Nevertheless, closed-form expressions for equivalent circuit models of these discontinuities are still useful whenever they are appropriate. These expressions are used in many circuit analysis programs. There are numerous closed form expressions for microstrip discontinuities available, for convenience some typical ones are given as follows.

3.2.1 Steps in Width

For a symmetrical step, the capacitance and inductances of the equivalent circuit indicated below may be approximated by the following formulation

$$C = 0.00137h \frac{\sqrt{\epsilon_{rel}}}{Z_{c1}} \left(1 - \frac{W_2}{W_1}\right) \left(\frac{\epsilon_{rel} + 0.3}{\epsilon_{rel} - 0.258}\right) \left(\frac{W_1/h + 0.264}{W_1/h + 0.8}\right) (\text{pF})$$

$$L_1 = \frac{L_{w1}}{L_{w1} + L_{w2}} L, \quad L_2 = \frac{L_{w2}}{L_{w1} + L_{w2}} L$$

with

$$L_{wi} = Z_{ci} \sqrt{\epsilon_{rei}} / c$$

$$L = 0.000987h \left(1 - \frac{Z_{c1}}{Z_{c2}} \sqrt{\frac{\epsilon_{rel}}{\epsilon_{re2}}}\right)^2 (\text{nH})$$

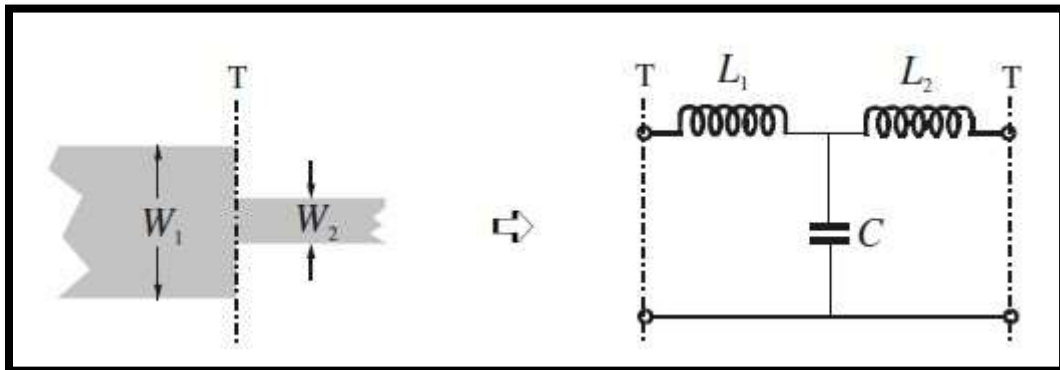


Figure 3.2 Microstrip Discontinuity (Steps in Width)

where L_{wi} for $i = 1, 2$ are the inductances per unit length of the appropriate micro strips, having widths W_1 and W_2 , respectively. While Z_{ci} and ϵ_{rei} denote the characteristic impedance and effective dielectric constant corresponding to width W_i , c is the light velocity in free space, and h is the substrate thickness in micrometres.

3.2.2 Open Ends

At the open end of a micro strip line with a width of W , the fields do not stop abruptly but extend slightly further because of the fringing field. This effect can be modelled either with an equivalent shunt capacitance C_p or with an equivalent length of transmission line Δl , as shown in the following figure. The equivalent length is usually more convenient for filter design. The relation between the two equivalent parameters may be found by

$$\Delta l = \frac{c Z_c C_p}{\sqrt{\epsilon_r}}$$

Where c is the light velocity in free space. A closed-form expression for $\Delta l/h$ is given by

$$\frac{\Delta l}{h} = \frac{\xi_1 \xi_3 \xi_5}{\xi_4}$$

where

$$\begin{aligned}\xi_1 &= 0.434907 \frac{\varepsilon_{re}^{0.81} + 0.26(W/h)^{0.8544} + 0.236}{\varepsilon_{re}^{0.81} - 0.189(W/h)^{0.8544} + 0.87} \\ \xi_2 &= 1 + \frac{(W/h)^{0.371}}{2.35\varepsilon_r + 1} \\ \xi_3 &= 1 + \frac{0.5274 \tan^{-1}[0.084(W/h)^{1.9413/\xi_2}]}{\varepsilon_{re}^{0.9236}} \\ \xi_4 &= 1 + 0.037 \tan^{-1}[0.067(W/h)^{1.456}] \cdot \{6 - 5 \exp[0.036(1 - \varepsilon_r)]\} \\ \xi_5 &= 1 - 0.218 \exp(-7.5W/h)\end{aligned}$$

The accuracy is better than 0.2% for the range of $0.01 \leq w/h \leq 100$ and $\varepsilon_r \leq 128$

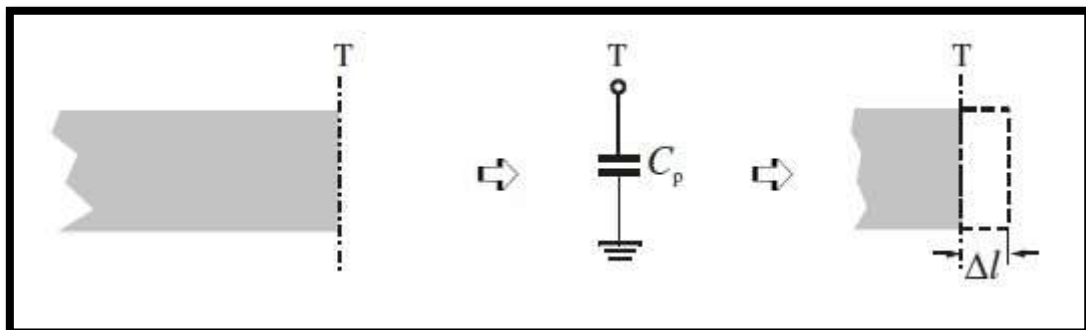


Figure 3.3 Microstrip Discontinuity (Open End)

3.2.3 Gaps

A microstrip gap can be represented by an equivalent circuit, as shown in the following figure. The shunt and series capacitances C_p and C_g may be determined by

$$C_p = 0.5C_e$$

$$C_g = 0.5C_o - 0.25C_e$$

where

$$\frac{C_o}{W} \text{ (pF/m)} = \left(\frac{\epsilon_r}{9.6} \right)^{0.8} \left(\frac{s}{W} \right)^{m_o} \exp(k_o)$$

$$\frac{C_e}{W} \text{ (pF/m)} = 12 \left(\frac{\epsilon_r}{9.6} \right)^{0.9} \left(\frac{s}{W} \right)^{m_e} \exp(k_e)$$

with

$$m_o = \frac{W}{h} [0.619 \log(W/h) - 0.3853] \quad \text{for } 0.1 \leq s/W \leq 1.0$$

$$k_o = 4.26 - 1.453 \log(W/h)$$

$$m_e = 0.8675$$

$$k_e = 2.043 \left(\frac{W}{h} \right)^{0.12} \quad \text{for } 0.1 \leq s/W \leq 0.3$$

$$m_e = \frac{1.565}{(W/h)^{0.16}} - 1 \quad \text{for } 0.3 \leq s/W \leq 1.0$$

$$k_e = 1.97 - \frac{0.03}{W/h}$$

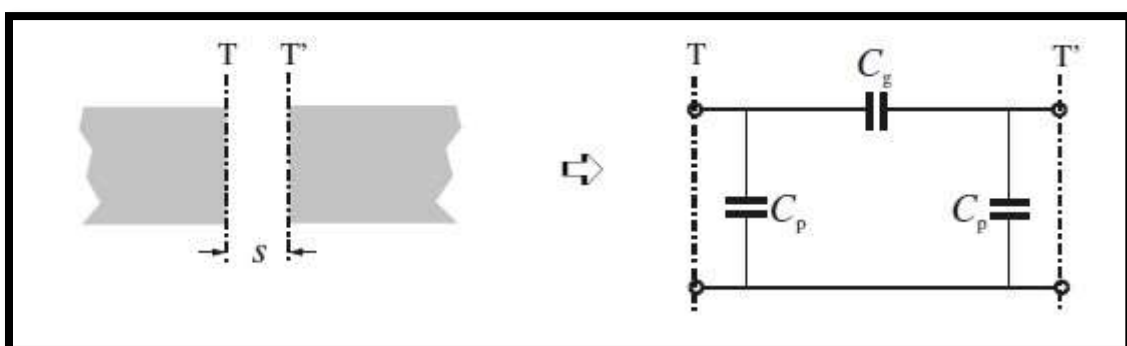


Figure 3.4 Microstrip Discontinuity (Gap)

3.2.4 Bends

Right-angle bends of microstrips may be modeled by an equivalent T-network, as shown in the figure below. The expressions for evaluation of capacitance and inductance is given by:

$$\frac{C}{W} \text{ (pF/m)} = \begin{cases} \frac{(14\epsilon_r + 12.5)W/h - (1.83\epsilon_r - 2.25)}{\sqrt{W/h}} + \frac{0.02\epsilon_r}{W/h} & \text{for } W/h < 1 \\ (9.5\epsilon_r + 1.25)W/h + 5.2\epsilon_r + 7.0 & \text{for } W/h \geq 1 \end{cases}$$

$$\frac{L}{h} \text{ (nH/m)} = 100 \left\{ 4 \sqrt{\frac{w}{h}} - 4.21 \right\}$$

The accuracy on the capacitance is quoted as within 5% over the ranges of $2.5 \leq \epsilon_r \leq 15$ and $0.1 \leq W/h \leq 5$. The accuracy on the inductance is about 3% for $0.5 \leq W/h \leq 2.0$.

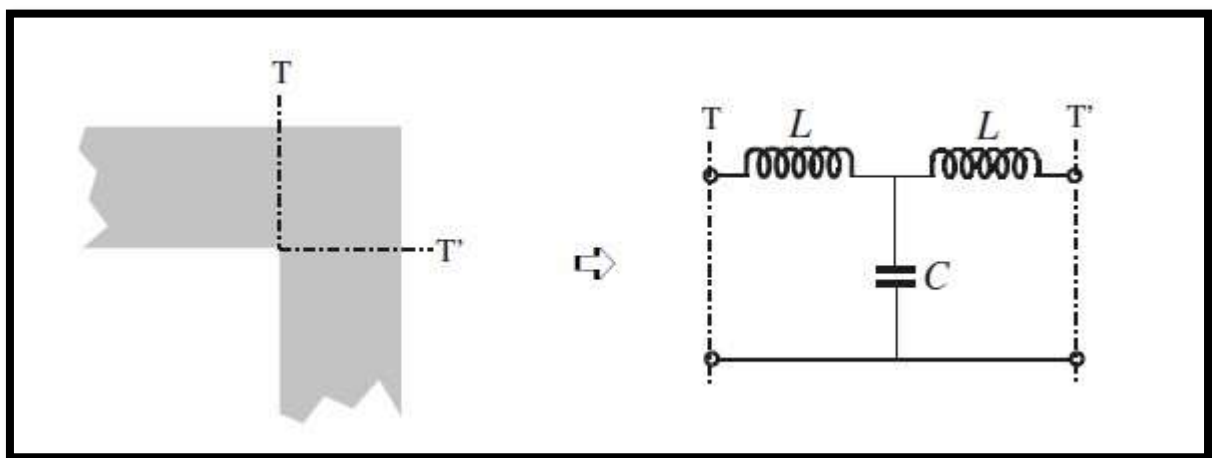


Figure 3.5 Microstrip Discontinuity (Bend)

In the practical designing of the filter these discontinuity concepts are extensively used.

3.3 Quasilumped Elements

Micro strip line short sections and stubs, whose physical lengths are smaller than a quarter of guided wavelength λ_g at which they operate, are the most common components for approximate microwave realization of lumped elements in micro strip filter structures, and are termed quasi lumped elements. They may also be regarded as lumped elements if their dimensions are even smaller, say smaller than $\lambda_g/8$. Some important micro strip quasi lumped elements are discussed in this section.

3.3.1 High- and Low-Impedance Short Line Sections

A short length of high-impedance (Z_c) lossless line terminated at both ends by relatively low impedance (Z_0) is represented by a π -equivalent circuit. For propagation constant $\beta = 2\pi/\lambda_g$ of the short line, the circuit parameters are given by

$$x = Z_c \sin\left(\frac{2\pi}{\lambda_g}l\right) \quad \text{and} \quad \frac{B}{2} = \frac{1}{Z_c} \tan\left(\frac{\pi}{\lambda_g}l\right)$$

which can be obtained by equating the ABCD parameters of the two circuits. If $l < \lambda_g/8$ then

$$x \approx Z_c \left(\frac{2\pi}{\lambda_g} l \right) \quad \text{and} \quad \frac{B}{2} \approx \frac{1}{Z_c} \left(\frac{\pi}{\lambda_g} l \right)$$

It can be further be shown that for $Z_c \gg Z_0$, the effect of the shunt susceptance may be neglected, and this short line section has an effect equivalent to that of a series inductance having a value of $L = Z_c l / v_p$, where $v_p = \omega/\beta$ is the phase velocity of propagation along the short line.

For the dual case shown, a short length of low-impedance (Z_c) loss-less line terminated at either end by relatively high impedance (Z_0) us represented by a T-equivalent circuit with the circuit parameters

$$B = \frac{1}{Z_c} \sin\left(\frac{2\pi}{\lambda_g}l\right) \quad \text{and} \quad \frac{x}{2} = Z_c \tan\left(\frac{\pi}{\lambda_g}l\right)$$

For $l < \lambda_g/8$ the values of the circuit parameters can be approximated by

$$B \approx \frac{1}{Z_c} \left(\frac{2\pi}{\lambda_g} l \right) \quad \text{and} \quad \frac{x}{2} \approx Z_c \left(\frac{\pi}{\lambda_g} l \right)$$

Similarly, if $Z_c \ll Z_0$, the effect of the series reactance may be neglected, and this short line section has an effect equivalent to that of a shunt capacitance $C = 1/(Z_c v_p)$. To evaluate the quality factor Q of these short-line elements, losses may be included by considering a lossy transmission line with a complex propagation constant $\gamma = \alpha + j\beta$. The total equivalent series resistance associated with the series reactance is then approximated by $R \approx Z_c \alpha l$, whereas the total equivalent shunt conductance associated with the shunt susceptance is $G \approx \alpha l / Z_c$. Since $Q_Z = x/R$ for a lossy reactance element and $Q_Y = B/G$ for a lossy susceptance element, it can be shown that the total Q-factor ($1/Q = 1/Q_Z + 1/Q_Y$) of the short-line elements is estimated by

$$Q = \frac{\beta}{2\alpha}$$

Where β is in radians per unit length and α is in nepers per unit length.

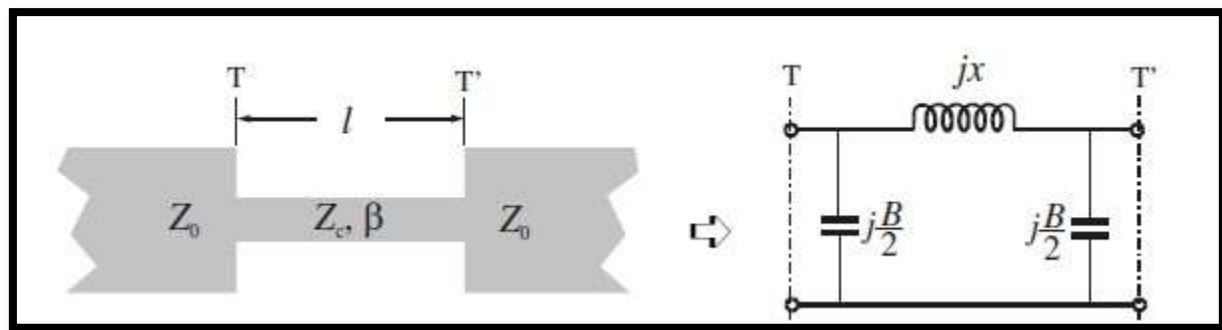


Figure 3.6 High-impedance short-line element

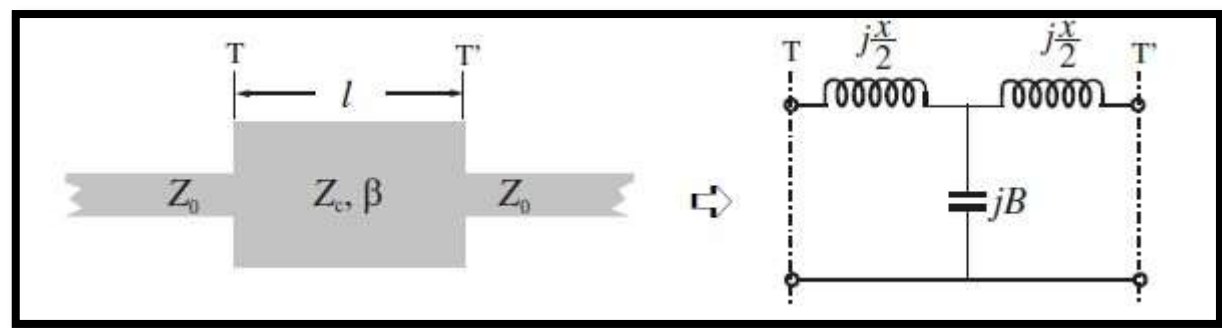


Figure 3.7 Low-impedance short-line element

3.3.2 Open- and Short-Circuited Stubs

We will now demonstrate that a short open circuited stub of lossless micro strip line can be equivalent to a shunt capacitor and that a similar short-circuited stub can be equivalent to a shunt inductor.

According to the transmission line theory, the input admittance of an open-circuited transmission line having a characteristic admittance $Y_c = 1/Z_c$ and propagation constant $\beta = 2\pi/\lambda_g$ is given by

$$Y_{in} = jY_c \tan\left(\frac{2\pi}{\lambda_g}l\right)$$

Where l is the length of the stub. If $l < \lambda_g/4$ this input admittance is capacitive. If the stub is even shorter, say $l < \lambda_g/8$, the input admittance may be approximated by

$$Y_{in} \approx jY_c \left(\frac{2\pi}{\lambda_g}l\right) = j\omega \left(\frac{Y_c l}{v_p}\right)$$

Where v_p is the phase velocity of propagation in the stub. It is now clearer that such a short open-circuited stub is equivalent to a shunt capacitance $C = Y_c l / v_p$. For the dual case, the input impedance of a similar short-circuited transmission line is given by

$$Z_{in} = jZ_c \tan\left(\frac{2\pi}{\lambda_g} l\right)$$

This input impedance is inductive for $l < \lambda_g/4$. If $l < \lambda_g/8$, an approximation of the input impedance is

$$Z_{in} \approx jZ_c \left(\frac{2\pi}{\lambda_g} l \right) = j\omega \left(\frac{Z_c l}{v_p} \right)$$

Such a short section of the short-circuited stub functions, therefore, as a shunt lumped element inductance $L = Z_c l / v_p$.

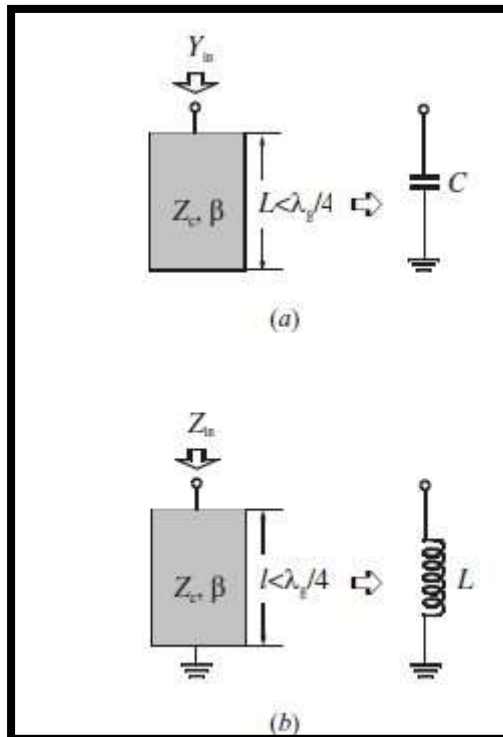


Figure 3.8 Short stub elements: (a) open-circuited stub; (b) short-circuited stub

These stub elements serve as the foundational resonators in the band pass filter design presented later in this work.

3.4 Resonators

A micro strip resonator is any structure that can contain at least one oscillating electromagnetic field. There are numerous forms of micro strip resonators. In general, micro strip resonators for filter designs may be classified as lumped-element or quasi lumped-element resonators and distributed line or patch resonators. Some typical configurations of these resonators are illustrated below.

Lumped-element or quasi lumped-element resonators, formed by the lumped or Quasilumped inductors and capacitors as shown, will obviously resonate at $\omega_0 = 1/\sqrt{LC}$. However, they may — resonate at some higher frequencies at which their sizes are no longer much smaller than a wavelength, and thus, by definition, they are no longer lumped or quasilumped elements. The distributed line resonators shown below may be termed quarter-wavelength resonators, since they are $\lambda_{g0}/4$ long, where λ_{g0} is the guided wavelength at the fundamental resonant frequency f_0 . They can also resonate at other higher frequencies when $f \approx (2n - 1) f_0$ for $n = 2, 3, \dots$. Another typical distributed line resonator is the half-wavelength resonator, which is $\lambda_{g0}/2$ long at its fundamental resonant frequency, and can also resonate at $f \approx nf_0$ for $n = 2, 3, \dots$. In our filter designing these resonating structures play a crucial role.

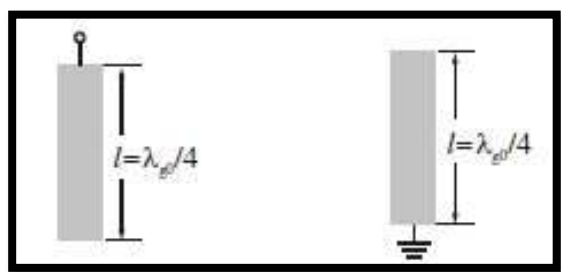


Figure 3.9 Quarter-wave resonators

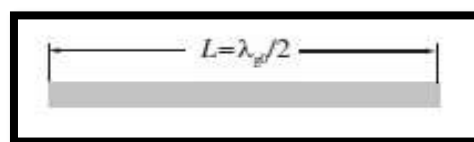


Figure 3.10 Half-wave resonators

The stub-loaded resonators used in this design are based on open-circuited stubs integrated into micro strip line sections to control resonant frequency and bandwidth.

3.5 Scattering Parameters (S-Parameters)

Scattering parameters, or S-parameters, are fundamental tools used to describe the electrical behaviour of high-frequency (microwave and RF) networks. Instead of using voltages and currents directly, S-parameters relate the **incident** and **reflected power waves** at the ports of a device.

For a two-port network:

- S_{11} : Input reflection coefficient (how much power is reflected back at port 1)
- S_{21} : Forward transmission coefficient (how much power is transmitted from port 1 to port 2)
- S_{12} : Reverse transmission coefficient (port 2 to port 1)
- S_{22} : Output reflection coefficient (port 2 reflection)

Why Use S-Parameters Instead of Z, Y, or H Parameters?

1. High-Frequency Suitability:

At microwave frequencies, the dimensions of circuits are comparable to the signal wavelengths, and parasitic effects become significant. Traditional parameters like **impedance (Z)** or **admittance (Y)** are based on **voltage and current**, which are difficult to define and measure precisely in these regimes.

2. Practical Measurement:

S-parameters are measured using a **vector network analyser (VNA)**, which directly measures the magnitude and phase of reflected and transmitted signals (power waves), making them highly convenient and accurate for high-frequency components.

3. Compatibility with Wave Behaviour:

Microwave signals propagate as **electromagnetic waves** through transmission lines, and power wave analysis (as used in S-parameters) better represents this behaviour than circuit theory-based parameters.

4. Port-Based Analysis:

S-parameters naturally fit multi-port devices (e.g., filters, amplifiers, antennas), allowing engineers to easily evaluate performance aspects like:

- **Return Loss** (via S_{11} , S_{22})
- **Insertion Loss** (via S_{21})
- **Isolation** (via S_{12})

5. Passive and Active Device Modelling:

They can describe both **linear passive** (like filters, couplers) and **active** (like amplifiers) components, making them universally applicable in RF and microwave design.

S-parameters are the preferred choice in microwave engineering due to their **measurement practicality**, **suitability for wave-based systems**, and **direct relevance to key performance metrics** in high-frequency circuits.

CHAPTER-4 FILTER - 1: FILTER DESIGN METHODOLOGY

After discussing all the prerequisites in the first two chapters, this chapter marks the starting of the discussion related to the filter design that is to be practically implemented.

4.1 Problem Statement (Filter Specifications)

The filter design that is to be done is a **band pass filter using lumped elements** having centre frequency at 312.5 MHz. The insertion loss should be lesser than 3dB. The stopband rejection (312.5 ± 125 MHz) should be > 20 dBc. The substrate that is to be used is Duroid 6010, having relative dielectric constant, $\epsilon_r = 10.2$ and conductor thickness is $17\mu\text{m}$. The following table shows the entire specification in a tabular format.

Table-1 Filter Specifications

Parameters	Value/Name
Centre Frequency (F_c)	312.5 MHz
0.5dB Bandwidth	312.5 ± 50 MHz
1 dB Bandwidth	312.5 ± 60 MHz
Insertion Loss	< 3 dB
Filter Stop Band with > 20dBc rejection	312.5 ± 125 MHz
Return Loss	>15 dB
Maximum Size	$\frac{3}{4}$ - inch x $\frac{3}{4}$ - inch

4.2 Literature Survey

For the design of the Band Pass Filter using Lumped Elements much literature review was not required. Only referred materials were the textbooks mentioned in [6] and [7].

This includes understanding the fundamentals of EM Theory, Transmission Lines and Waveguides, Resonators, Microstrip Line, Filter Design Theory. All the content refer from these Chapters are mentioned in the report in CHAPTER-1 and CHAPTER-2.

Some websites were also referred, just get an idea about how filters look after being fabricated and what their physical sizes are.

4.3 Theoretical Approach

Before approaching the practical designing process, theoretical calculations are done to choose the type of response, order of the filter which can cater all the constraints.

4.3.1 Substrate Analysis

The design is implemented on an Duroid 6010 substrate, which is a commonly used material in RF and microwave circuits due to its excellent electrical and mechanical properties [8]. Below mentioned are some of the key substrate parameters:

- Substrate Height (H): 25 mils (0.635 mm)
- Relative Dielectric Constant (ϵ_r): 10.2
- Loss Tangent (Tan D): 0.002
- Conductor Material: Gold (Au)
- Conductor Thickness (T): 17 um
- Conductivity: 4.1E+7
- Upper Housing Height (Hu): 11 mm
- Substrate Area: $\frac{3}{4}$ - inch x $\frac{3}{4}$ - inch - (≈ 19 mm x 19 mm)

Duroid 6010 is selected as the dielectric substrate for its high permittivity ($\epsilon_r = 10.2$), which enables miniaturization of the resonator structures and helps achieve compact layout within the given area constraint of $\frac{3}{4}$ - inch \times $\frac{3}{4}$ - inch. Its low loss tangent (0.002) is ideal for microwave frequencies, contributing to low insertion loss and improved quality factor (Q).

The conductor material is gold, which, although slightly less conductive than copper, is chosen for its excellent surface conductivity, resistance to oxidation, and stable performance over time, especially beneficial at high frequencies where the skin effect confines current to the surface. The 17 μm thickness ensures adequate conduction while maintaining fine patterning precision. The 11 mm upper housing height is considered in EM modelling to account for shielding and possible cavity resonance effects.

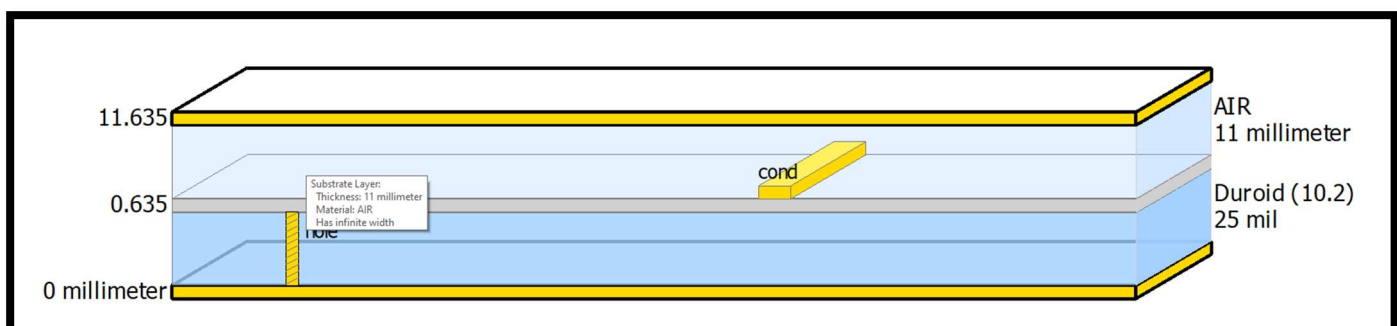


Figure 4.1 Substrate structure used for design

4.3.2 Filter Design Analysis

At first to satisfy the given filter specifications, both Butterworth and Chebyshev responses were tried out. **The Butterworth response is selected**, for it smoother pass band. The given order to us is N = 3. **But we first start with a higher order to get the correct and then we will move on to improvise the response.**

Order of the filter (n): 3

4.4 Practical Implementation

As computed from the theoretical analysis the design is supposed to be a 3th order BPF having a Butterworth Response. First there are certain formulae that are needed to be used for computing.

$$\epsilon_{\text{eff}} \approx [(\epsilon_r + 1) / 2]$$

$$\lambda_g = [c / (f_c * \epsilon_{\text{eff}})]$$

$$\omega_c = 2 * \Pi * f_c$$

Further, we use the g-values table from [6], to calculate the values of L and C. The formulae for the same are given below.

$$L'_k = \frac{R_0 L_k}{\omega_c},$$

$$C'_k = \frac{C_k}{R_0 \omega_c}.$$

Here, L_k and C_k take values from g-values and finally we get the values of Inductances and Capacitances in nH and pF respectively. Further, we create a Schematic followed by Layout or directly start with a layout. Accordingly, we perform tuning operations for enhancing the response and run EM simulations with various physical parameters to get the most accurate response of the filter. Here, we work with Co-Simulations. Finally, the layout is ready for fabrication after exporting “.gds” file.

4.4.1 3rd Order Lumped Band Pass Filter Design

The following table consists of all the values of L and C.

Table-2 Obtained values for 3rd order Lumped Band Pass Filter

i	L (nH)	C (pF)
1	56.58	4.58
2	5.729	45.27
3	56.58	4.58
4	9.75	36.3s

Schematic View:

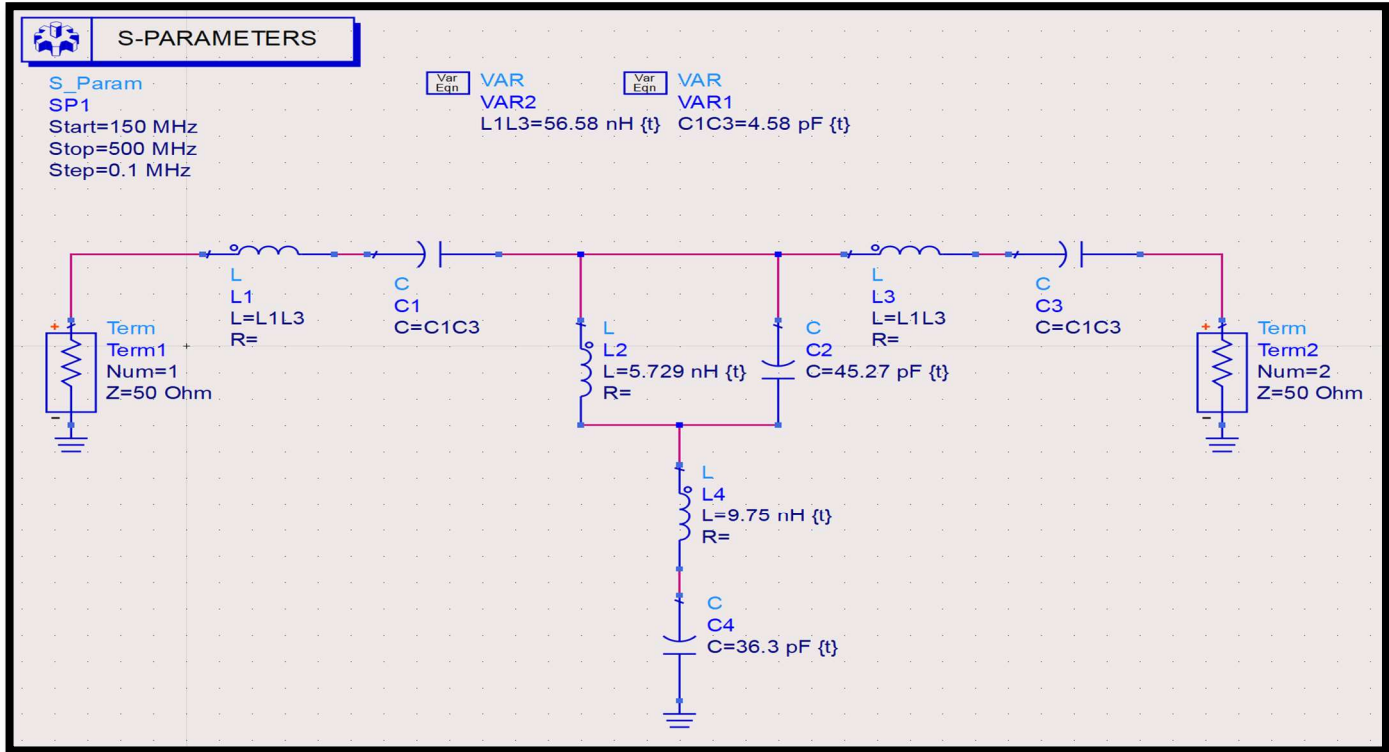


Figure 4.2 Schematic representation of the 3rd order filter

Schematic Simulation Result:

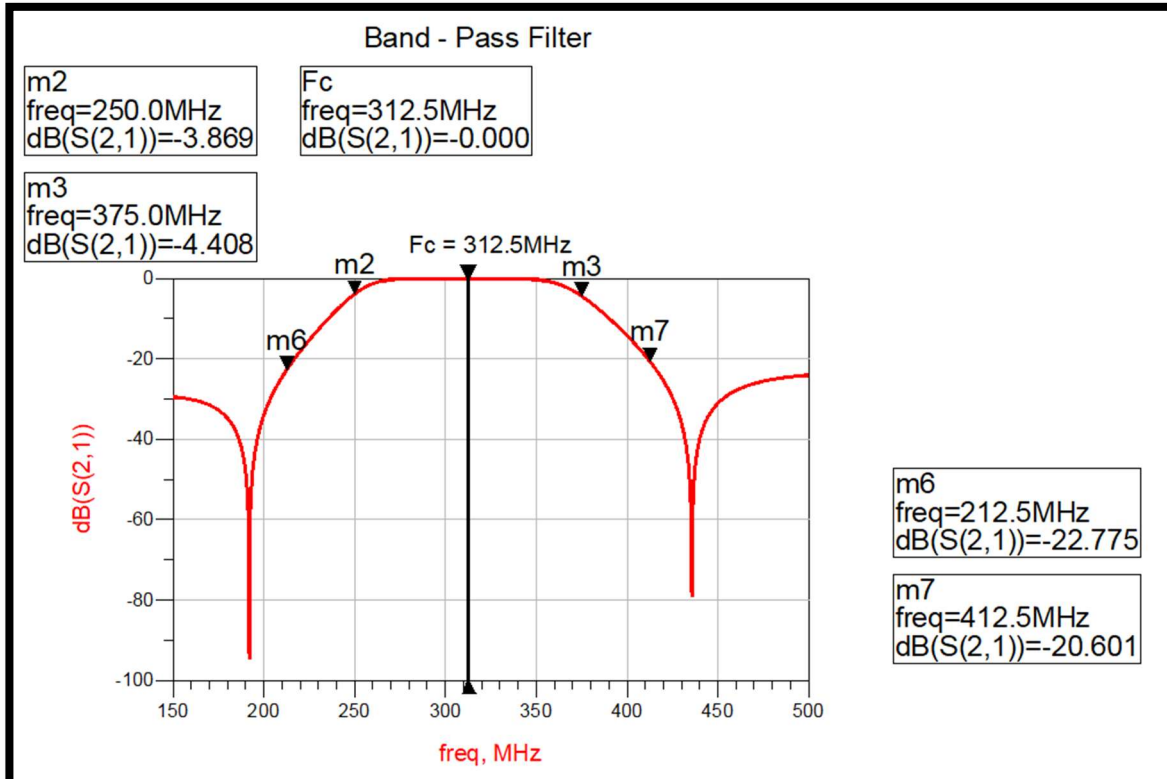


Figure 4.3 S-Parameters from schematic simulation

As from the schematic simulation it is observed that we need to increase the pass band wideness.

Observation: The obtained response, clearly, is not at all what are specifications are except the cut-off frequency which is nearly correct.

Further optimizations are not carried out.

4.4.2 4th Order Lumped Band Pass Filter Design with Ideal Elements

The following table consists of all the values of L and C.

Table-3 Obtained values for 4th order Lumped Band Pass Filter Optimized

i	L (nH)	C (pF)
1	65.5	4.155
2	8.6315	30
3	65.5	4.155
4	18	18
5	14.9235	19.5
6	10.8	18

Schematic View:

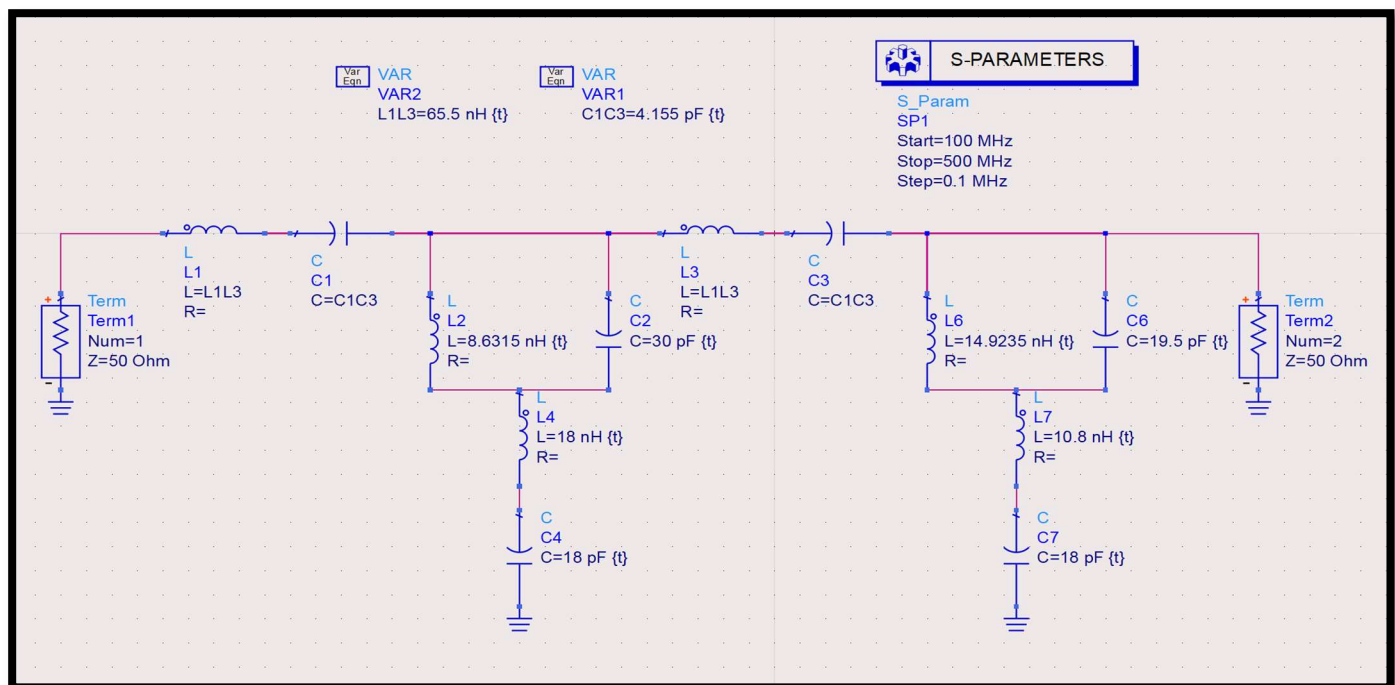


Figure 4.4 Schematic representation of 4th order filter

Schematic Simulation Result:

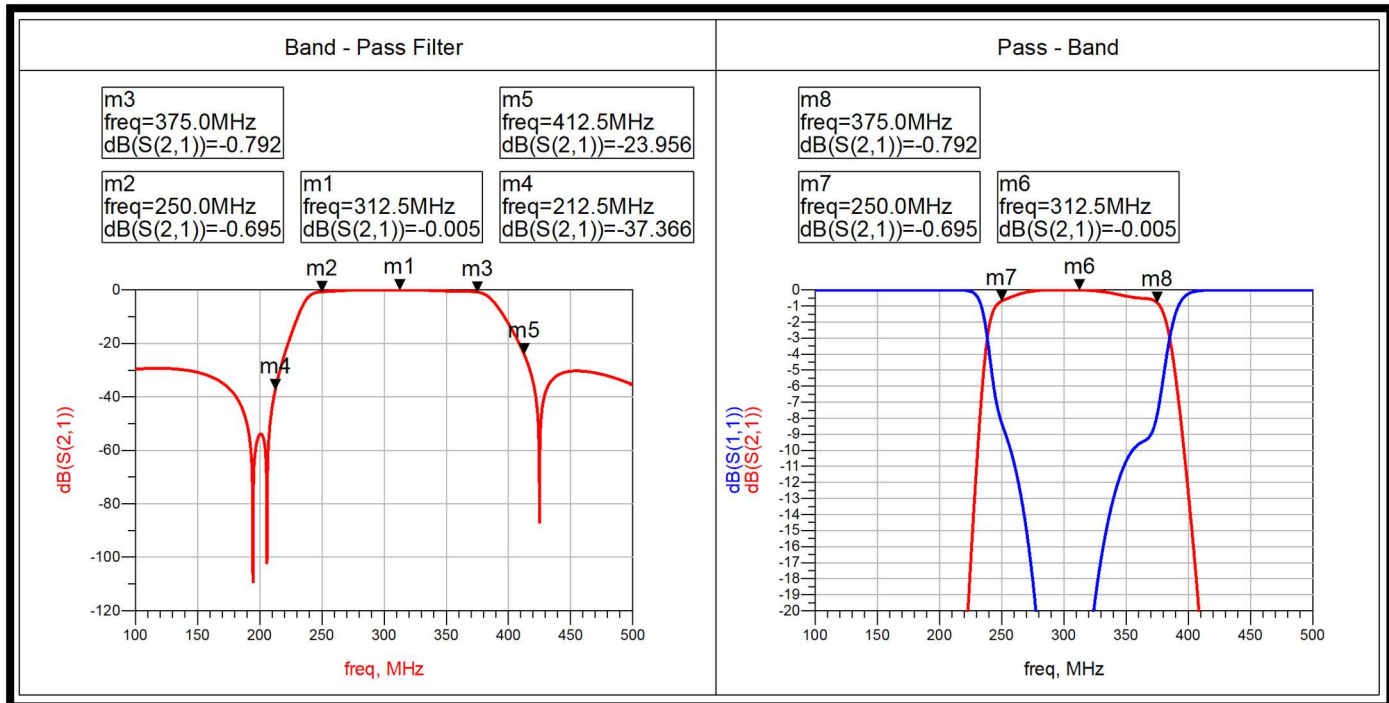


Figure 4.5 S-Parameters from schematic simulation (4th order)

The above response is much better than the previous result.

Observation: The schematic includes 4 sections consisting of 2 m-derived sections for sharp cut-off. The schematic simulation clearly matches with our desired specifications. The pass band is also good and flat with stop band completely below 20dB. Roll-off is also perfect.

Conclusion: The design is very good and can be improved further, but our task is to make a filter of 3 sections that is, N = 3. So, now we move back to 3rd order filter in order to make filter realizable.

4.4.3 3rd order Lumped Band Pass Filter with Non-Ideal Elements

To reduce the size of the filter we move back to 3rd order filter but with Q Components with include parasitic effects of the Lumped Components when realizing practically. Q = 25

Table-4 Obtained values for 3rd order Filter

i	L (nH)	C (pF)
1	65.5	3.0695
2	10.353	23.4
3	65.5	3.0695
4	14.58	69.97

Schematic View:

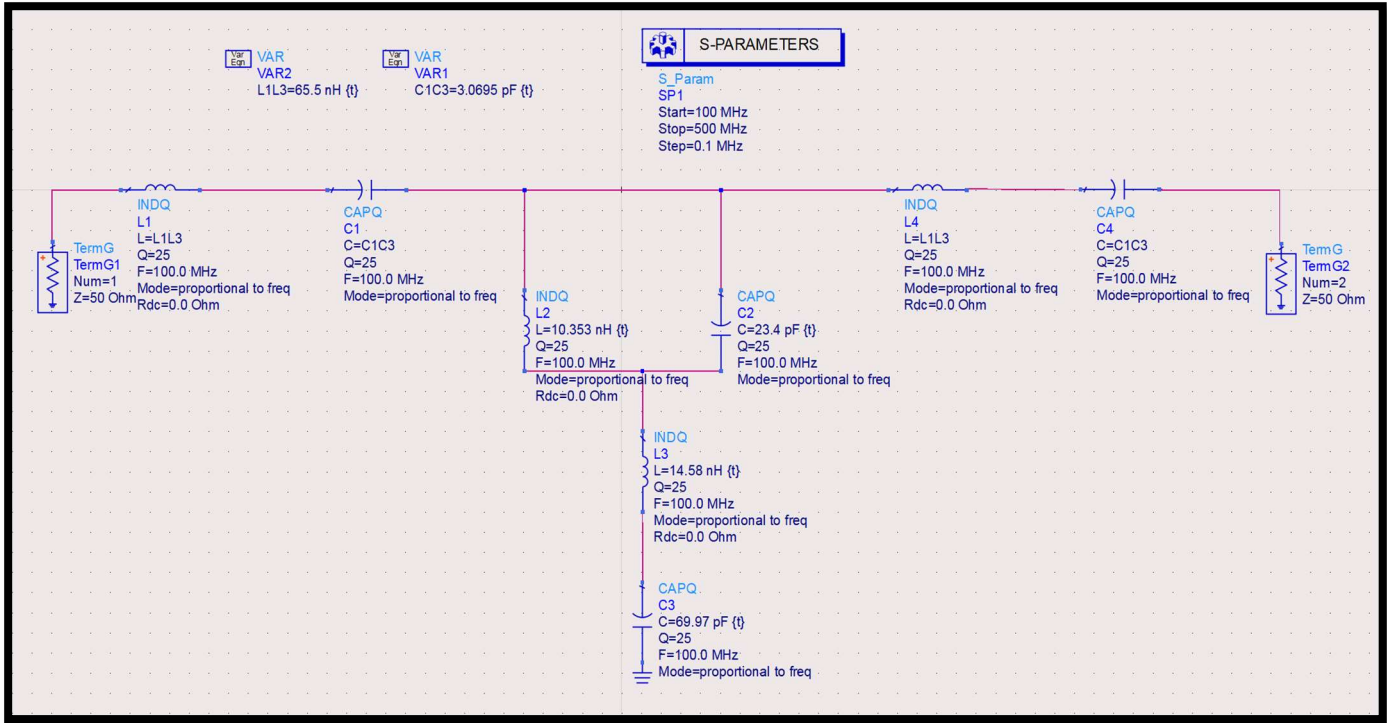


Figure 4.6 Schematic representation of 3rd order filter with Non-Ideal Elements

Schematic Simulation Result:

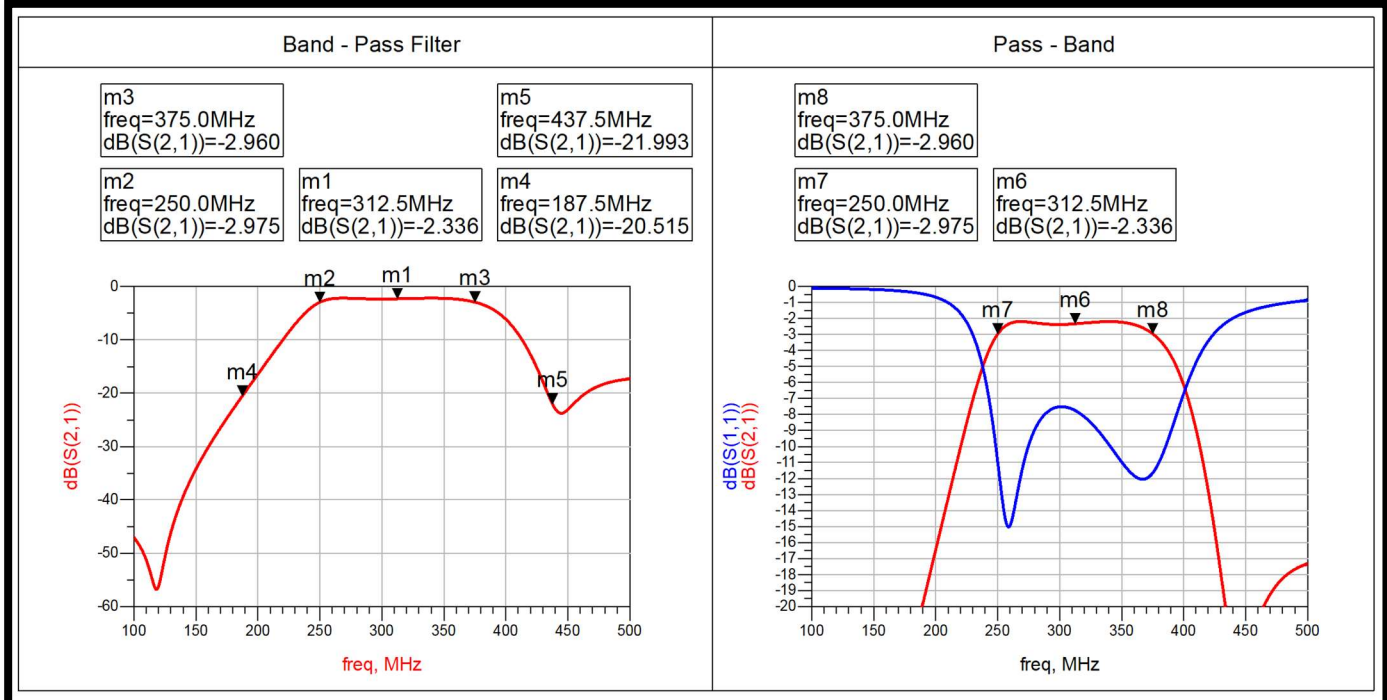


Figure 4.7 S-Parameters from schematic simulation (3rd order) with Ideal Elements

The schematic simulation shows promising results, satisfying most of the specifications with some minor tunings. Still, in the passband the insertion loss and return loss are too high to be of practical implementation.

Observation: The simulated result from the schematic shows promising results satisfying most of the given specifications as well, without doing any major changes and the size of the filter is comparable in accordance to the substrate size mentioned.

Conclusion: The schematic for this design gives good results and some minor tuning and optimizations will lead us to our desired response.

Note:

Further, we make a layout for elements to be soldered when fabricated. The layout will be simulated and then we use Co-Simulations followed by some tuning and converting actual values of L and C to practically available values, to obtain final results of the design to be fabricated.

CHAPTER-5 FILTER - 2: FILTER DESIGN METHODOLOGY

After discussing all the prerequisites in the first two chapters, this chapter marks the starting of the discussion related to the filter design that is to be practically implemented.

5.1 Problem Statement (Filter Specifications)

The filter design that is to be done is a low pass filter having a passband from 0 GHz to 2.475 GHz. The insertion loss should be lesser than 3dB while maintaining a return loss lesser than -15dB. The stopband rejection (2.750 – 17.250 GHz) should be > 20 dBc. Also, the image frequency rejection (7.725 – 10.125 GHz) should be > 30dBc. The substrate that is to be used is Alumina (Al_2O_3), having relative dielectric constant, $\epsilon_r = 9.9$ and conductor thickness is $8\mu\text{m}$. The following table shows the entire specification in a tabular format.

Table-5 Filter Specifications

Parameters	Value/Name
Range of Pass Band Frequency	DC - 2.475 GHz
0.5dB Bandwidth	DC - 2.475 GHz
1 dB Bandwidth	DC - 2.500 GHz
Insertion Loss	< 3dB
Image Rejection Band with > 30dBc rejection	7.725 – 10.125 GHz
Filter Stop Band with > 20dBc rejection	2.750 – 17.250 GHz
Return Loss	> 15 dB
Maximum Size	$\frac{3}{4}$ - inch x $\frac{3}{4}$ - inch

5.2 Literature Survey

In a previous work [1], In this paper, a novel low-pass filter using spiral compact microstrip resonant structure for size reduction and broad pass-band is presented. The proposed low-pass filter is designed, fabricated and tested. The insertion loss of the filter is less than 0.1dB in the frequency range from DC to 3.5 GHz. The novel low-pass filter has the advantages of low insertion loss in the pass-band, high and wide rejection in the stop-band and compact size. The performances of the proposed filter are demonstrated by measured results, which are good agreement with the simulation ones.

In another work [2], A lowpass filter with wideband stopband is developed using microstrip line and proposed in this paper. It consists of shunt stepped-impedance open-circuited stubs and unit elements. The electrical length of the open-circuited stubs is chosen to be twice the length of the unit elements at a specific frequency. As a result, the filter can exhibit additional transmission zeros inside the rejection band and close to the cut-off frequency. Hence, the filter can provide an equal ripple performance with very high selectivity. The proposed design is verified by EM-simulations and experiment. A good agreement is attained between the calculated, simulated and measured results. The measured filter shows excellent performance with an extended stopband.

Work [3] presents design, implementation and performance evaluation of a 2.8 GHz low-pass filter using microstrip resonator. The 3D planar electromagnetic simulator ADS Momentum is used for the layout design and the performance characterization. This filter has a Chebyshev response with 0.02 dB of ripple and a cutoff frequency located at 2.8 GHz. The attenuation of this filter is measured at 3.3 GHz. Theoretical frequency response from analytical calculations in MATLAB and ideal transmission line simulation in ADS are almost identical. The filter finds its application in telecommunication systems. Designed filter has been fabricated and measurements greatly coincide with simulation results.

In work [4] a compact microstrip low-pass filter (LPF) using T-shaped resonator with wide stopband is presented. The proposed LPF has capability to remove the eighth harmonic and a low insertion loss of 0.12 dB. The bandstop structure using stepped impedance resonator and two open-circuit stubs are used to design a wide stopband with attenuation level better than -20 dB from 3.08 up to 22 GHz. The proposed filter with -3 -dB cutoff frequency of 2.68 GHz has been designed, fabricated, and measured. The operating of the LPF is investigated based on equivalent circuit model. Simulation results are verified by measurement results and excellent agreement between them is observed.

Work [5] presents a novel lowpass filter (LPF) structure which consists of a section of high-impedance microstrip line (HIML) with a pair of radial stubs (RSs) loaded at its center and a pair of stepped-impedance open stubs (SIOSSs) loaded on both ends of HIML. The RSs loaded HIML exhibits a lowpass property and has a wide stopband. The loaded SIOSSs not only can improve the roll-off rate of LPF significantly but also is able to extend the stopband. Based on such a LPF structure, a pair of highpass shorted HIMLs are paralleled on both sides of LPF to construct a wideband bandpass filter (BPF) with wide stopband. To validate the proposed method, two filters, i.e., a LPF with cutoff frequency at 1.07 GHz and a BPF centered at GHz with dB fractional bandwidth of 87%, are designed and fabricated. The measured results show the fabricated LPF has a dB isolation bandwidth from to while the fabricated BPF has a dB isolation bandwidth from to. Moreover, the fabricated LPF and BPF also have the compact size of and, respectively. Good agreement can be observed between the simulation and measurement.

5.3 Theoretical Approach

Before approaching the practical designing process, theoretical calculations are done to choose the type of response, order of the filter which can cater all the constraints.

5.3.1 Substrate Analysis

The design is implemented on an Alumina (Al_2O_3) substrate, which is a commonly used ceramic material in RF and microwave circuits due to its excellent electrical and mechanical properties [8]. Below mentioned are some of the key substrate parameters:

- Substrate Height (H): 25 mils (0.635 mm)
- Relative Dielectric Constant (ϵ_r): 9.9
- Loss Tangent (Tan D): 0.007
- Conductor Material: Gold (Au)
- Conductor Thickness (T): 8 μm
- Conductivity: $4.1\text{E}+7$
- Upper Housing Height (H_u): 11 mm
- Substrate Area: $\frac{3}{4}$ - inch $\times \frac{3}{4}$ - inch - ($\approx 19 \text{ mm} \times 19 \text{ mm}$)

Alumina is selected as the dielectric substrate for its high permittivity ($\epsilon_r = 9.9$), which enables miniaturization of the resonator structures and helps achieve compact layout within the given area constraint of $\frac{3}{4}$ - inch $\times \frac{3}{4}$ - inch. Its low loss tangent (0.0007) is ideal for microwave frequencies, contributing to low insertion loss and improved quality factor (Q).

The conductor material is gold, which, although slightly less conductive than copper, is chosen for its excellent surface conductivity, resistance to oxidation, and stable performance over time, especially beneficial at high frequencies where the skin effect confines current to the surface. The 8 μm thickness ensures adequate conduction while maintaining fine patterning precision. The 11 mm upper housing height is considered in EM modelling to account for shielding and possible cavity resonance effects.



Figure 5.1 Substrate structure used for design

5.3.2 Filter Design Analysis

At first to satisfy the given filter specifications, both Butterworth and Chebyshev responses were tried out. The Chebyshev response is selected, for it higher roll-off rate necessary to meet the required specifications. In case of Chebyshev, the 0.1dB Low – Pass prototype was chosen. Now the process is to determine the order of the filter to design the prototype low pass filter at first. Below show all the initial calculations done.

Order of the filter (n):

$$n \geq \frac{\cosh^{-1} \sqrt{\frac{10^{0.1L_{As}} - 1}{10^{0.1L_{Ar}} - 1}}}{\cosh^{-1}(\frac{\omega_1}{\omega_C})}$$

Here one considerations are taken for getting the normalised filter element values for Chebyshev response, the values are taken from predefined tables mentioned in [6]. In that the passband ripple L_{Ar} is considered is around 0.1 dB.

After putting the values, we get the filter order to be approximately a 13th order filter. Now it different design topologies are to explored to satisfy our requirement.

The Fractional Bandwidth can be calculated from the given formulae:

$$FBW = \frac{\omega_2 - \omega_1}{\omega_0}$$

where,

$$\omega_0 = \frac{\omega_1 + \omega_2}{2}$$

- Wide Fractional Bandwidth Handling

Open-stub topologies are inherently well-suited for wideband responses. Unlike narrowband resonator designs (e.g., coupled lines or hairpins), open stubs allow more flexibility in shaping the frequency response over large bandwidths with controlled return loss and ripple.

- High Design Compactness

With a high dielectric constant substrate ($\epsilon_r = 9.9$) and small layout constraint (1 inch × 1 inch), open-stub filters can achieve greater miniaturization. The quarter-wavelength stubs can be tightly packed or meandered while maintaining their electrical length, enabling a compact layout without compromising performance.

- Low Insertion Loss Potential

Open stubs, when implemented with high-quality conductors like gold, exhibit very low conductor loss due to minimal discontinuities and short line sections. Combined with the low-loss Alumina substrate, this supports specification of insertion loss < 3 dB.

- Good Return Loss Performance

The Chebyshev-based open-stub design can be tuned to achieve the required return loss < 15 dB across the passband. Matching networks at input/output can further optimize VSWR without excessive complexity.

- Simplicity of EM Simulation and Tuning

Open-stub filters are relatively easy to model and simulate using full-wave EM tools. Their performance can be fine-tuned by adjusting stub lengths and spacing, without needing complex 3D structures or multilayer configurations.

- Flexibility in Topology Variations

Open stubs can be configured in shunt, series, or pseudo-lumped forms, and can easily integrate with other filter sections or impedance matching networks. This makes them flexible for integration into broader microwave systems.

5.4 Practical Implementation

As computed from the theoretical analysis the design is supposed to be a 13th order LPF having a Chebyshev Response. First there are certain formulae that are needed to be used for computing the lengths and thickness of the stubs.

$$\epsilon_{\text{eff}} \approx [(\epsilon_r + 1) / 2]$$

$$\lambda_g = [c / (f_c * \epsilon_{\text{eff}})]$$

$$\omega_c = 2 * \pi * f_c$$

Clearly, each section length will be $l = \lambda_g / 8$. The calculated value of l comes out to be 6.18 mm. Here, ω_c comes out to be $16.328 * 10^9$ rad/sec. The calculated value of λ_g is 49.43 mm at our cut-off frequency of 2.475 GHz, along with ϵ_{eff} being 5.45.

Further, we use the g-values table from [], to calculate the values of L and C. The formulae for the same are given below.

$$L'_k = \frac{R_0 L_k}{\omega_c},$$

$$C'_k = \frac{C_k}{R_0 \omega_c}.$$

Here, L_k and C_k take values from g-values and finally we get the values of Inductances and Capacitances in nH and pF respectively.

Now, we use the Richards Transformation to convert these lumped elements values to microstrip line values consisting of Ws and Ls.

$$\Omega = \tan \beta \ell = \tan \left(\frac{\omega \ell}{v_p} \right)$$

From the above formula, we get θ or bl , which is the electrical length. Finally, we use the LineCalc tool from ADS to calculate the physical widths and lengths. We can also calculate the W , L manually but the software gives us more accurate parameters and considers some more conditions which we usually ignore.

Given below is the example of using the LineCalc tool in ADS.

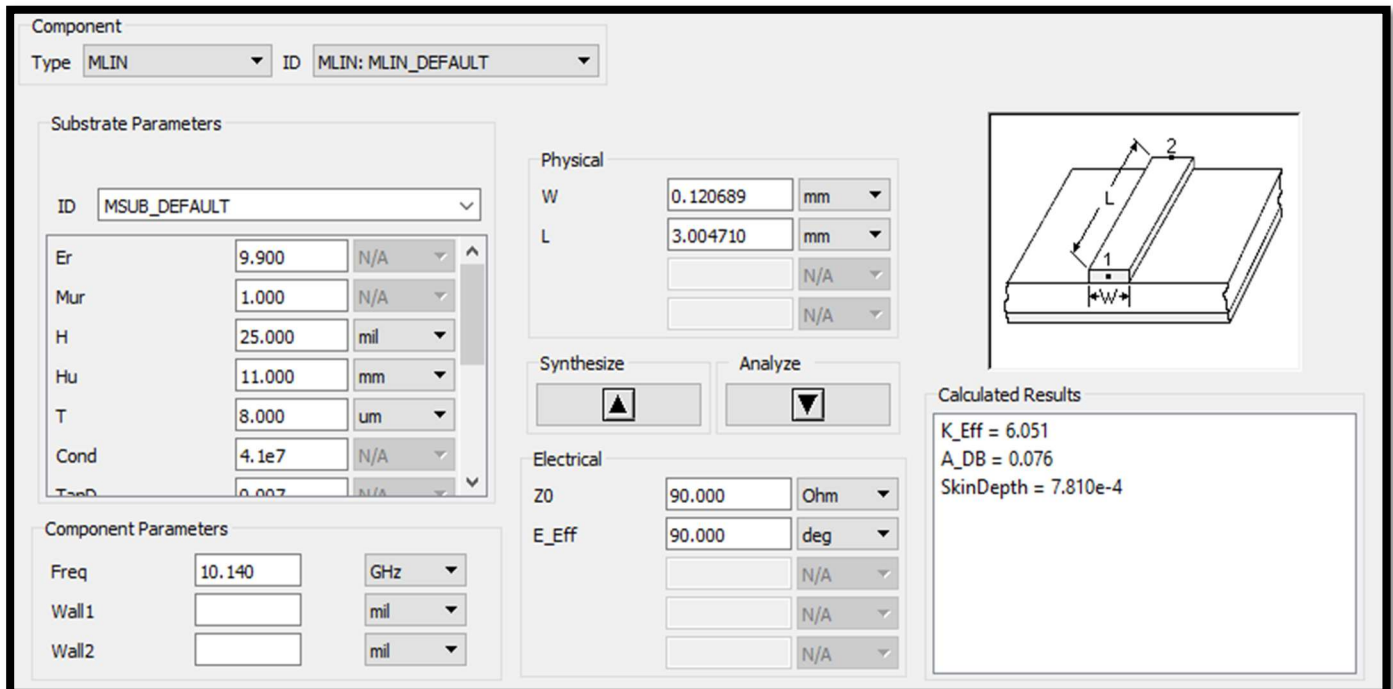


Figure 5.2 LineCalc tool in ADS

Further, we create a Schematic followed by Layout or directly start with a layout. Accordingly, we perform tuning operations for enhancing the response and run EM simulations with various physical parameters to get the most accurate response of the filter. Once the filter has achieved the desired response in EM simulations then we add tuning pads and further flatten the design followed by union operation. Finally, the layout is ready for fabrication after exporting “.gds” file.

5.4.1 6th Order Stepped-Impedance Filter Design

The following table consists of all the values of L and W.

Table-6 Obtained values for 6th order Stepped-Impedance Filter

i	L _i (mm)	W _i (mm)
1	2.05	11.3
2	6.63	0.428
3	7.69	11.3
4	9.04	0.428
5	5.63	11.3
6	2.41	0.428

Schematic View:

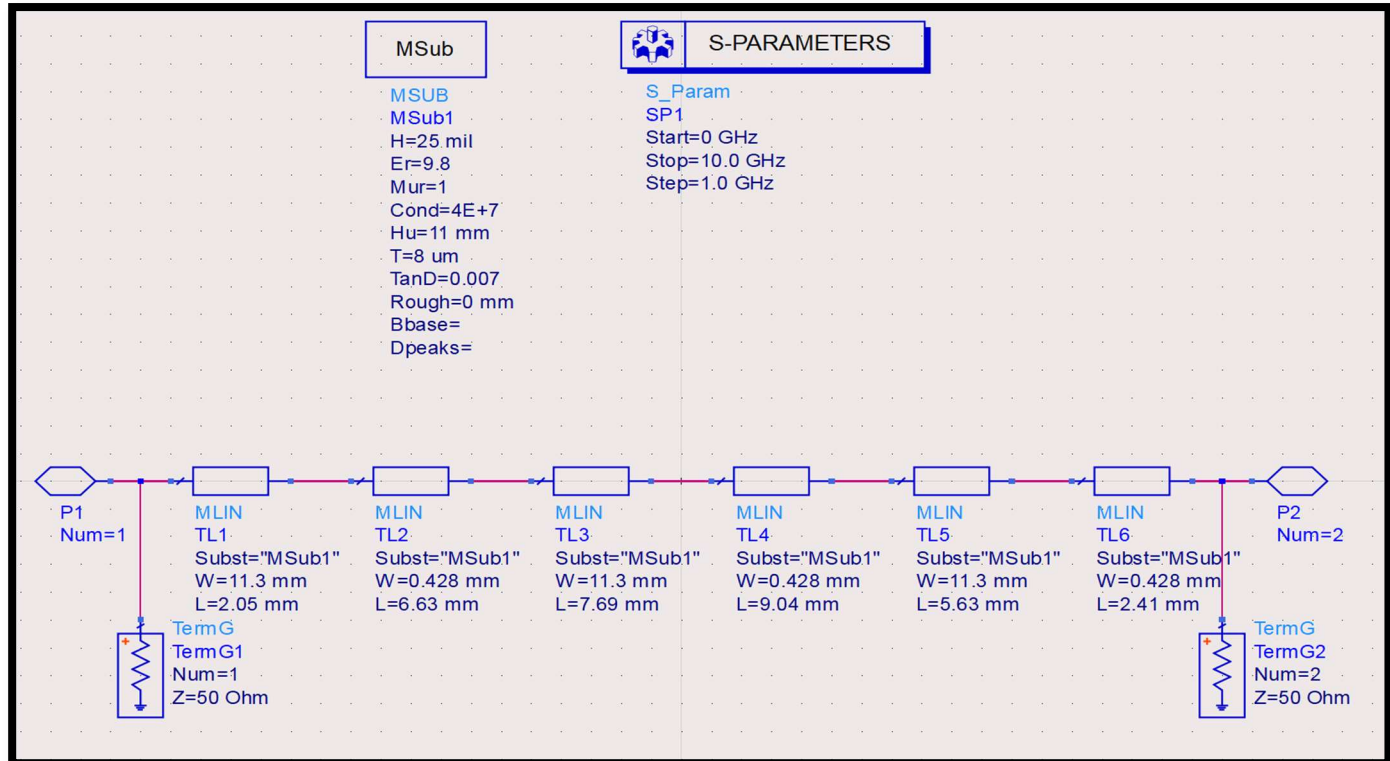


Figure 5.3 Schematic representation of the 6th order filter

Schematic Simulation Result:

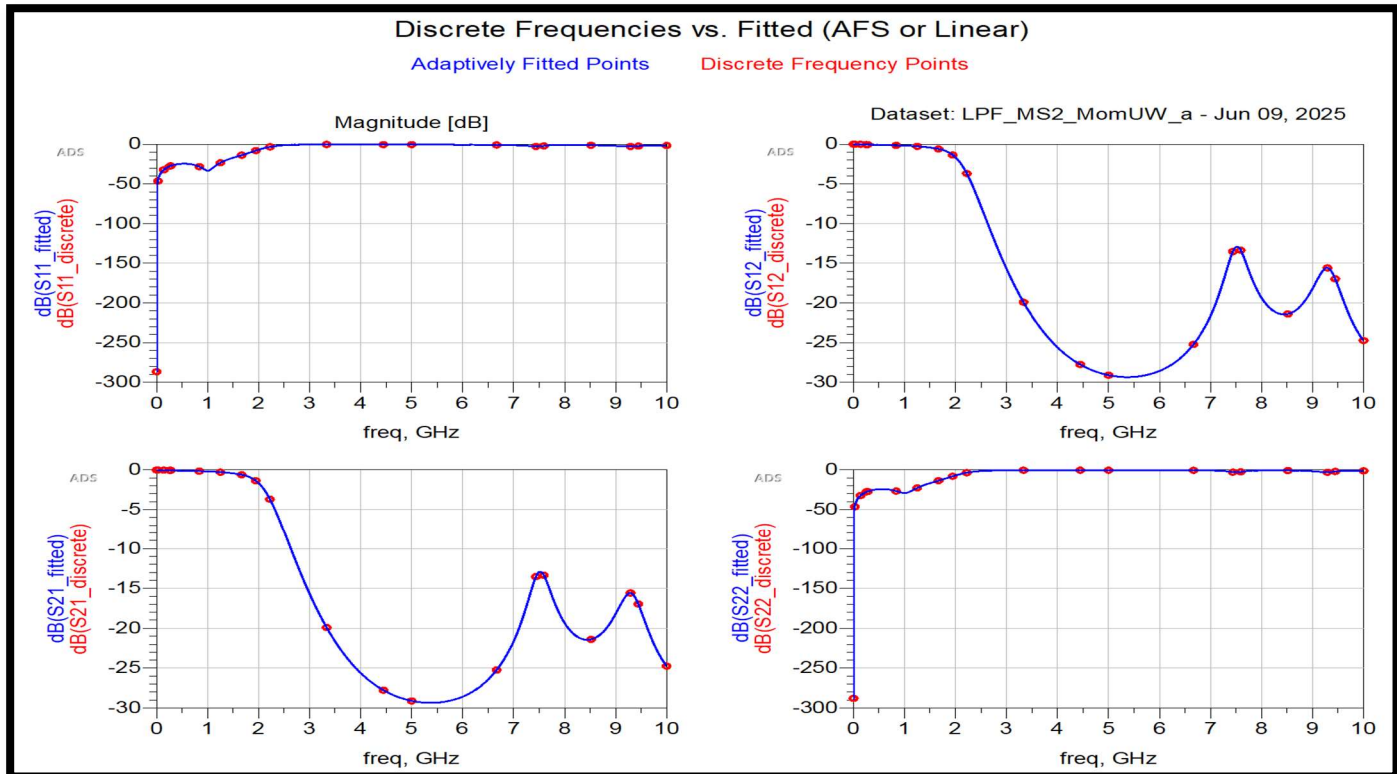


Figure 5.4 S-Parameters from schematic simulation

As from the schematic simulation it is observed that the result is not what should have happened, so for a better result we need to increase the order as well as we need to suppress frequencies emerging in the stop band.

Observation: The obtained response, clearly, is not at all what are specifications are except the cut-off frequency which is nearly correct.

Conclusion: As a result, any further attempt for optimisation is not performed on this design.

It is to be considered that because of lack of some specs required to design any filter, there are assumptions that are made because of which the calculated also needs some hit and trial approach.

5.4.2 10th Order Stepped-Impedance Filter Design

Every calculation procedure remains the same, the main change occurs in the computational values, which is because of the change in the normalised filter element values that too because of the change in the order of the filter.

Table-7 Obtained values for 10th order Stepped-Impedance Filter

i	L _i (mm)	W _i (mm)
1	2.5	0.05
2	2	3.6
3	6	0.05
4	5.5	3.6
5	2.7	0.05
6	8	3.6
7	3.6	0.05
8	7.5	3.6
9	4	0.05
10	4	3.6

Schematic View:

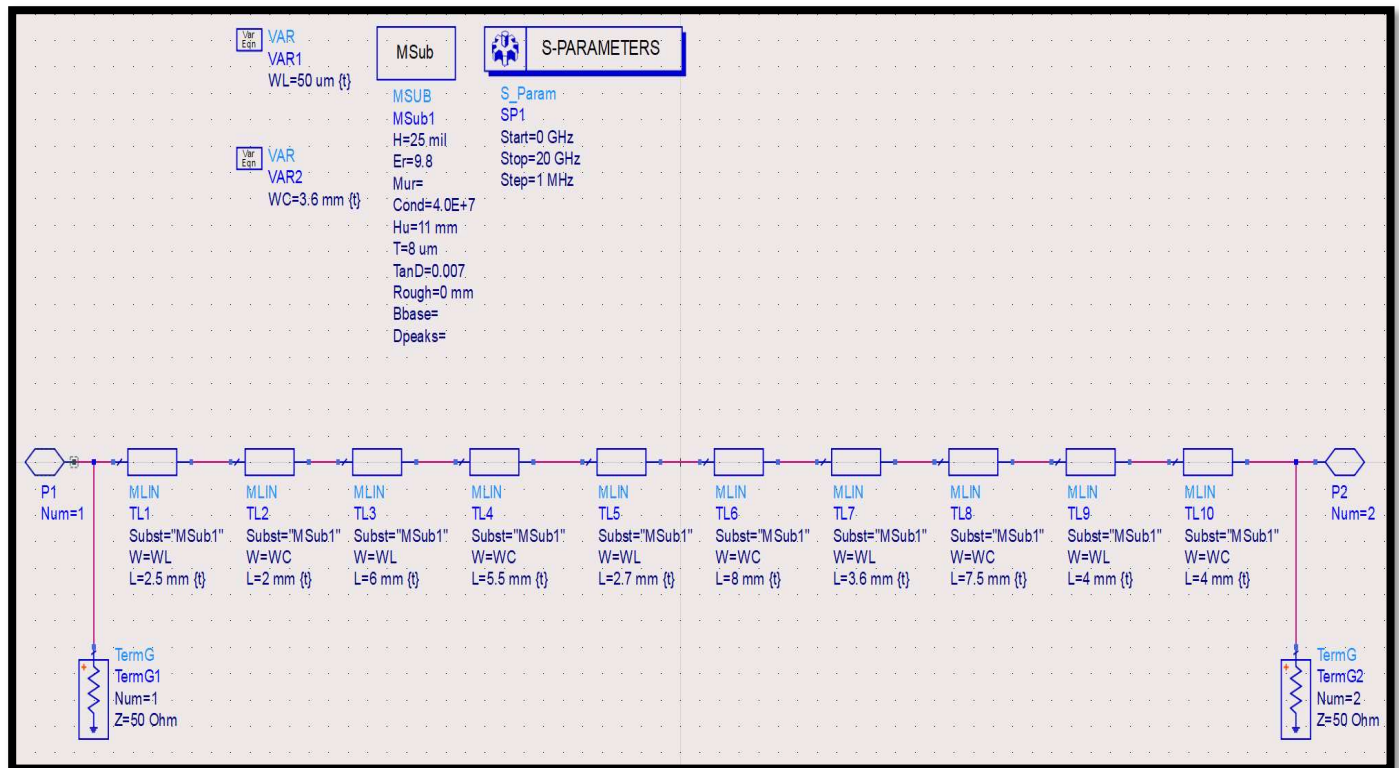


Figure 5.5 Schematic representation of 6th order filter

Schematic Simulation Result:

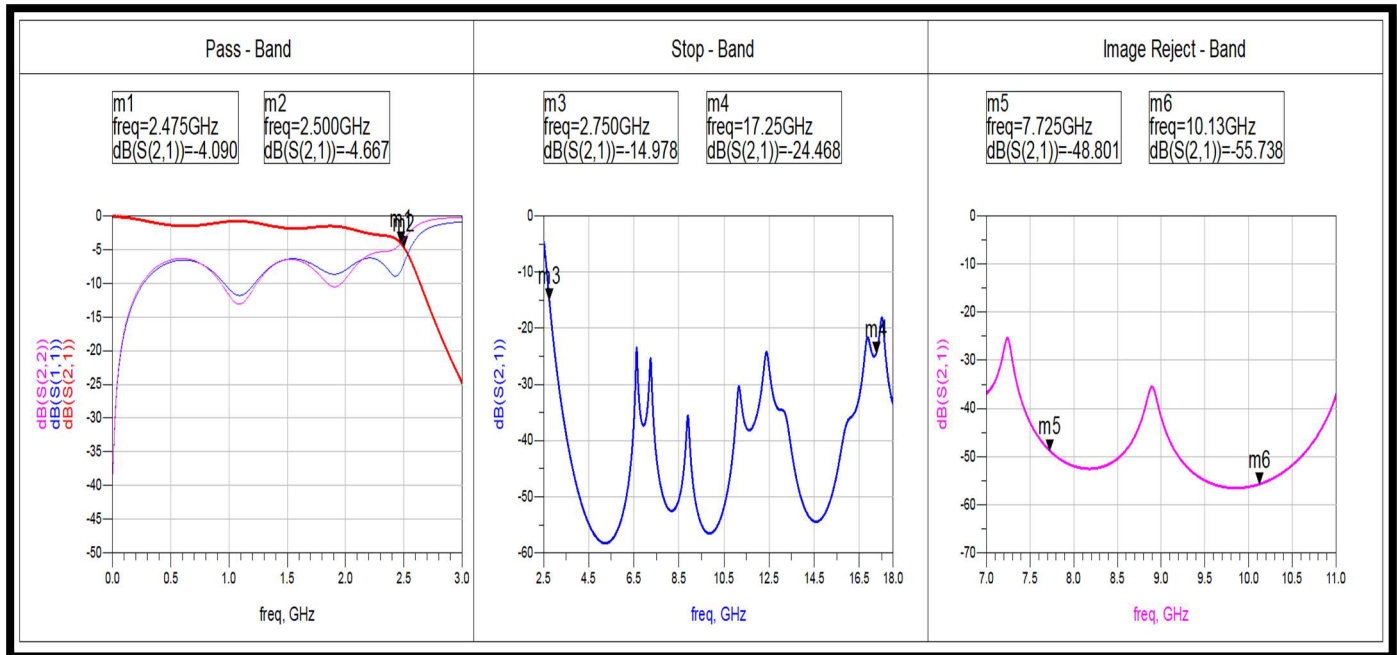


Figure 5.6 S-Parameters from schematic simulation (10th order)

The schematic simulation response for the 10th order filter improves from that of the 6th order filter. However there the response does not fully satisfy in the passband. Also, the return losses are way too high then what is required.

Observation: The schematic simulation does show that the design covers a better portion of the passband than that of the 6th order filter however it is observed that the S₁₁ parameter worsens from the layout simulation of that of 6th order filter. Also, the stop-band and image-reject band can satisfy the required specification.

Conclusion: The pass band is not at all tolerable, although the other requirements are matches. Therefore, this design is also not further tuned to get the output.

5.4.3 10th Order Open-Stub Filter Design

To get a sharper roll-off rate, we tried to implement the 10th order filter using open-stub topology.

Table-8 Obtained values for 10th order Stepped-Impedance Filter

i	L _i (mm)	W _i (mm)
1	2.5	0.05
2	2	3.6
3	6	0.05
4	5.5	3.6
5	2.7	0.05
6	8	3.6
7	3.6	0.05
8	7.5	3.6
9	4	0.05
10	4	3.6

Schematic View:

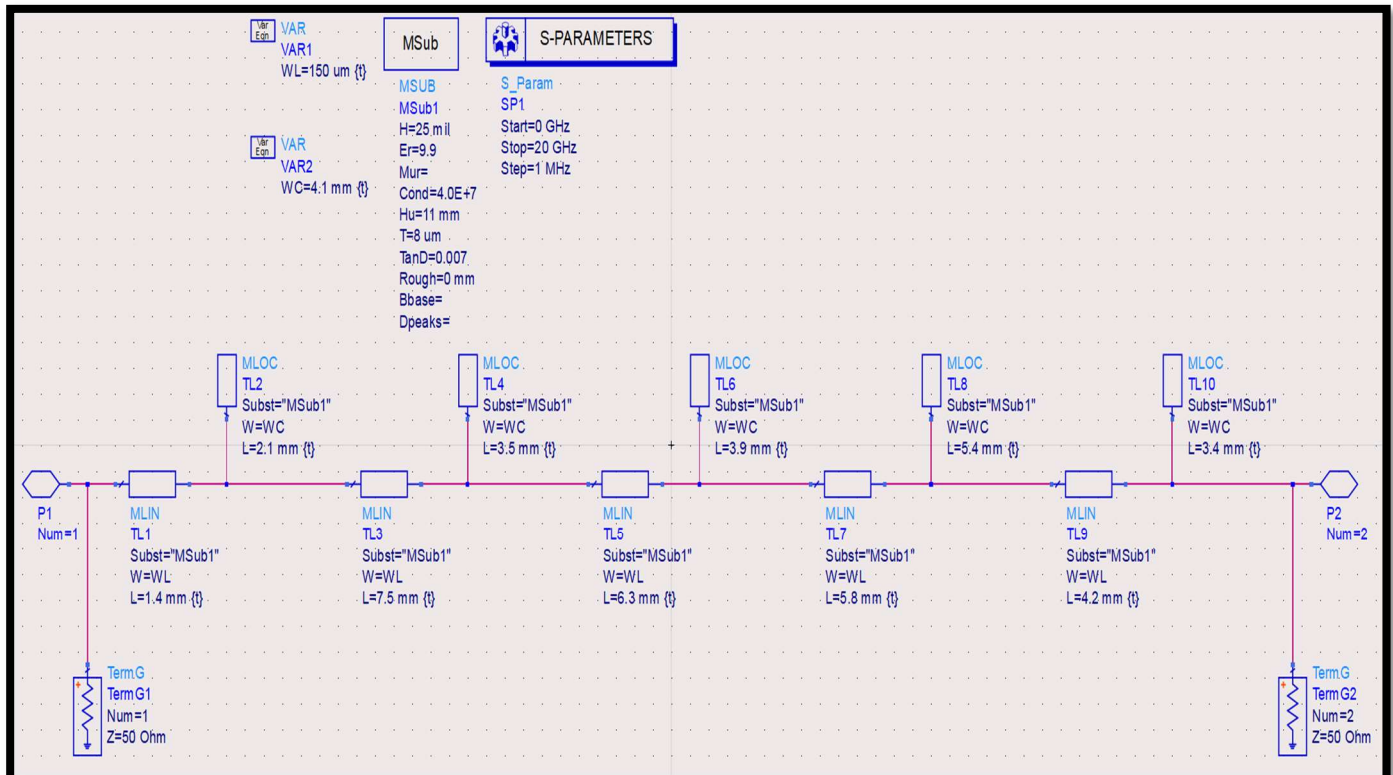


Figure 5.7 Schematic representation of 10th order filter

Schematic Simulation Result:

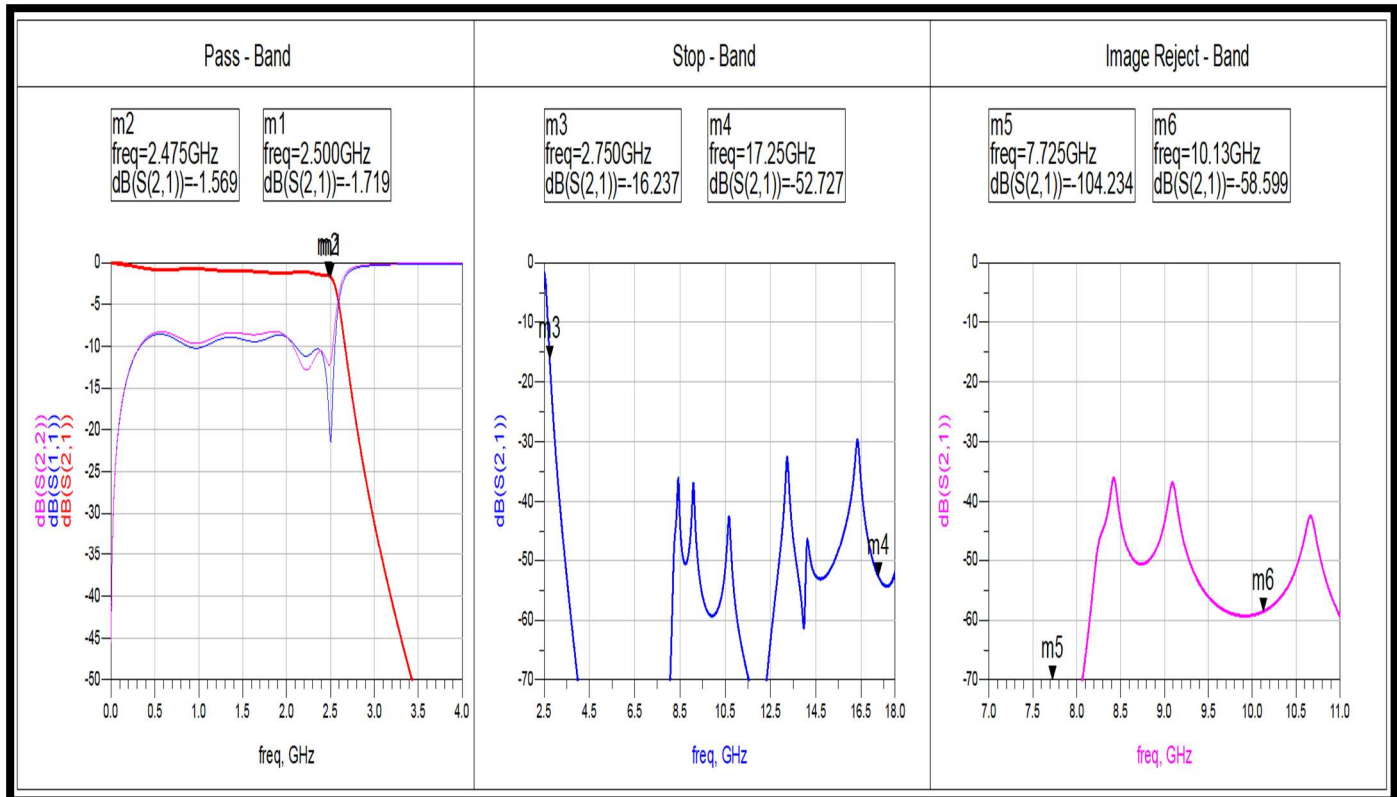


Figure 5.8 S-Parameters from schematic simulation (10th order)

The schematic simulation shows promising results, satisfying most of the specifications with some minor tunings. Still, in the passband the insertion loss and return loss are too high to be of practical implementation. So, the further not moved to layout for actual response.

Observation: The simulated result from the schematic shows promising results satisfying most of the given specifications as well, without doing any major changes and the size of the filter is comparable in accordance to the substrate size mentioned.

Conclusion: The schematic for the 10th order filter shows the best response among all the three filter that are tried. Also, there is scope of making the design compact to satisfy the substrate area constraint.

5.4.4 7th Order Stepped-Impedance with $\lambda/4$ Open-Circuited Stubs Filter Design

To get a sharp-roll and reduce losses we move to 0.5dB Chebyshev prototype with 9th order filter with $\lambda/4$ stubs to suppress peaks occurring in the stop band.

Table-9 Obtained values for 7th order Stepped-Impedance Filter

i	L _i (mm)	W _i (mm)
1	5.5	0.3
2	1.6	7.7
3	5.5	0.073
4	2	8.3
5	5.5	0.073
6	1.6	7.7
7	5.5	0.3

Schematic View:

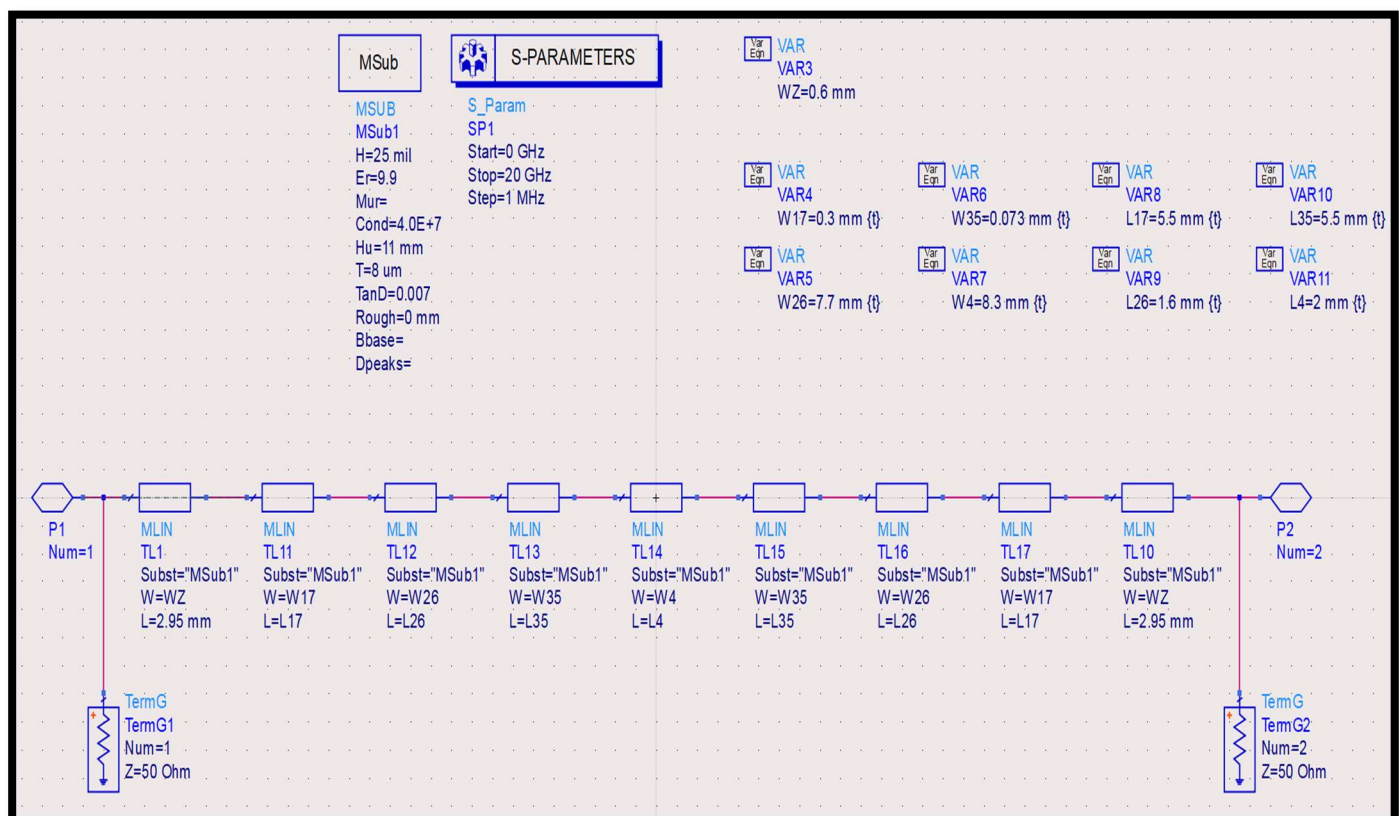


Figure 5.9 Schematic for the 7th order filter design

Layout View:

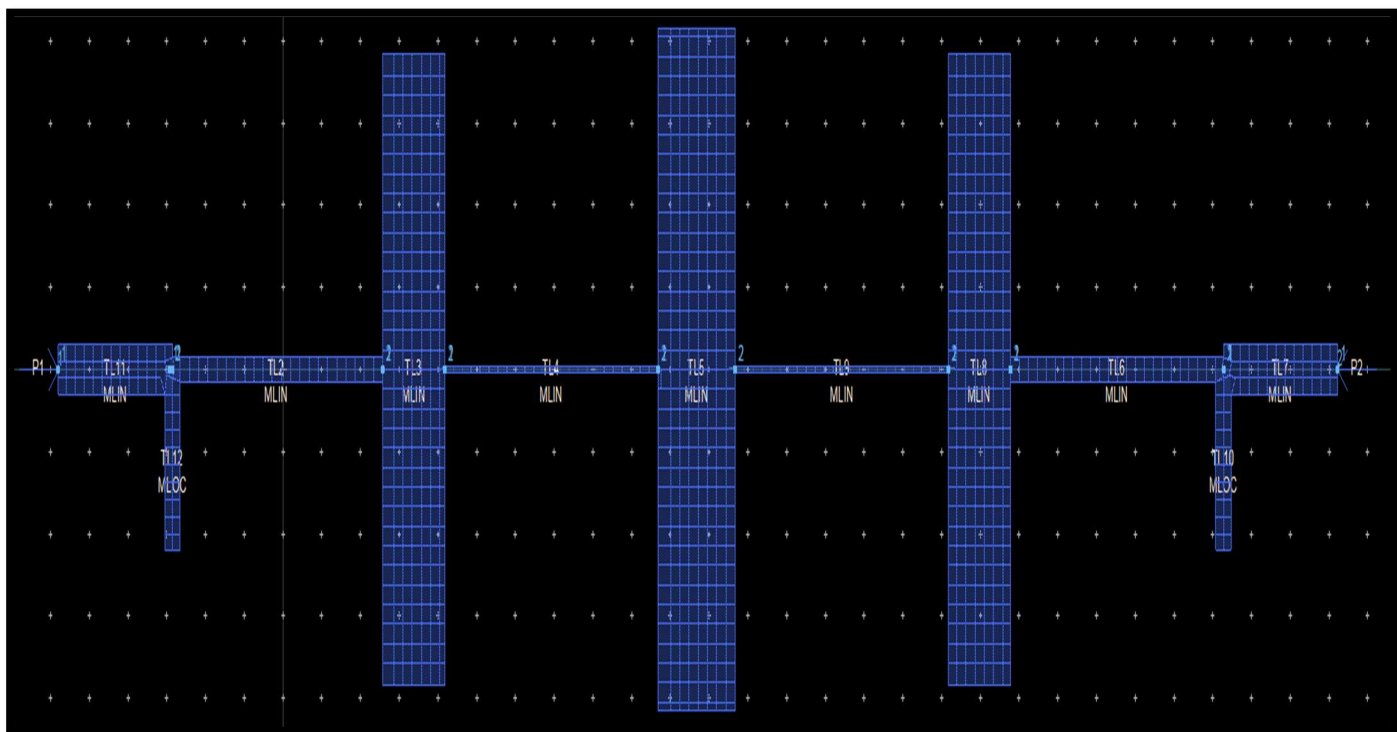


Figure 5.10 Layout for the 7th order filter design

Layout Simulation Result:

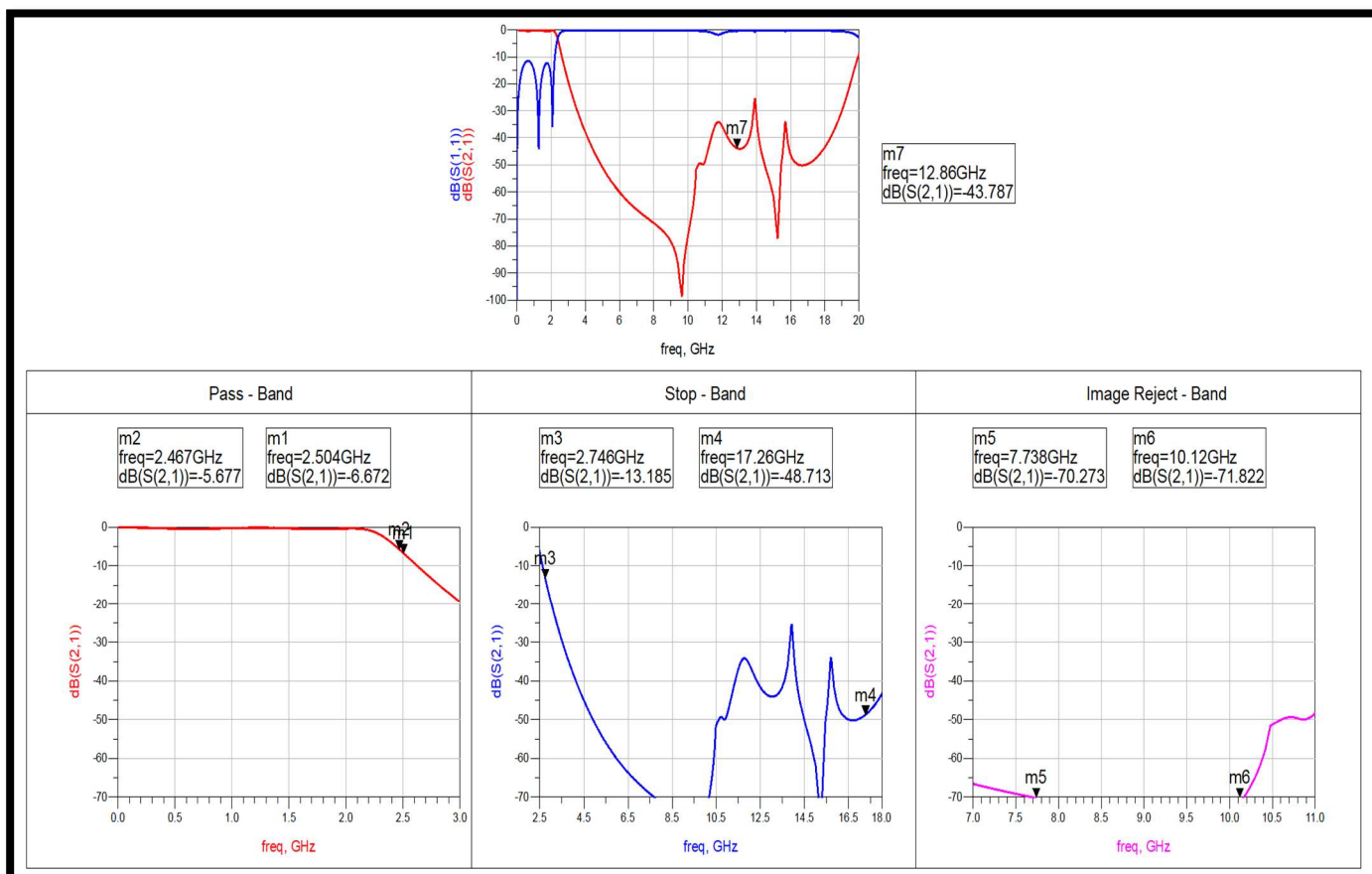


Figure 5.11 S-Parameters from layout simulation (7th order)

The layout simulation shows promising results, satisfying most of the specifications with some minor tunings. We can see that now the passband is much flatter than previous which lead to reduction in return loss as well as insertion loss.

Observation: The simulated result from the layout shows promising results satisfying most of the given specifications as well, without doing any major changes and the size of the filter is comparable in accordance to the substrate size mentioned.

Conclusion: The schematic for the 7th order filter shows the best response among all the four filter that are tried. Also, there is scope of making the design compact to satisfy the substrate area constraint. Still the roll-off is to be tackled before finalization. **Now onwards, we directly design a layout as simulation results are way far from the EM Simulations results.**

5.4.5 7th Order LC Open-Stub Filter Design

To get a flatter pass band with minimal insertion loss and maximum return loss, we used LC open stub filter design as shown below. Here, the g-values for LC Stub are taken same for L and C. To achieve impedance matching on both the sides, we have used 50 Ohm sections for matching. The calculation method remains same as discussed above.

Layout View:



Figure 5.12 Layout for 7th order filter

Layout Simulation Result:

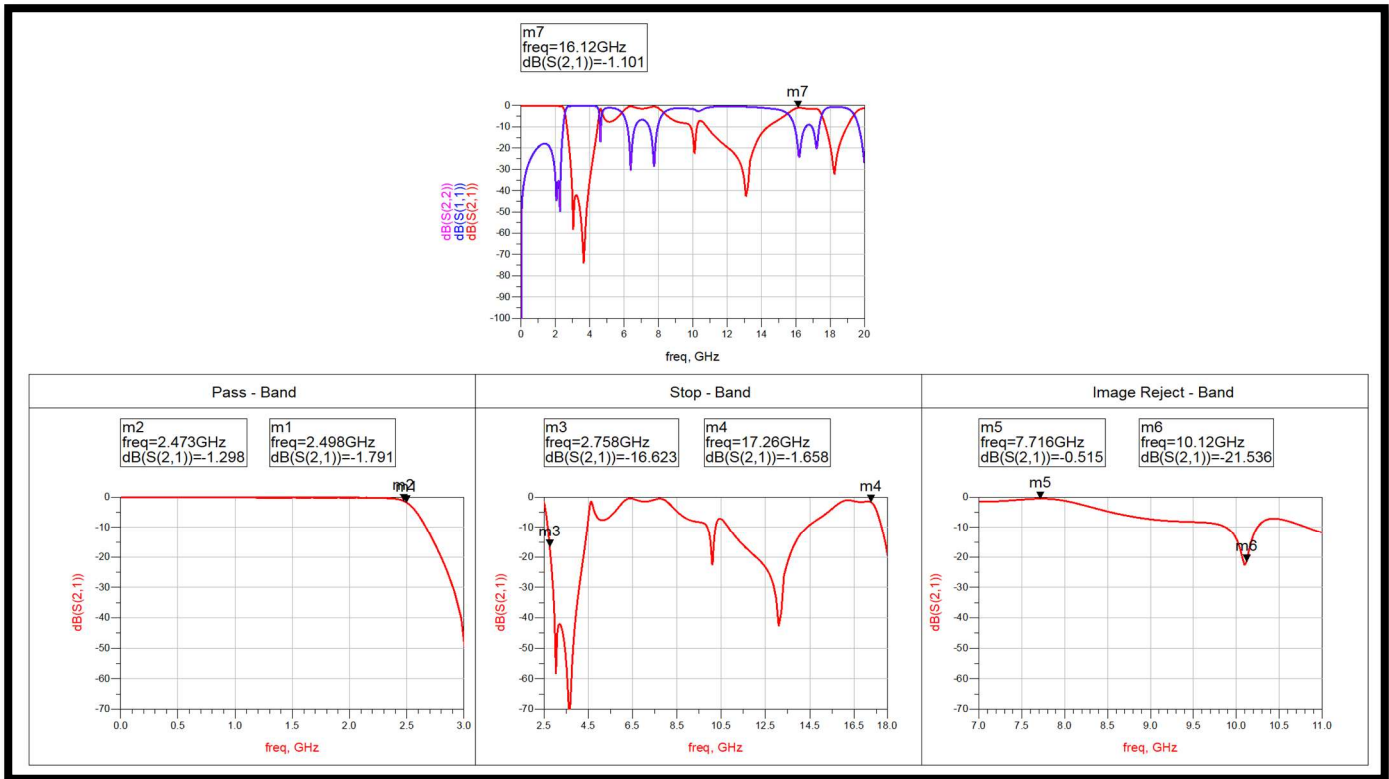


Figure 5.13 S-Parameters from layout for 7th order filter

Observation: The S-Parameter response satisfies the Pass Band requirements of Cut-off, return loss below 15 dB and nearly achieves Roll-off at 20dB on M3. But, in Stop Band the response is not even near to the actual desired response.

Conclusion: The design can be further added with stubs to suppress the frequencies emerging in the Stop-Band.

5.4.6 7th Order LC Open-Stub Filter Design with Radial Stubs

In the previous design, we found that we need to suppress frequencies emerging in the Stop-Band to match our requirements. Here we use radial stubs to get a wide band of frequencies being rejected.

Layout View:

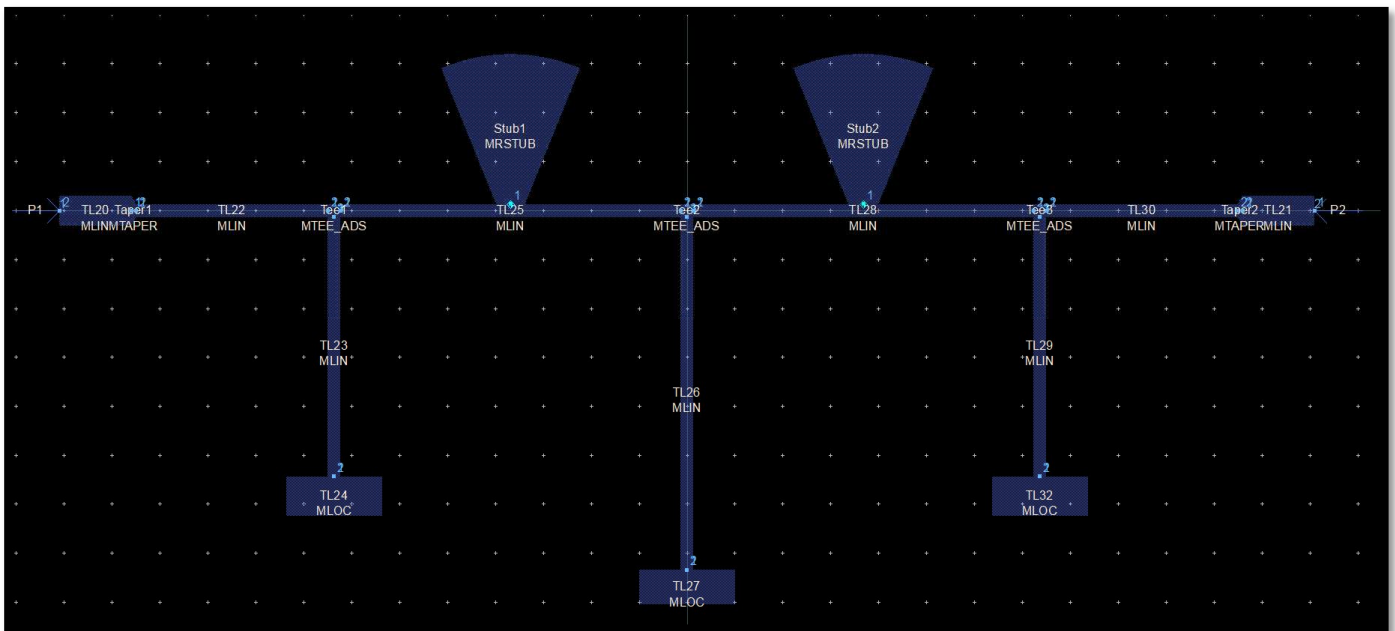


Figure 5.14 Layout representation of 7th order filter with Radial Stubs

Layout Simulation Result:

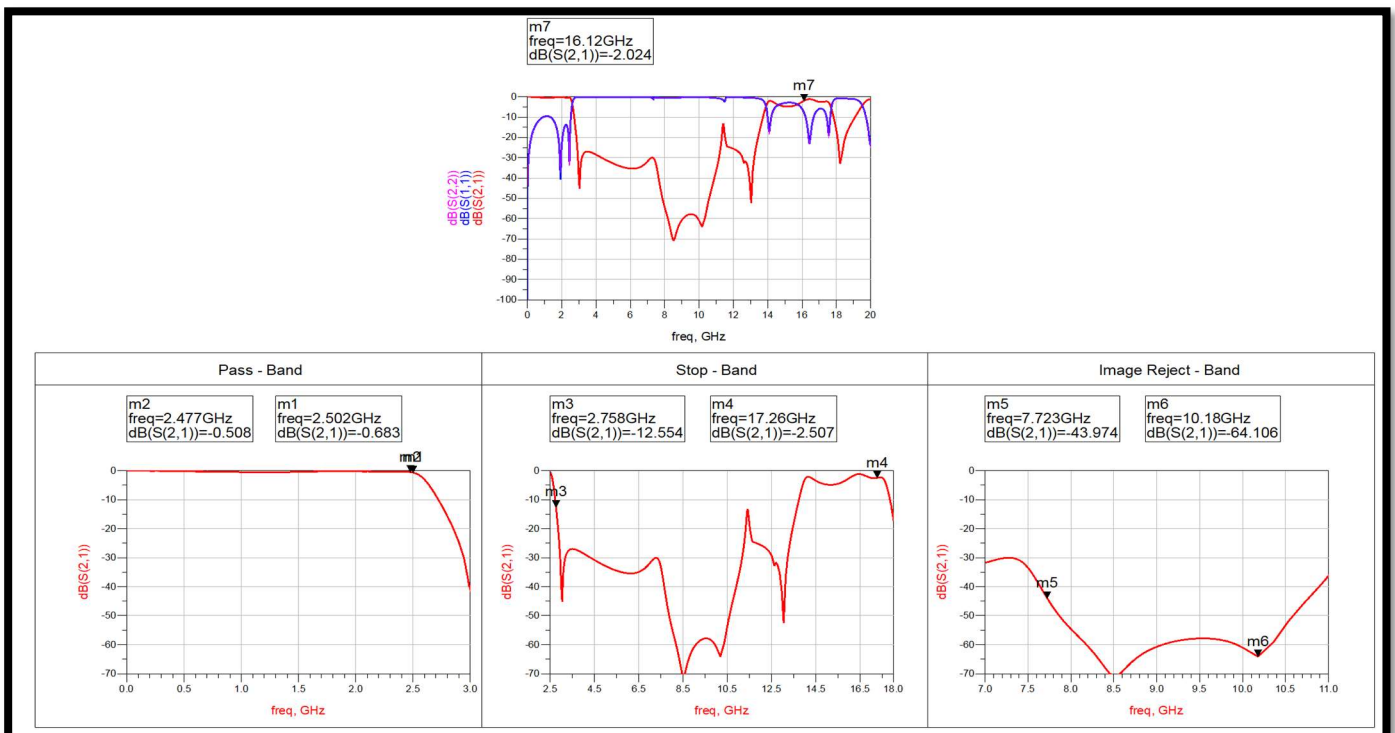


Figure 5.15 Layout Simulation Result of 7th order filter with Radial Stubs

Observation: Clearly, we can see that the radial stubs are very much effective in suppressing frequencies from nearly 3.5 GHz to 10.5 GHz. Still the frequencies beyond the 10.5GHz are not suppressed. So, still more improvisations can give the desired response followed by some fine tuning.

Layout View:

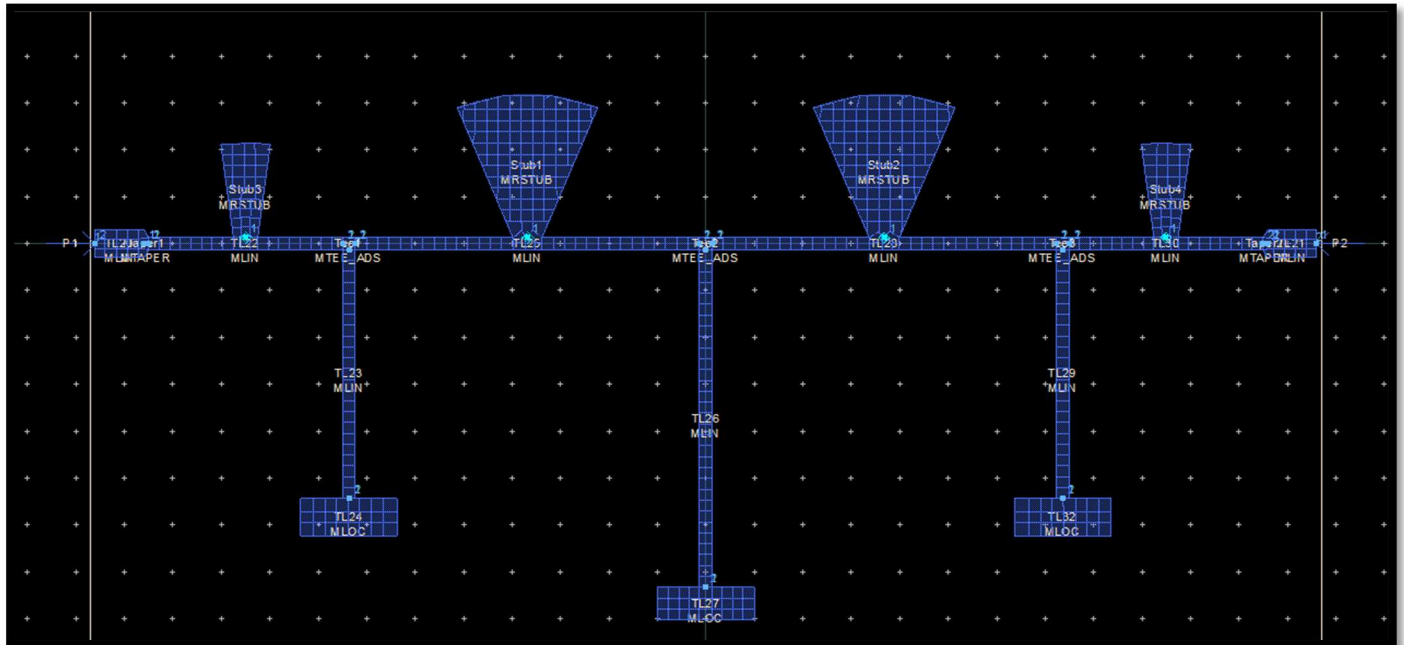


Figure 5.16 Layout representation of 7th order filter with more Radial Stubs

Layout Simulation Result:

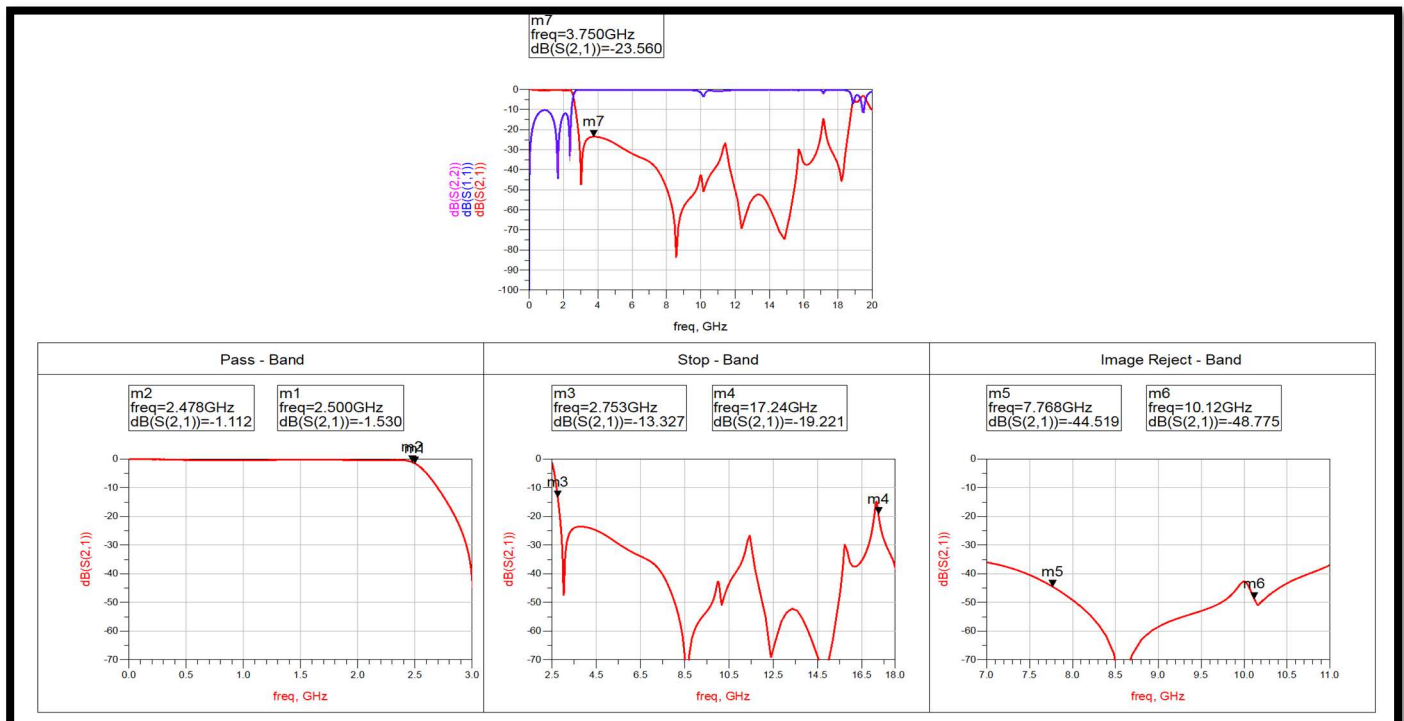


Figure 5.17 Layout Simulation Result of 7th order filter with more Radial Stubs

Observation: Clearly, we can see that the radial stubs are very much effective in suppressing frequencies from nearly 3.5 GHz to 17 GHz. Still, we are not able to match Roll-off M3 should be below 20dB. So, we need to rework and recalculate the design to achieve it.

Conclusion: This design is good enough but some parameters need to recalculated to get a good roll off.

5.4.7 7th Order LC Open-Stub Filter Design with Radial Stubs – 2

In the previous design, we found that we need to suppress frequencies emerging in the Stop-Band to match our requirements. Here we use radial stubs to get a wide band of frequencies being rejected. We also wanted to get a sharper roll off so we reworked the design.

Layout View:

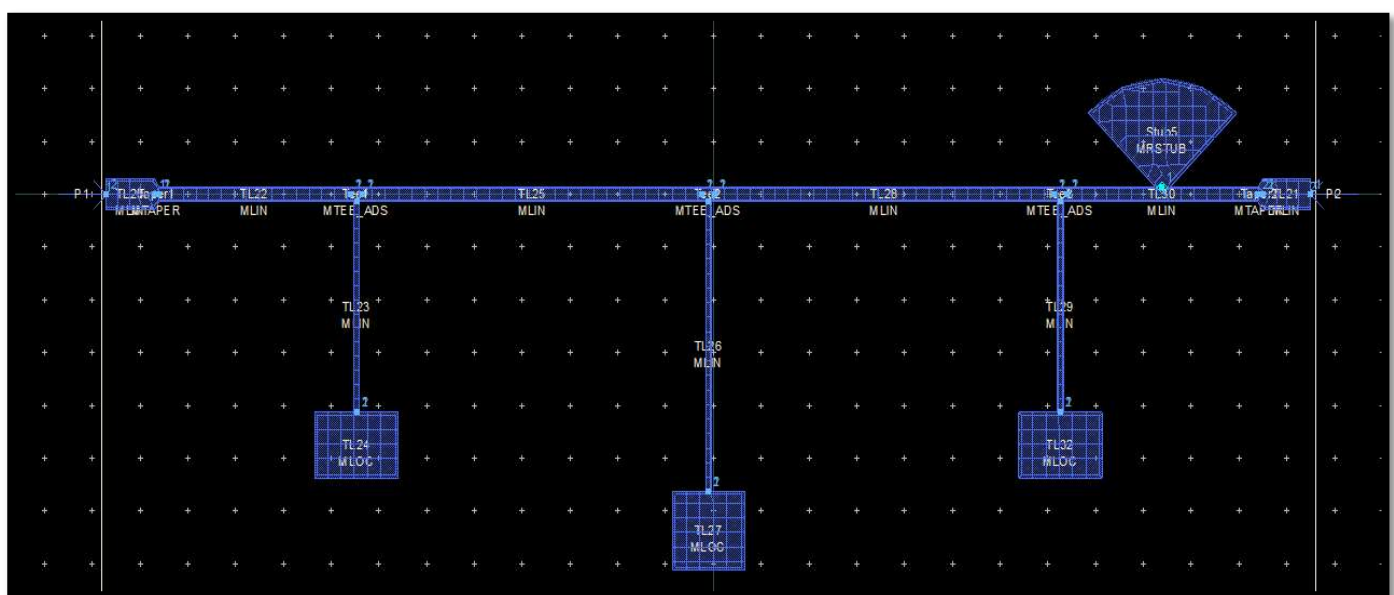


Figure 5.18 Layout representation of 7th order filter with Radial Stubs - 2

Layout Simulation Result:

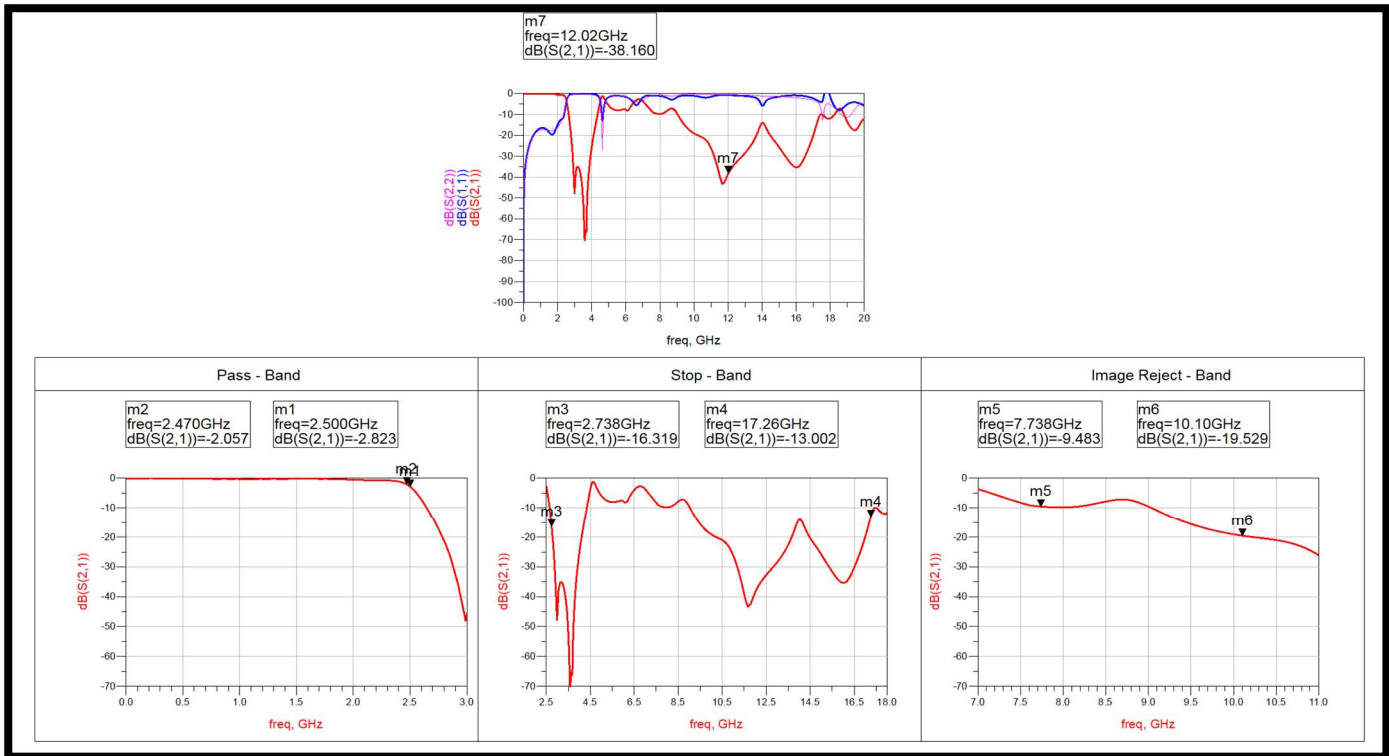


Figure 5.19 Layout Simulation Result of 7th order filter with more Radial Stubs

Observation: This is an another way for same filter. Again, the pass band is obtained as required but we need to reject the harmonic frequencies emerging in stop band.

This design is further worked upon to obtain the actual response. Here, an LPF filter is cascaded with original LPF filter centred at 3 GHz to reject frequencies from 4 to 10 GHz.

Layout View:

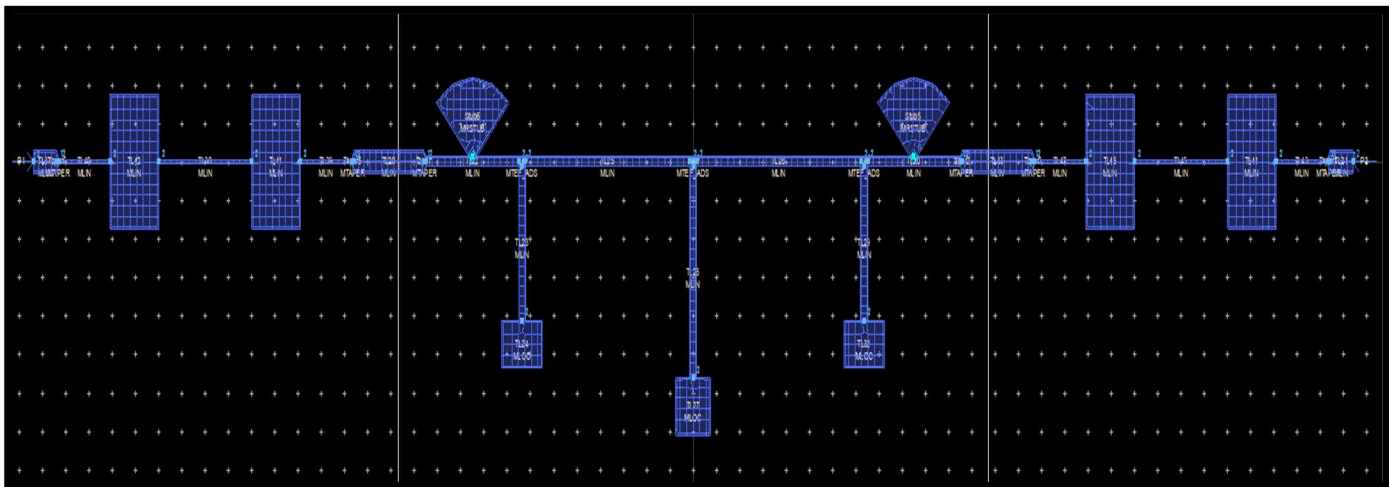


Figure 5.20 Layout representation of 7th order filter + 5 th order filter with radial stubs

Layout Simulation Result:

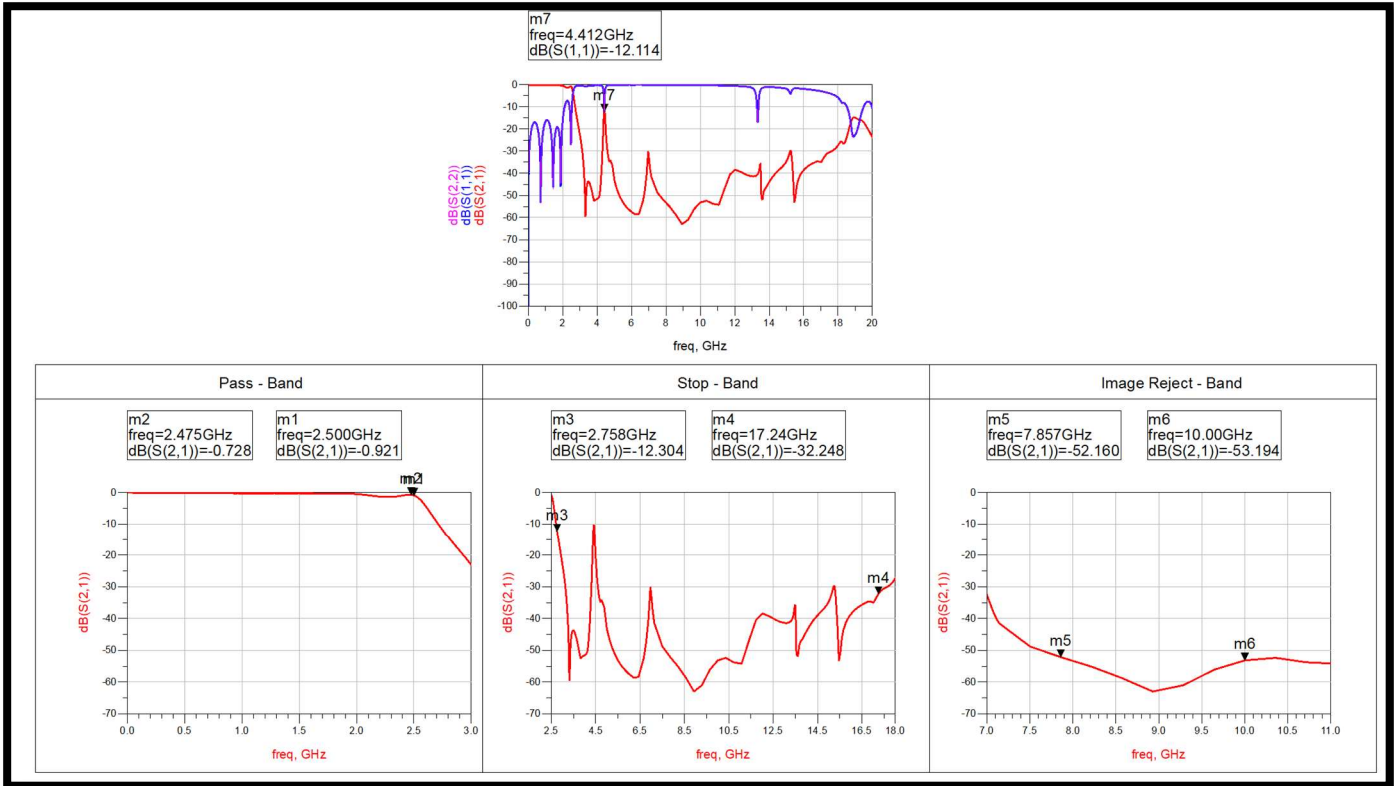


Figure 5.21 Layout Simulation Rwesult of 7th order filter + 5th order filter with radial stubs

Observation: Here, we used 2 radial stubs to suppress frequencies above 10 GHz and further cascaded another Stepped – Impedance LPF of 5th order to suppress frequencies from 4.5 GHz to 10.5 GHz. The 5th order LPF is cascaded on both the sides in order match S11 and S22 parameters.

Conclusion: Here, we are still not getting Roll-Off as required, so further we extend the work on this design and this design give promising results in Stop-Band as well as Pass Band and even maintains Return loss below 15dB.

5.4.8 LPF+LPF Finalizing the Design

In the previous design, we need to improve ripple in Pass – Band and suppress some remaining peaks in the Stop – Band also try to improve Roll-Off. Also, we now try to fit the design in 1-inch x 1-inch area.

Layout View:

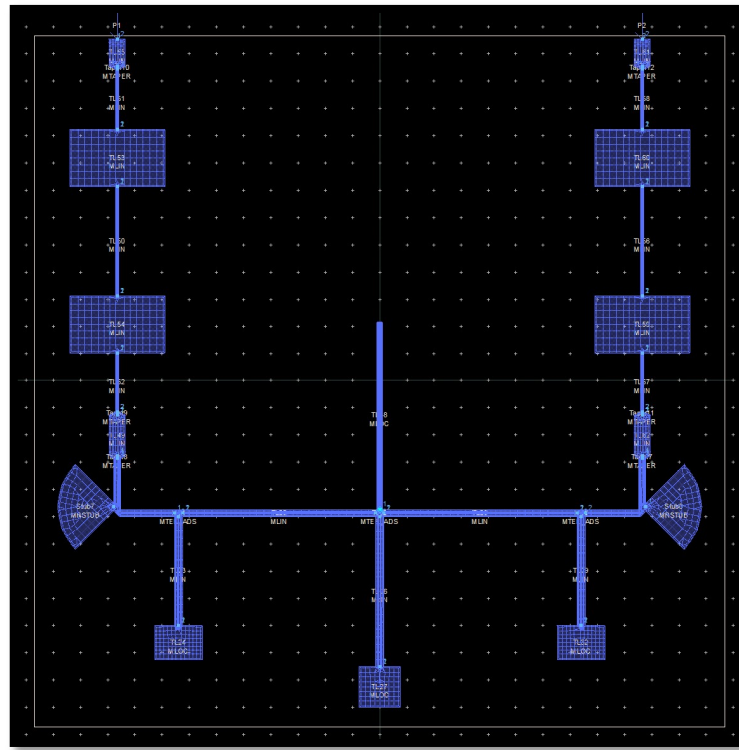


Figure 5.22 Layout representation for LPF+LPF Filter

Layout Simulation View:

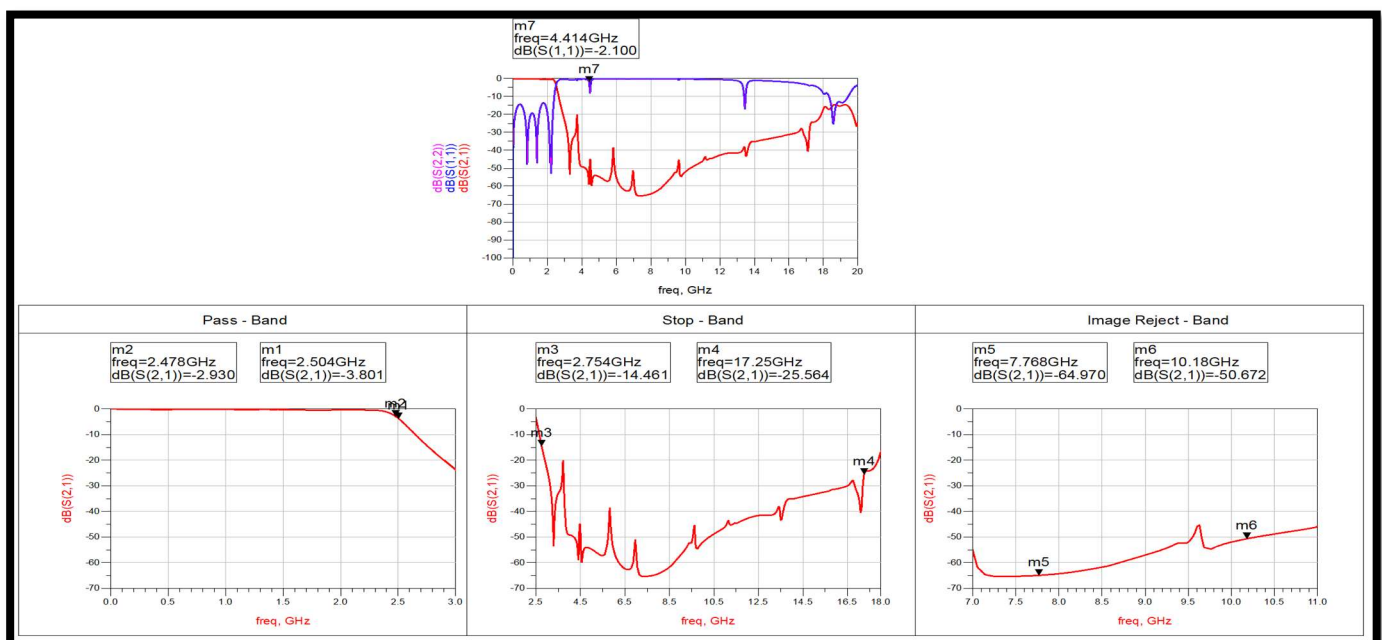
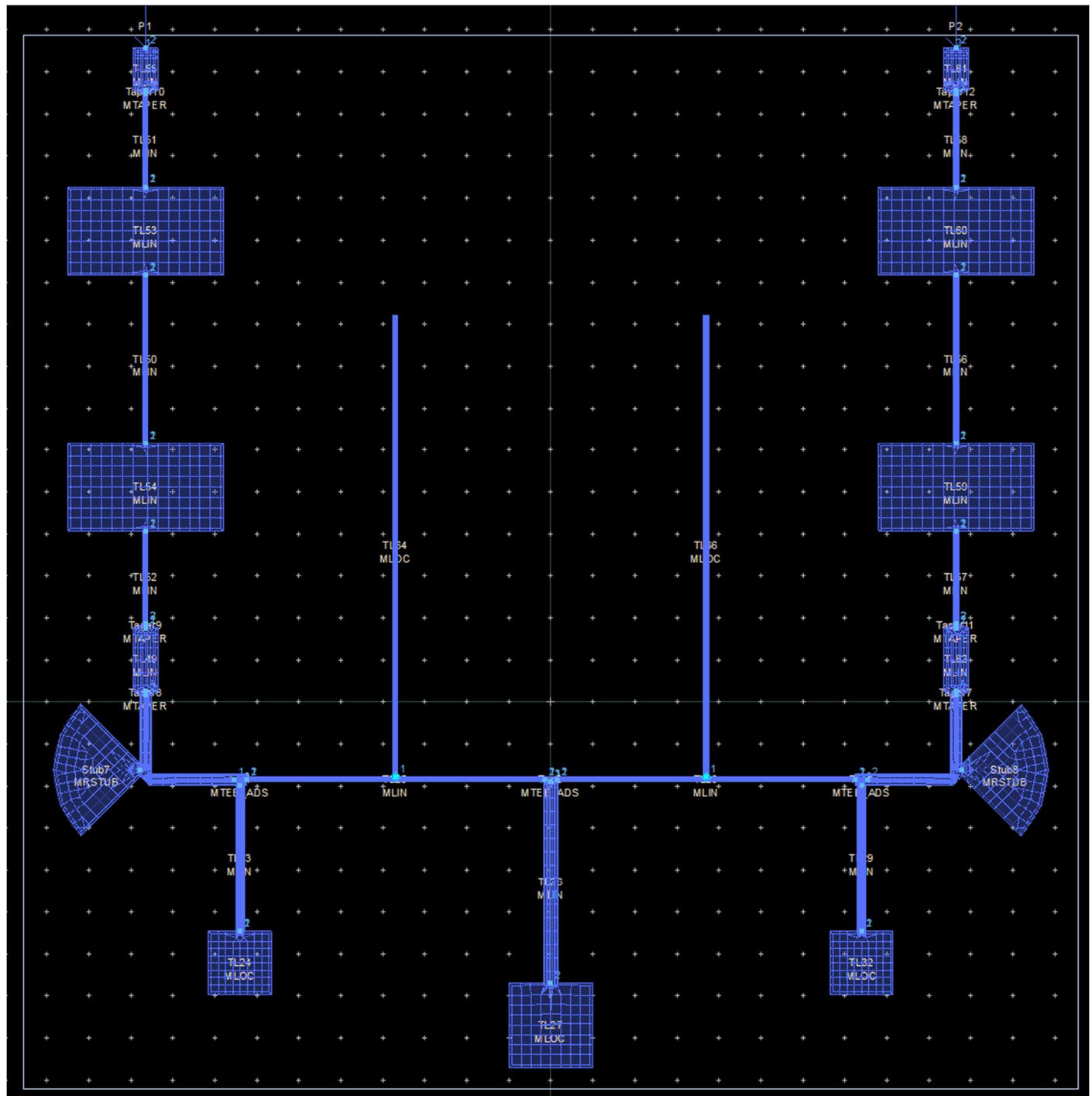


Figure 5.23 Layout Simulation Result of LPF+LPF Filter

Observation: Here, we used mitred lines to bend the lines and fit the layout within the given area. Also, we added a stub at the centre for suppressing peaks. Here, in the simulation view we can see that Stop-Band requirements are completely satisfied. The pass band requirements are also satisfied including the insertion loss and return loss. The only change required now is to sharpen the Roll-Off of the filter.

Here, we increased the order of the main filter by 2 to achieve the Sharp Roll Off.

Layout View:



Layout Simulation View:

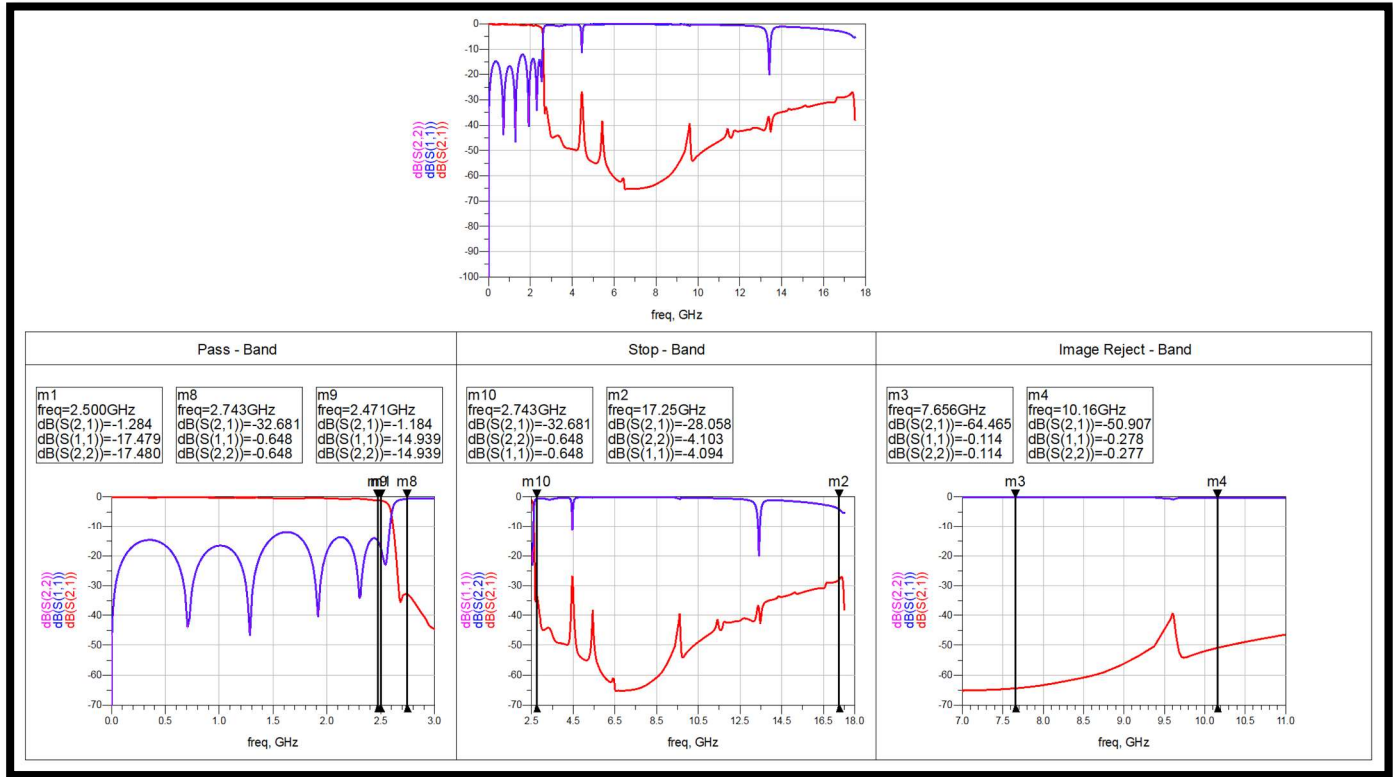


Figure 5.25 Layout Simulation Result of LPF+LPF Filter with increased order

Observation: Here, in the simulation view, we have achieved all specification exactly. This filter is completed just some optimizations and tuning is required.

Conclusion: The major change now required is to further reduce area to $\frac{3}{4} \times \frac{3}{4}$ inch² area and also set the two input and output ports at opposite sides and centre.

CHAPTER-6 FINAL PROPOSED DESIGNS

6.1 Band Pass Filter using Lumped Components (Filter – 1)

6.1.1 Layout Designed for BPF using Lumped Elements

Here, we have pre-defined footprints for L and C. Also, we have used Via for grounding, the yellow holes in the layout shows vias.

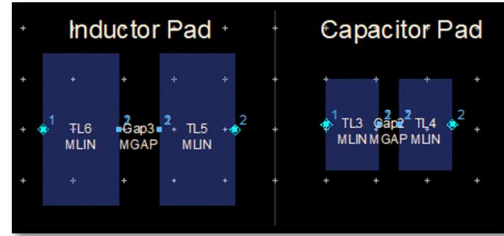


Figure 6.1 Footprints for Lumped Elements

Layout View:

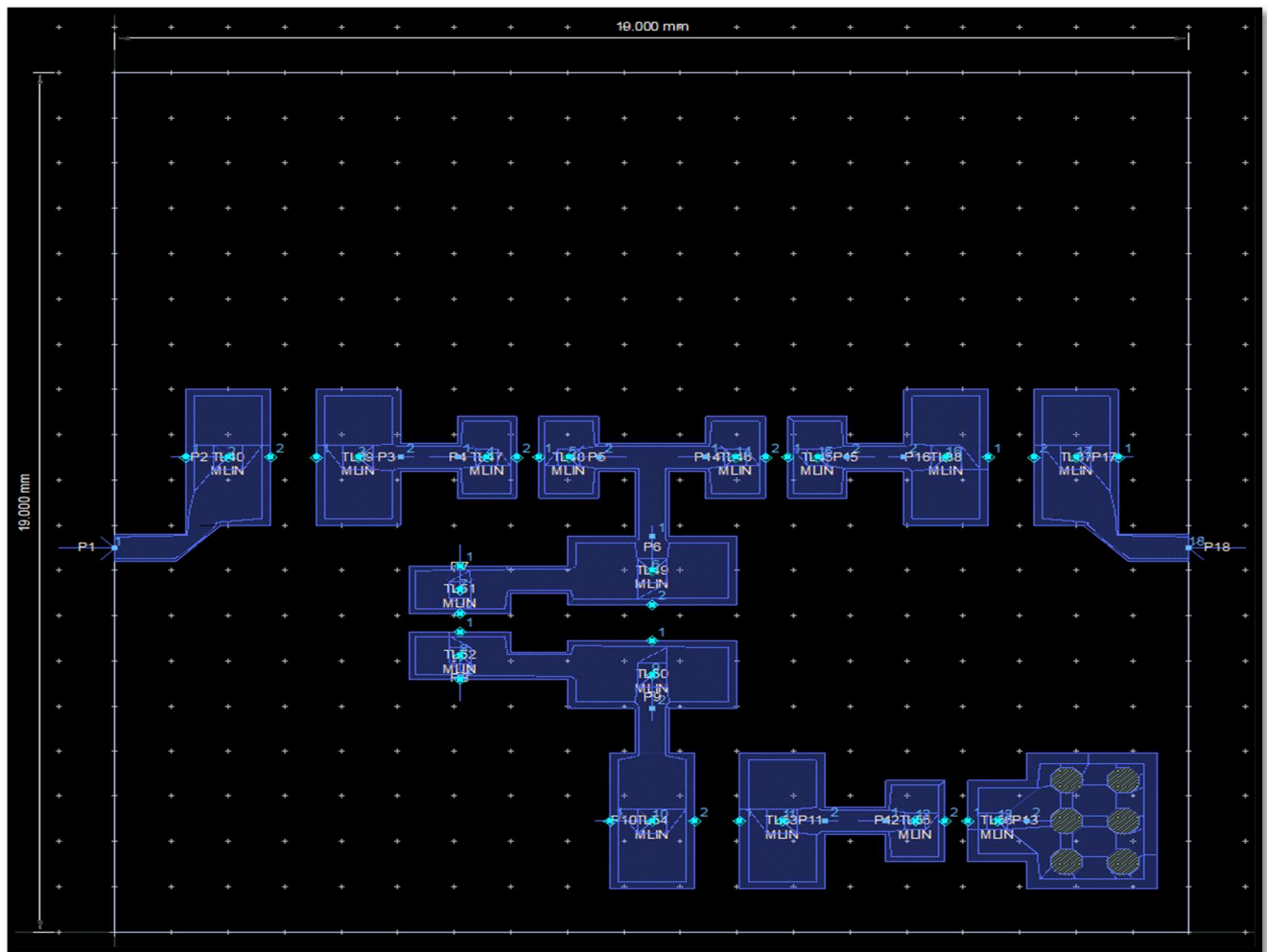


Figure 6.2 Layout for BPF using Lumped Elements

The above shown layout is the final proposed layout that will be used in Co-Simulations as an EM-Model.

6.1.2 Schematic with Co-Simulation

The below image shows Co-Simulations for the Layout designed for Lumped Elements.

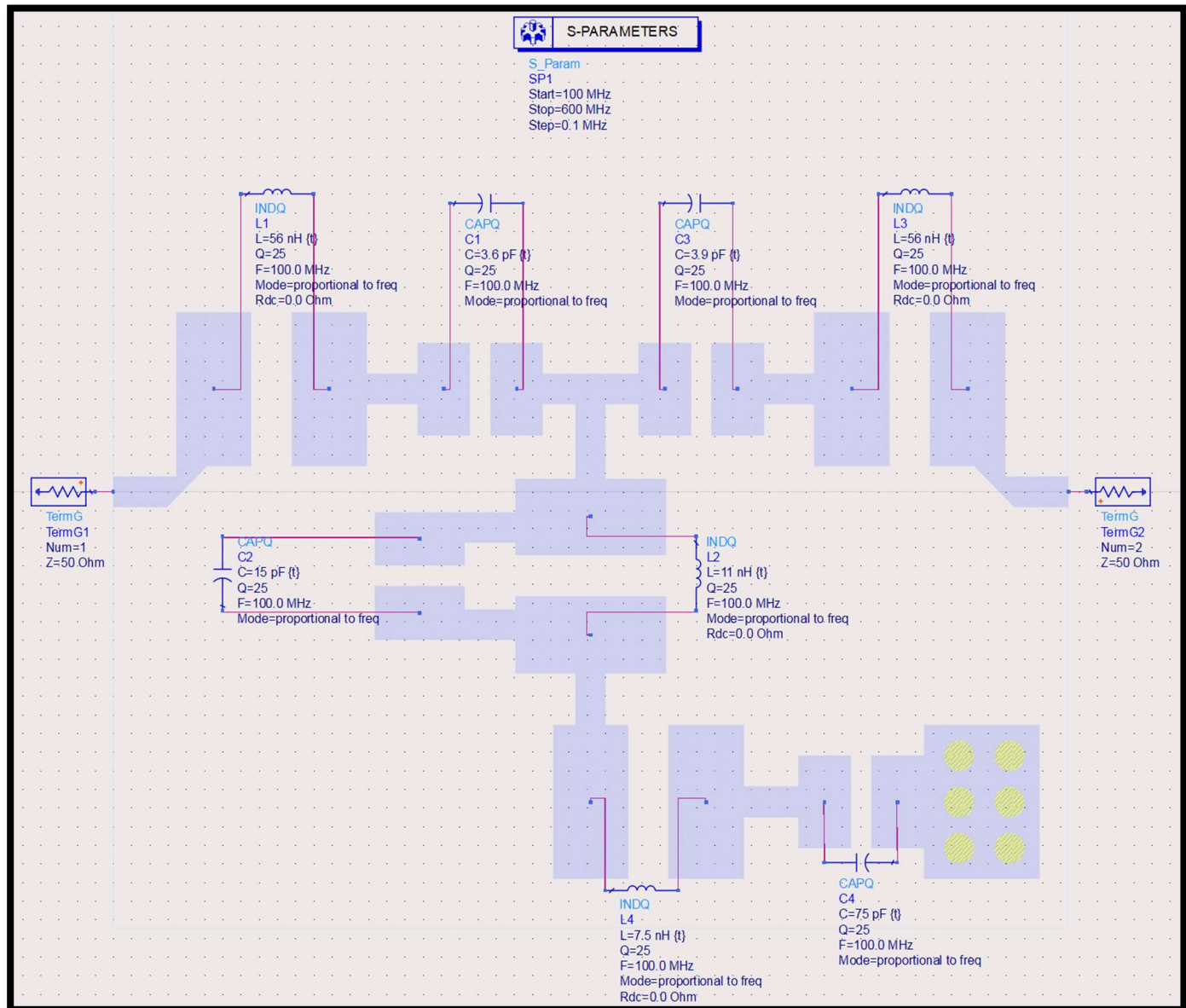


Figure 6.3 Co-Simulation Schematic for BPF using Lumped Elements

6.1.3 S-Parameters for Co-Simulation

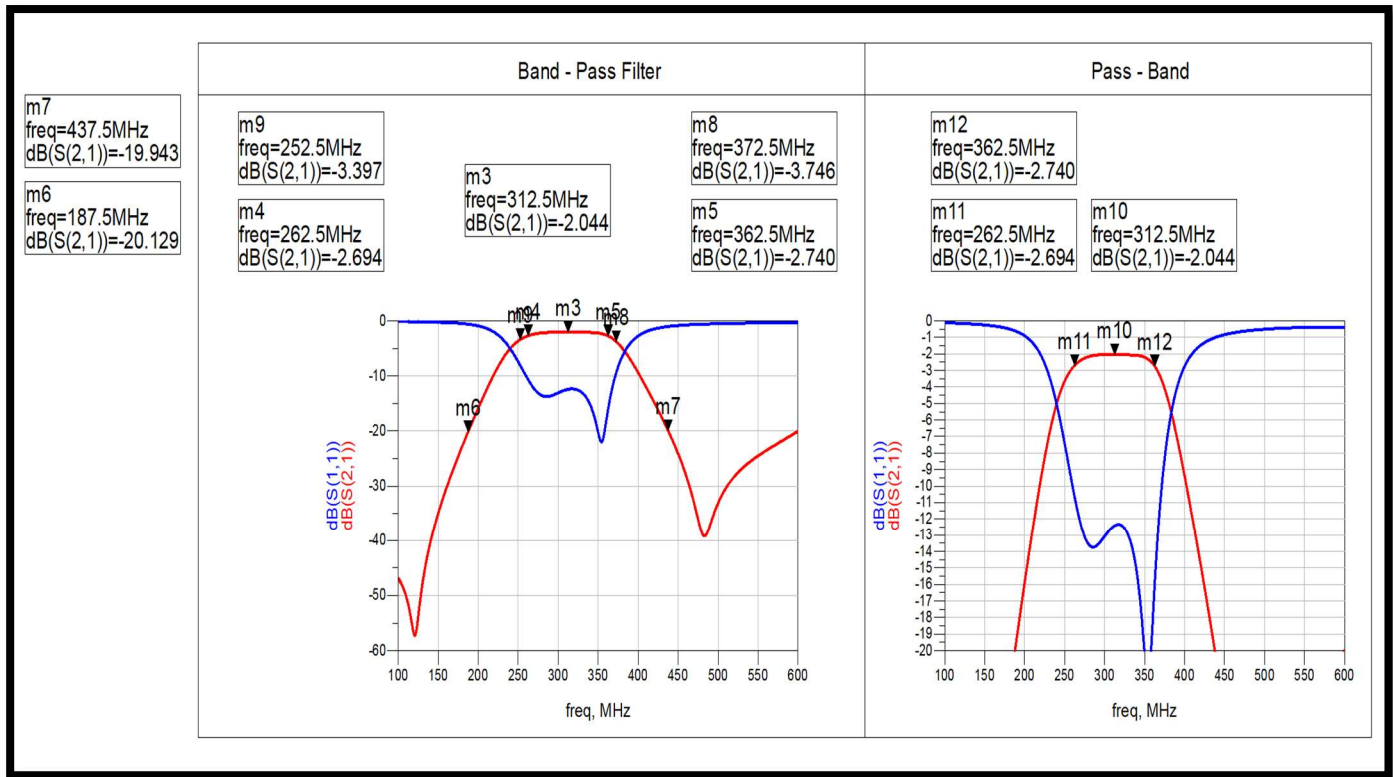


Figure 6.4 S-Parameters for Co-Simulations

Here, we can clearly see that the parameters are matching our actual desired response. **Now, the filter is ready for fabrication.**

Further, the final practical values decided for BPF are:

Table-10 Final values for 3rd order BPF

i	L (nH)	C (pF)
1	56	3.6
2	11	15
3	56	3.9
4	7.5	75

Observation: The co-simulated result showed deviation from simulated results. So, tuning again and size reduction helped to get the desired output.

Conclusion: The proposed design successfully satisfies the required specifications along with physical size constraints and is ready for fabrication. Further, we will test the response after the design is fabricated.

6.2 Micro-strip Low Pass Filter (Filter – 2)

6.2.1 Layout Designed for Micro-Strip LPF Layout

The below design shows the proposed final layout for meeting the given specifications for Low-Pass Filter mentioned above.

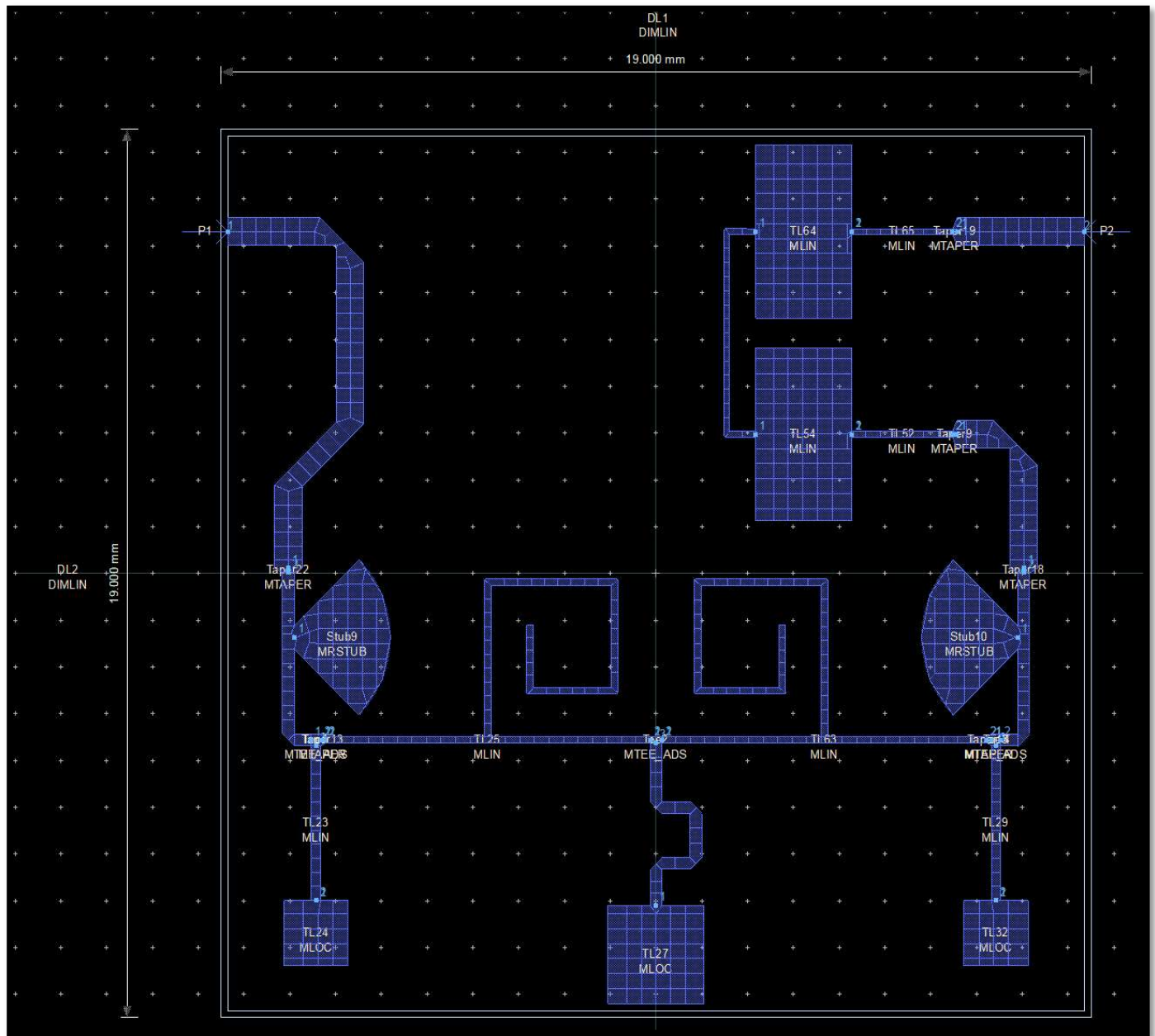


Figure 6.5 Layout for Final Micro strip LPF

Here, we have used 11th Order LPF with 2 Radial Stubs followed by 5th Order LPF.

Radial Stubs Suppress the Higher Stop band Frequencies and 5th Order LPF suppress Lower Stop band Frequencies.

6.2.2 S-Parameters for Final Micro Strip LPF

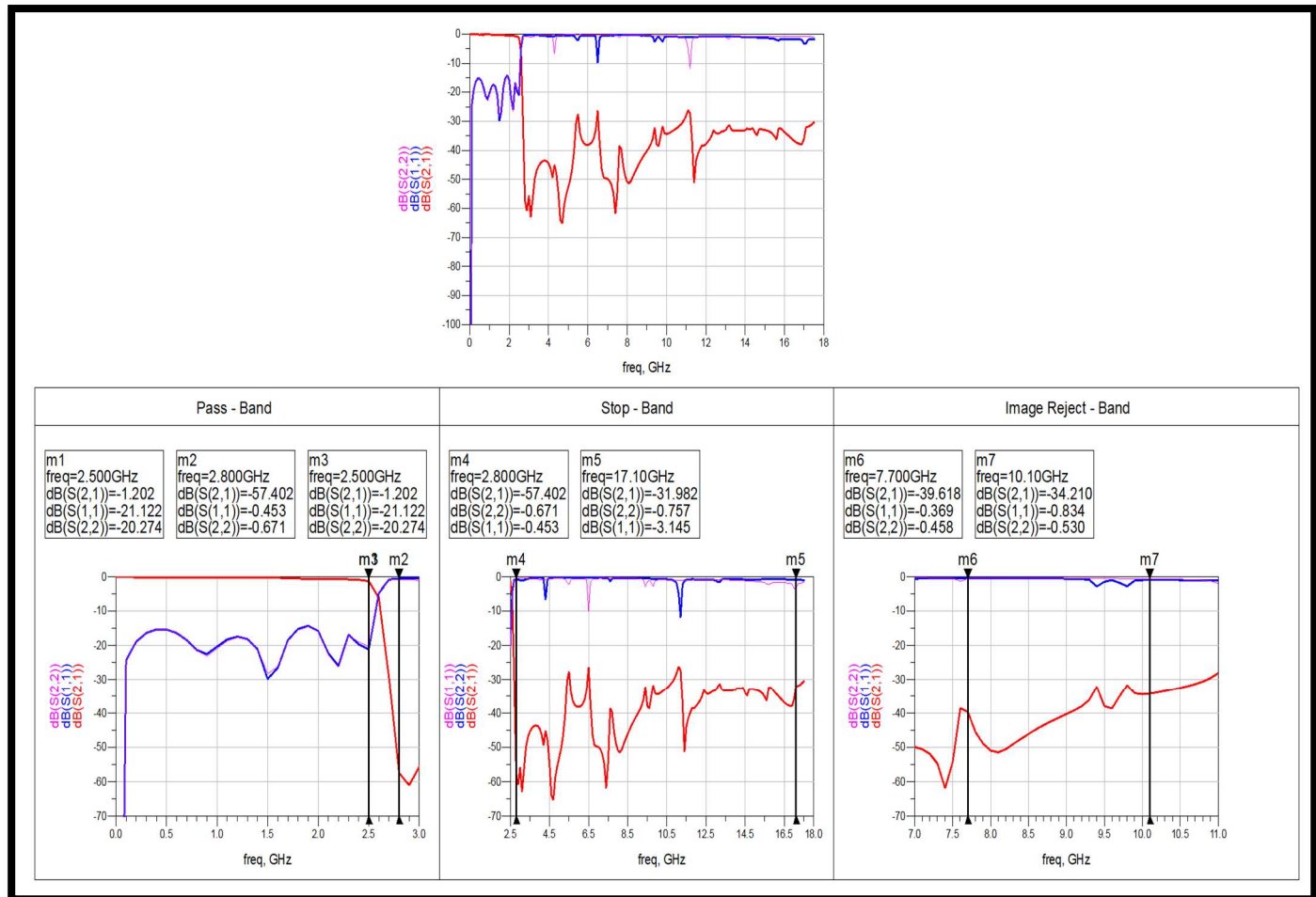


Figure 6.6 S-Parameters for Final Micro strip LPF

Here, we can clearly see that the parameters are matching our actual desired response. **Now, the filter is ready for fabrication.**

Observation: The filter is completely fitted in $\frac{3}{4}$ inch x $\frac{3}{4}$ inch area. The simulations show that the filters response is meeting the given specifications. Also, still some updates can be done including the port to be at the centre which will help it to fit better and require less area in the payload.

6.2.3 Layout for Final Micro Strip LPF with Tuning Pads

The tunings pads are used as a safety measure because sometimes the filter response may shift a bit here and there after fabrication. So, to adjust and nullify these errors we used Tuning Pads.

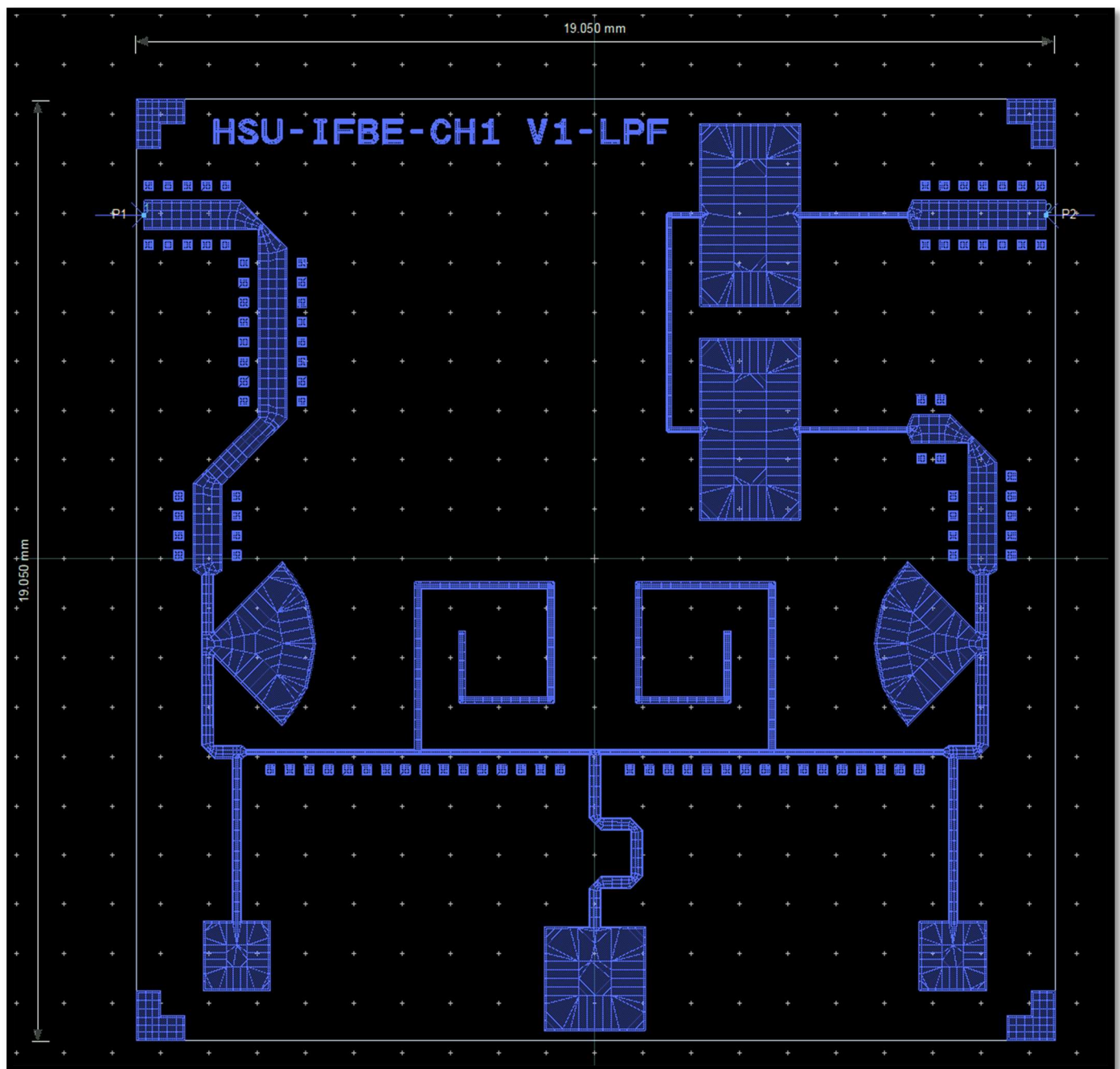


Figure 6.7 Layout for Final Micro strip LPF with Tuning Pads

Conclusion: The filter is matching with all the requirements including Area, Output Response and practicality of Fabrication possible. Hence, the layout is converted to “. gds” file for fabrication.

CONCLUSION

The purpose of the report is to provide an in-depth procedure driven approach into designing of wideband micro strip Low pass filter and Band pass filter using Lumped Elements. The discussion first starts with basic theoretical concepts that are needed to be done in a brief before starting with the designing purpose. Thereafter, the entire design process starts from basic equations and a theoretical approach after which the practical designing is started. It is to be noted that the exact theoretical approach did not give the expected response when converted to the practical design. This might be due to the fact of making some assumptions for some filter specifications and using a set of different normalised prototype component values than that of the expected values.

Final design consists of a 3rd order LC Band Pass Filter satisfying the specifications. It also meets the desired specifications and fits in the area of $\frac{3}{4}$ inch x $\frac{3}{4}$ inch.

The design for micro strip Low Pass Filter also matches the specifications given and has been fitted in an area of $\frac{3}{4}$ inch x $\frac{3}{4}$ inch also.

Both the filters are nearly ready for fabrication stage and afterwards we will be comparing the filters practical and simulated results.

SCOPE OF FUTURE WORK

The micro strip LPF can still be optimized in size as well as ports placed at centre. Further, after both the filters are fabricated, we will test their response in Vector Network Analyser (VNA) and verify the Simulated and Practically obtained results for the both the filters.

The other areas to be explored includes Mixers, Amplifiers, etc.

REFERENCES

- [1] Song, Mei-jing, and Jiu-sheng Li. "A compact microstrip lowpass filter using spiral resonant structure." 2011 4th IEEE International Symposium on Microwave, Antenna, Propagation and EMC Technologies for Wireless Communications. IEEE, 2011.
- [2] Alyahya, Meshaal, et al. "Compact microstrip lowpass filter with ultra-wide rejection-band." 2017 International Conference on Wireless Technologies, Embedded and Intelligent Systems (WITS). IEEE, 2017.
- [3] Ahmad, Jameel, et al. "Design and Fabrication of a Low-Pass Filter based on a Microstrip Resonator for Microwave Applications." 2021 International Conference on Electrical, Computer, Communications and Mechatronics Engineering (ICECCMEE). IEEE, 2021.
- [4] Sheikhi, Akram, Abbas Alipour, and Abdolali Abdipour. "Design of compact wide stopband microstrip low-pass filter using T-shaped resonator." IEEE Microwave and Wireless Components Letters 27.2 (2017): 111-113.
- [5] Xu, Jin, et al. "Design of miniaturized microstrip LPF and wideband BPF with ultra-wide stopband." IEEE Microwave and wireless components letters 23.8 (2013): 397-399.
- [6] Jia-Sheng Hong, M.J.Lancaster. "Microstrip Filters for RF/Microwave Applications".
- [7] David M. Pozar. "Microwave Engineering", 4th Edition.
- [8] T.C Edwards, M.B Steer. "Foundations of Interconnect and Microstrip Design", 3rd Edition.